

Thesis  
1632

FAST ION CONDUCTION IN MIXTURES OF SALT  
WITH COMB-SHAPED POLYMERS BASED ON  
MACROCYCLIC AND LINEAR POLYETHERS

THIS SUBMITTED TO UNIVERSITY OF STIRLING  
FOR THE COMPLETION OF DOCTORATE OF PHILOSOPHY  
IN CHEMISTRY

KAMBIZ SADAGHIANIZADEH

UNIVERSITY OF STIRLING



3044 9930

2/01

**THE BRITISH LIBRARY DOCUMENT SUPPLY CENTRE**

# **BRITISH THESES NOTICE**

The quality of this reproduction is heavily dependent upon the quality of the original thesis submitted for microfilming. Every effort has been made to ensure the highest quality of reproduction possible.

If pages are missing, contact the university which granted the degree.

Some pages may have indistinct print, especially if the original pages were poorly produced or if the university sent us an inferior copy.

Previously copyrighted materials (journal articles, published texts, etc.) are not filmed.

Reproduction of this thesis, other than as permitted under the United Kingdom Copyright Designs and Patents Act 1988, or under specific agreement with the copyright holder, is prohibited.

**THIS THESIS HAS BEEN MICROFILMED EXACTLY AS RECEIVED**

**THE BRITISH LIBRARY  
DOCUMENT SUPPLY CENTRE  
Boston Spa, Wetherby  
West Yorkshire, LS23 7BQ  
United Kingdom**

To

Professor G.M.G. Cowie

## ACKNOWLEDGEMENTS

I wish to express my sincere thanks to Professor J.M.G. Cowie for his invaluable support and guidance throughout this work. I would also like to say that working with Prof. has been pleasurable and I am especially grateful to him for giving me and my colleagues the freedom of initiative whilst maintaining a high academic standard. As a token of my gratitude, this work is dedicated to him.

I am grateful, too, to the technical members of staff for providing valuable support without which this work would not have been possible.

I would like to mention here Doctors R. Ferguson, I. Macewan, H. Hunter, J. Wu, A. Riley and A. Miles, the friends with whom I worked for two and half years in the polymer group, whose friendship made this work more enjoyable.

And last, but not least, if it was not because of the sacrifices of my wife Fatemah, this thesis could not have been completed, so, I would like to express a special thanks to her.



## ABSTRACT

In the first part of this work samples of the poly(vinyl ether) having 3 ethylene oxide units in the side chain were crosslinked to varying degrees and doped with  $\text{LiClO}_4$ . The glass transition,  $T_g$ , was increased by about 20 K at 11% crosslinking, but the levels of conductivity remained the same as those for the uncrosslinked material up to 5% crosslinking. The temperature dependence of the a.c. conductivity was predominately non-Arrhenius and the data were analysed using the *Vogel-Tammann-Fulcher (VTF)* equation and the *Adam-Gibbs* configurational entropy model. Both approaches appear valid at low crosslink densities but may not be applicable at higher levels of crosslinking. Activation energies associated with the segmental motion in the polymer were around  $55 \text{ kJ mol}^{-1}$ .

Conductivity levels increased significantly when the number of EO units in the side chain increased to 5 (mono-dispersed) or 6/7 (average number of EO units). Ionic conductivity in these samples doped with salts are noticeably higher than those reported for MEEP or polysiloxane electrolytes. The temperature dependence of the a.c. conductivity of these polymers doped with  $\text{LiClO}_4$  and  $\text{NaClO}_4$  were predominately Arrhenius at low to medium salt concentrations, over the temperature range

studied. Activation energies associated with the segmental motion in these systems were also calculated.

In the second part of this work, a series of polyphosphazenes with pendant crown ethers were prepared. A 16-crown-5 unit was attached to the polymer backbone using methylene spacer units to modify the initial  $T_g$  of the polymer. Spacers with 0, 3 and 6 methylene units were examined and the  $T_g$ s were observed to decrease with the increasing of the spacer units. The conductivity of mixtures of these polymers with  $LiClO_4$  and  $NaClO_4$  were measured as a function of temperature and it was found that the conductivity was highest for the system with the longest spacing unit which also has the lowest  $T_g$ . Also for comparison a 15-crown-5 and 12-crown-4 derivative with one methylene spacing unit were prepared and examined.

The dependence of conductivity on temperature of these materials was found to be non-Arrhenius and the data were analysed according to VTF equation and Adam-Gibbs configurational model. This predicts that  $(T_g - T_0)$  has a value of about 50 K, but only in the case of  $n = 0$  does this criterion come close to being satisfied and this may not to be the best model to use in these systems.

## CONTENTS

<b>1.</b>	<b>CHAPTER ONE - INTRODUCTION</b>	
1.1	Background	1
1.2	Developments in solvent-free polymer electrolytes	
1.2.1	Poly(ethylene oxide) chemistry	5
1.2.2	Formation of polymer/salt complexes	9
1.2.3	Salt characteristics	12
1.2.4	The effect of salt addition on polymer properties	14
1.3	Electrolyte theory and conductivity studies in polymer/salt complexes	
1.3.1	The origin of electrolyte theory	18
1.3.2	The measurement of ionic conductivity and other transport properties	21
1.3.3	Identity of charge carriers	23
1.3.4	Conductivity studies in polymer salt complexes	24
1.4	Improvement of ionic conductivity by polymer modification	27
1.4.1	Crystallinity reduction	28
1.4.2	Reduction in Tg	31

1.5	Self ionisable polymer electrolytes	33
1.6	Increased solvating capability and polymer modification	36
1.6.1	Polyimines	36
1.6.2	Poly(alkalene) sulphides	36
1.6.3	Polyesters and other solvating polymers	37
1.7	Application of solid polymer electrolytes	38
1.7.1	Batteries	39
1.7.2	Additives to battery electrodes	39
1.7.3	Electrochromic displays	40
1.7.4	Chemical Sensors	40
1.7.5	Fuel cells	40

## 2. CHAPTER TWO - AIMS AND OBJECTIVES

2.1	Polymer electrolyte network structures	42
2.2	Synthesis and characterisation of a new type polymer electrolytes	46

## 3. CHAPTER THREE - EXPERIMENTAL

3.1	Instrumentation	49
3.1.1	General notes	49
3.1.2	Differential scanning calorimetry (DSC)	50

3.1.3	Conductivity instrumentation	52
3.1.4	Preparation of polymer salt complexes	56
3.1.5	Network swelling	58
3.2	Synthesis and characterisation of vinyl ether monomers	59
3.2.1	Synthesis of mono- and divinyl ethers of oligooxy-ethylens	59
3.2.1.1	Synthesis of triethylene glycol monomethyl vinyl ether	60
3.2.1.2	Synthesis of pentaethylene glycol monomethyl vinyl ether	62
3.2.1.3	Synthesis of vinyl ether macromonomer with a mixed number of EO units	66
3.2.1.4	Synthesis of triethylene glycol divinyl ether	67
3.3	Preparation of linear and crosslinked polyvinyl ethers	71
3.3.1	Preparation of PVO <sub>3</sub>	74
3.3.2	Preparation of network polymers based on PVO <sub>3</sub>	75
3.3.3	Preparation of PVO <sub>5</sub>	77
3.3.4	Preparation of PVO <sub>5</sub> - 5 & C-L	78
3.3.5	Preparation of PVO <sub>6,7</sub>	79
3.3.6	Preparation of PVO <sub>6,7</sub> - 5 & C-L	80

3.4	Preparation of macrocyclic oligomers of ethylene oxide (CROWN ETHERS)	82
3.4.1	Facile one pot synthesis of Hydroxy-Substituted 16-crown-5	83
3.4.2	Preparation of hydroxy 16-crown-5 derivative with methylene spacer units	87
3.4.3	Preparation of hydroxy 16-crown-5 derivative with 6 methylene spacer units	91
3.4.4	Preparation of 2-hydroxy methyl 15-crown-5	95
3.4.4.1	Precursors for the preparation of 2-hydroxy methyl 15-crown-5	96
3.4.4.2	Cyclisation to produce [2-(benzyloxy(methyl))-15-crown-5	101
3.4.4.3	2-(hydroxymethyl)-15-crown-5	102
3.4.5	Preparation of 2-hydroxymethyl 12-crown-4	104
3.4.5.1	Preparation of benzyloxy methyl 12-crown-4	105
3.4.5.2	Preparation of 2-hydroxy methyl-12-crown-4	106
3.5	Preparation of polyphosphazenes with crown ether side groups	108
3.5.1	Poly[bis(trifluoroethoxy)phosphazene]	110
3.5.2	Preparation of polymers PPC1, PPC2	114

	and PFC3	
3.5.3	Preparation of the polymer PFC4	116
3.5.4	Preparation of the polymer PFC5	118
3.5.5	Preparation of the polymer PFC6	119

**4. CHAPTER FOUR -**

**POLYVINYL ETHER ELECTROLYTES**

4.1	Polymer preparation	120
4.2	Formation of polymer-salt complexes	122

**5. CHAPTER FIVE - EFFECT OF CROSSLINKING IN**

**THE A.C. CONDUCTIVITY AND OTHER PHYSICAL**

**PROPERTIES OF POLYVINYL ETHER ELECTROLYTES**

5.1	Swelling studies	125
5.2	Glass transition (T <sub>g</sub> ) studies	128
5.3	Effect of salt addition on T <sub>g</sub>	128
5.4	Effect of crosslinking on conductivity	138
5.5	Isothermal conductivity	145

**6. CHAIN EXTENDED POLYVINYL ETHER**

**ELECTROLYTES**

6.1	Introduction	157
6.2	Swelling studies	158
6.3	Glass transition temperature	161

6.4	Conductivity studies	178
6.4.1	Isothermal conductivity	180

**7. THEORETICAL TREATMENT OF CONDUCTIVITY-  
TEMPERATURE DATA**

7.1	VTF analysis and theoretical models	205
7.2	VTF analysis of the conductivity data	208
7.3	VTF analysis of the crosslinked PVO, conductivity data	209
7.4	VTF analysis of the chain extended polyvinyl ether conductivity data	212

**8. IONIC CONDUCTION IN MIXTURES OF SALTS AND  
POLYPHOSPHAZENES WITH PENDANT CROWN ETHERS**

8.1	Crown ether chemistry	225
8.2	Ionic conduction in mixtures of salts and polyphosphazenes with pendant 16-crown-5 ethers	232
8.3	The effect of spacer length on the conductivity of the <u>PPCl</u> /sodium perchlorate mixtures	239
8.4	Ionic conduction in mixtures of salts and polyphosphazenes with pendant 15-crown-5 and 12-crown-4 ethers	245
8.5	VTF analysis of the conductivity-	258



temperature data

**9. CONCLUSIONS AND FUTURE WORK**

9.1	Effect of crosslinking on polymer properties	263
9.2	The effect of chain extension on the properties of polyvinyl ethers	265
9.3	Polyphosphazene-crown ether electrolytes	266
9.4	Closing remarks and future work	267
	References	274

CHAPTER ONE

INTRODUCTION

## 1.1 Background

Plastic ion conductors appear to be the best compromise between hard solid electrolytes like  $\beta$ -alumina and liquid solvents, whose stability is limited. Polymers have mainly been developed for structural and insulating properties, and the possibility of inducing electronic or ionic conductivity as an intrinsic feature of macromolecular materials has only recently been appreciated <sup>1,2</sup>. Such plastic conductors differ from metal or carbon-filled plastics, for which the electronic conductivity is achieved through a dispersed percolating phase or from ionic gels and ion-exchange membranes, whose ionic conductivity relies upon the presence of water or a polar solvent.

For the latter compounds, a wealth of practical and theoretical literature is available; for instance, the conformation of biological polymers is dependent upon the water-mediated interaction between the charged backbone and ions. Also, ionic groups are incorporated in non-polar polymers to improve their mechanical strength<sup>3</sup>.

Here we discuss the properties and applications of solvent free polymer electrolytes obtained through the direct interaction of a salt and a macromolecule. This new class of materials was first studied by Wright et al.<sup>4</sup>, while recognition of such systems as practical

solid electrolytes, and much of the early development, was due to Armand and co-workers<sup>3</sup>.

Interest in such compounds rose rapidly after they were proposed as a new class of solid state electrolytes, especially in the area of large-scale rechargeable batteries. Attention was mainly focused on poly(ethylene oxide)-based materials, owing to their availability at various molecular weights and their attractive mechanical properties.

Current research in the field of polymer electrolytes may be divided into a number of principal areas:

(1) Synthesis of new polymers in order to form polymer electrolytes with optimised electrical, chemical and mechanical properties.

(2) Experimental and theoretical investigations directed towards an understanding of basic ion-polymer and ion-ion interactions involved in the formation of polymer electrolytes.

(3) Characterisation of the ion transport process and the development of models for its' description, and

(4) Studies of electrochemical cells based on polymer electrolytes, and development of practical devices based on them.

One of the most important steps to be taken in the

understanding of polymer electrolyte properties was the recognition by Berthier and co-workers<sup>6</sup> that ionic conductivity is a property of amorphous, elastomeric phases of PEO-salt complexes. High molecular weight amorphous polymers above their glass transition temperatures may exhibit mechanical properties which are similar in most ways to those of a true solid: this is a result of chain entanglement and cross linking of various types. At the microscopic level, however, local relaxation processes may still provide "liquid-like" degrees of freedom which are in some ways not significantly different from those in an ordinary molecular liquid. In this respect they are liquid-like, but they do not behave as normal free-flowing fluids because the molecular size reduces flow and creates visco-elastic behaviour.

Armand<sup>7</sup> has coined the phrase "the immobile solvent" to describe polymer electrolytes, since in general, ionic motion takes place with long-range net displacement of the polymer chains. There is now increasing evidence that ionic conduction takes place through the disordered part of the polymer matrix and is assisted by large-amplitude segmental motion of the polymer matrix. Fontanella and co-workers<sup>8,9</sup> have shown that for a large number of polymer-salt complexes the relaxation processes associated with the glass transition temperature ( $T_g$ ) and the ionic conductivity

have the same temperature and pressure dependence.

Polymer electrolytes offer at least the following advantages over materials containing liquid components:

- (1) Negligible vapour pressure
- (2) No transport of solvent along with ion
- (3) No long range mobile components except for ions
- (4) Suitable support for a thin film electrode.

The best known ion-solvating polymer is poly(ethylene oxide) (PEO) which can combine with a multitude of inorganic, organic and even polymeric<sup>10</sup> salts to form ion-conducting solutions in which the solvent is an elastomer.

These types of ion-containing polymers will be the subject of the remainder of this chapter. The following sections will discuss the chemistry and physical properties of polymer solvents and their complexes upon adding salt; the nature of the conduction process which is distinct from that understood to operate in liquids, solids or glasses; experimental methods used to determine the conductivity and transport processes; improvement of ionic conductivity by polymer modification, emphasising the role of glass transition temperature ( $T_g$ ) and finally the last section will outline the projected applications which has been the main stimulus for research in this area.

The literature on ion-conducting polymer systems has expanded profusely in the last decade, and detailed reviews and collections of papers may be found in a number of recent books and conference proceedings<sup>11-14</sup>.

## 1.2 Developments in Solvent-Free Polymer Electrolytes

### 1.2.1 Poly(ethylene oxide) chemistry

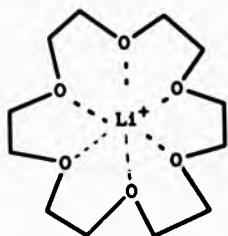
Electrolytes consisting of solid solutions, that is, solvating aprotic polymers containing metallic salts, fall into the category of charged polymers. Among research workers, Wright et al.<sup>4</sup> as early as 1973 reported the existence of crystalline complexes formed by poly(ethylene oxide) and various alkaline salts and pointed out that such complexes had a significant degree of conductivity. Since then, Armand suggested that aprotic electrolytes could be used in all solid lithium batteries<sup>2,20</sup>, launching an idea that has stimulated an ever-growing number of studies and development projects focused especially on polymers derived from ethylene oxide and their possible application in batteries.

There are several reasons for such popularity. From the chemical viewpoint, inertia of the ether function,

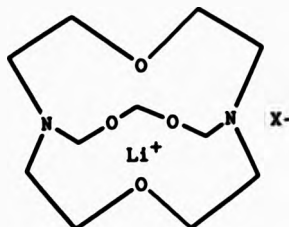
C-O-C, is an important property for liquid organic electrolytes. Polymers such as PEO show a higher stability of the ether functions than cyclic ethers (crown ethers) due to the absence of strain and, what is more, this stability is favoured kinetically by the solid state in the absence of convection. This gives the EO oxide chain enough flexibility to allow cation solvation by cage effect, which involves several donor heteroatoms. Neither the polyoxymethylene,  $-(CH_2)-$  which is rich in donor atoms but has a more rigid chain, nor polyoxacyclobutene  $-(CH_2CH_2CH_2O)-$ , with its flexible chain but more widely dispersed donor groups, possesses solvation properties equivalent to those of the PEO chain.

The solvation capacity of PEO chains is due to the multidentate nature of intermolecular solvation, enhanced by entropy, and is also a result of the chains ready ability to adopt a cage configuration in which the donor electrons of the oxygen are directed inward<sup>21</sup>. This solvation mechanism is well known for crown ethers, or cryptands, in which cages of synthetically predetermined size can specifically solvate cations of the corresponding radius as shown below:





18-Crown-6  
(2.6-3.2 Å cavity size)



Cryptand-211

The advantage of the linear chains of PEO in the fabrication of a polymer electrolyte is that they can form solvation cages that can self-adjust fairly well to the size of the cation. This solvation mechanism, which is at least partially intramolecular, is also reversible and can take into account the presence of ion pairs or even triplets, quadruplets or other complexes. Various degrees of participation of EO chains in cation solvation are therefore possible as illustrated in Figure 1.2.1.

The diversity and reversibility of the various possible conformations of PEO chain segments around cations also allow the latter to migrate from one solvating site to another.

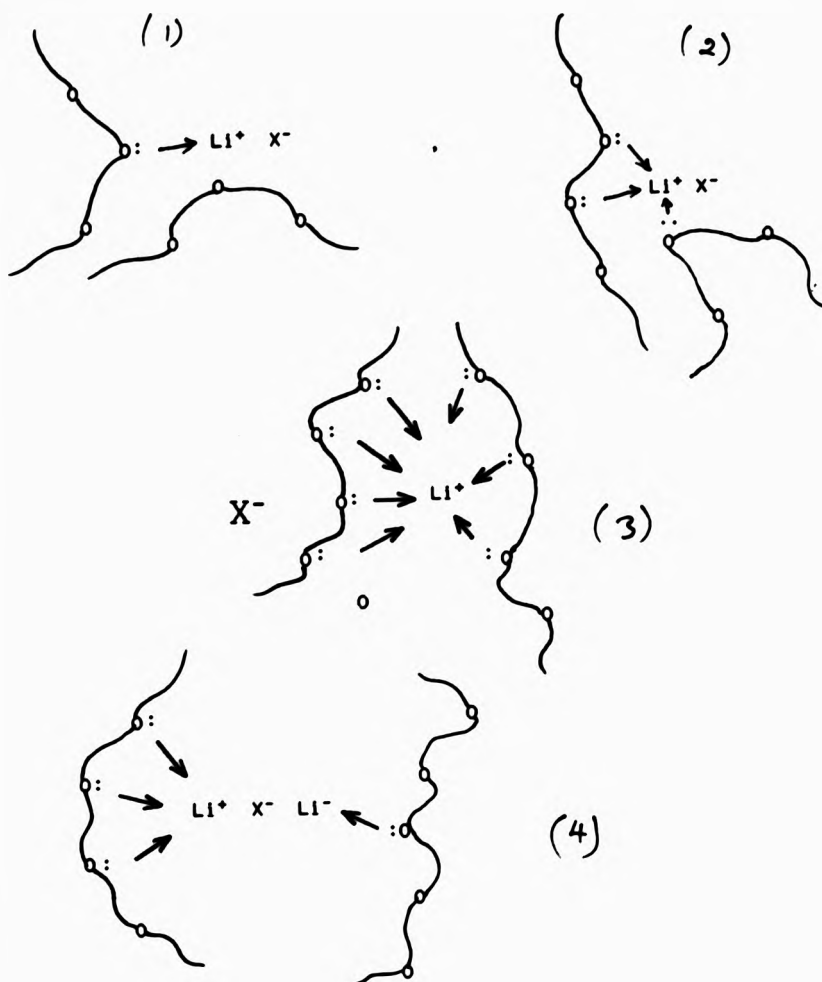
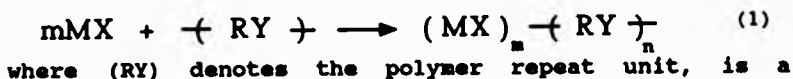


Figure 1.2.1 Illustration of conformational flexibility of line polyethers enhancing ion solvation

### 1.2.2 Formation of Polymer/Salt Complexes

The polymer electrolytes with which we are principally concerned are the complexes of alkali metal salts, denoted by MX, with polymer hosts. Both the precursor and the neat polymer are solid, so that the complex-forming reaction



where (RY) denotes the polymer repeat unit, is a solid/solid reaction. As with most other reactions of this type, the kinetics of (1) are unfavourable, even when the complex is stable. Although other schemes for accelerating (1) have been employed, including intimate grinding/mechanical mixing<sup>99</sup>, by far the most common method has been to dissolve or suspend both the MX salt and the host polymer in a common solvent and then to remove the solvent, producing the solvent-free polymer electrolyte in either bulk or thin-film form.

Care must be taken to purify the starting materials and (especially in the case of hygroscopic lithium electrolytes) to exclude water. Acetonitrile and methanol have been the solvents most commonly used. If the polymer-salt complex is partly crystalline, both the morphology and the transport properties of the electrolyte material produced may vary with choice of solvent.

For polymers the loss of transitional entropy caused by ion solvation is likely to be much less than that of the low molecular weight solvents, especially in situations where an ion is solvated by neighbouring coordination groups on the same chain. The entropy of solution will in general be positive, but fairly insensitive to variation of the salt. The solvation process is thus dominated by enthalpy changes, i.e. salts dissolve only in those polymers for which exothermic ion-polymer interactions compensate to a significant extent for the lattice energy<sup>15</sup>.

Specific anion solvation is known to arise mainly as a result of hydrogen bonding, but polymers in which a fraction of the hydrogen atoms bear a net positive charge, as when attached directly to an electronegative element, e.g. in polyacohols and polyamides, show extensive chain to chain interactions.

These interactions result in a high cohesive energy, and thus such polymers are quite an unfavourable media for diffusion in the absence of a aprotic, high dielectric constant plasticiser (water). In addition, labile hydrogen would be electronegative over a large range of chemical potentials, thereby reducing the use of materials for battery applications. Since the majority of polymer electrolytes have no hydrogen-bonding capabilities, the enthalpy of solvation is primarily a result of electrostatic interaction

between the positive charge on the cation and the negative end of dipolar groups belonging to the polymer, or partial sharing of a lone pair of electrons on coordinating atoms in the polymer, leading to the formation of a coordinate bond. In the absence of d-orbital involvements, the order of stability for the common coordinating group is



The various factors governing the formation of solvating polymer-alkali metal salt complexes have been determined by Chabagno<sup>2,139</sup>. As a rule, the competing phenomena are, on the one hand, the solvating power of the polymer, which promotes salt dissociation, and, on the other hand, the high lattice energy or cohesive energy values of the original products, which play the opposite role. The determining influence of the lattice energy has been clearly established by Shriver, who pointed out that in the case of salts with very high lattice energies, complexes are not usually formed.

The acceptable thresholds are nevertheless dependent on the cation used, since the latter also conditions the solvation energy of the complex. For example, a high threshold of -880 kJ/mol is acceptable for lithium salts because this cation has a strong polarising power with respect to the PEO. Dissolution of the salt to form a

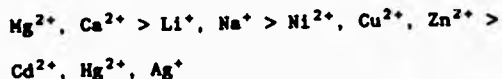
complex is governed by Lewis acid-base interactions, which are similar to those of polymers.

### 1.2.3 Salt characteristics

Until recently the great majority of polymer electrolyte studies were concerned with salts of alkali metals in PEO, and a simple approach of this type was adequate. With the recent interest in salts of alkaline earth and transition metal ions, a more comprehensive theory of ion-solvent forces must be used. The HSAB principle<sup>24,25</sup> recognises as hard bases molecules such as the ethers and certain amines which have donor atoms with high electronegativity but low polarisability. Polyethers are examples of soft bases which hold their electrons less firmly and are highly polarisable. Cations which may be characterised as hard acids have a small size, no unshared electron pairs in the valence shell and, in general, have low polarisability. In contrast, cations which are large, polarisable and have unshared pairs of electrons, act as soft acids. It is found that the most stable complexes are formed either by hard acids reacting with hard bases or by soft acids reacting with soft bases.

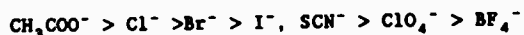
PEO may be regarded as a hard polybasic molecule. Of the complexes most studied, the hardness of the

constituent cations may be roughly placed in the order as follows:



Thus  $\text{Mg}^{2+}$  would be expected to form a very strong complex with PEO, while  $\text{Hg}^{2+}$  would interact only weakly with the hard ether oxygen. Note that the ability of a cation to form a stable complex, while enhancing the probability of dissolution of its salts in coordinating polymers, may also result in its low mobility. This area has been discussed further by Bruce et al<sup>26</sup>.

So far as the anions are concerned, there is considerable evidence to suggest that in dipolar aprotic solvents, including low molecular weight ethers, specific anion solvation is absent. The less important general solvation energies of anions do change as the solvent dielectric constant is varied, with destabilisation occurring on passing from polar to less polar media. This destabilisation is directly related to the charge density and basicity of the anion<sup>27</sup>:



Large "soft" anions such as  $\text{ClO}_4^-$  or  $\text{BF}_4^-$  which have low ion-dipole stabilisation energies, but relatively large energies of solvation due to mutual polarisability, are therefore likely to be the 'most

suitable choice for polymer electrolytes.

Table 1 lists most of the salts used to form lithium conducting electrolytes. When the electrolyte is to be used in a rechargeable battery, however, the number of available salts is far more limited. Various families of salts have been suggested<sup>28</sup>, to reconcile the stability, conductivity and redox stability requirements for polymer electrolytes. So far, only  $\text{LiClO}_4$  and  $\text{LiCF}_3\text{SO}_3$  have been used in rechargeable battery applications and, in fact, constituted the only salts recognised as fulfilling the electrochemical stability criteria and offering adequate conductivity. Recently, however, new salts have been successfully tested as substitutes for  $\text{LiClO}_4$  in high power cells applications<sup>29</sup>.

PEO metal salt complexes are now formed from a much wider range of products than the alkali metals and anions originally considered. Today, complexes involving alkaline earth salts and transition metals are known<sup>30-32</sup>, especially as a result of research on batteries<sup>33,34</sup>.

#### 1.2.4 The effect of salt addition on polymer electrolytes

On addition of a salt to a polymer, any interaction which occurs between the two species can be detected by



Table 1 List of salts proposed for Polymer-Lithium salt electrolytes.

<u>Common lithium salts:</u>	LiCl, LiBr, LiSCN, LiClO <sub>4</sub> .
<u>Monovalent anions</u>	: LiBF <sub>4</sub> , Li(C <sub>5</sub> H <sub>11</sub> -CmC) <sub>4</sub> B, Li(C <sub>4</sub> H <sub>9</sub> -CmC) <sub>4</sub> B, Li(C <sub>6</sub> H <sub>5</sub> -((CH <sub>2</sub> ) <sub>3</sub> -CmC) <sub>4</sub> B, R-COO-CH <sub>2</sub> CH <sub>2</sub> -SO <sub>3</sub> Li (R is non-solvating polymer chain)
<u>Divalent anions</u>	: LiB <sub>10</sub> Cl <sub>10</sub> , Li <sub>2</sub> B <sub>12</sub> Cl <sub>12</sub> , Li <sub>2</sub> B <sub>12</sub> H <sub>12</sub>
<u>Fluoride compounds</u>	: LiCF <sub>3</sub> SO <sub>3</sub> , LiC <sub>4</sub> F <sub>9</sub> SO <sub>3</sub> , LiC <sub>6</sub> F <sub>13</sub> SO <sub>3</sub> , LiCF <sub>3</sub> CO <sub>2</sub> , LiBF <sub>4</sub> , LiAsF <sub>6</sub> , LiN(CF <sub>3</sub> CO <sub>2</sub> ) <sub>2</sub>
<u>Divalent anions</u>	: LiOOC(CF <sub>2</sub> ) <sub>3</sub> COOLi, LiSO <sub>3</sub> (CF <sub>2</sub> ) <sub>2</sub> SO <sub>3</sub> Li

examination of certain physical properties of the polymer before and after incorporation of the salt. In addition to changes noted in the specific volume<sup>35,36</sup> and the viscosity<sup>35,37-40</sup> of the polymer, it is known that the addition of a salt to a polymer can have a profound effect on the temperature of the glass to rubber transition ( $T_g$ )<sup>36,41-49</sup>.

In amorphous polymers, below  $T_g$ , the free volume or unoccupied space in the polymer, which arises due to inefficient packing of the disordered chains, attains a particular value and remains constant as the temperature is reduced<sup>50</sup>. Alternatively, the configurational entropy of the system is limited at temperatures below  $T_g$ <sup>50</sup>. As the temperature is increased above  $T_g$ , the free volume or configurational entropy of the system increases with temperature and with a specific temperature increase above  $T_g$ , the polymer will possess a particular free volume or configurational entropy, relative to that present at  $T_g$ . This temperature increase is known as the reduced temperature.

$T_g$  is therefore the temperature above which long range segmental motion is possible in the polymer and the material changes from being in a glassy state to a rubber as the temperature is increased<sup>50</sup>. (In the glassy state, the polymer chains are frozen in a disordered state and only localised motions are possible within the matrix). At  $T_g$ , dramatic changes occur in the physical

properties of the polymer, and marked discontinuation can be noted in the specific volume, modulus, heat capacity and refractive index.

The Tg of the polymer is highly dependent on the chemical structure of the material<sup>50</sup>. Non-flexible units in the polymer chain, bulky side groups, dipole-dipole interactions between adjacent chains or crosslinks between the chains will hinder the movement of the polymer backbone and the Tg will be measured at a higher temperature since the temperature at which the Tg occurs reflects the energy required to overcome the rotational barriers in the polymer chain backbone.

The transition from a glass to a rubber is completely reversible in an amorphous polymer but the precise temperature which is measured for Tg is dependent on the experimental method used and the rate of heating or frequency of analysis.

In almost all of the polymer/salt complexes studied, it has been reported that interactions occurring between the polymer and the salt resulted in the Tg of the polymer increasing. If an ion can interact simultaneously with coordinating groups on two polymer molecules (or with two remote sites on the same polymer chain) then transient inter (and intra) molecular crosslinks will be formed which will have an effect on the segmental motion of the polymer chains and consequently on the mobility of ions.

This idea of ions acting as transient crosslinks which affect polymer properties was termed "physico-chemical crosslinking" by LeNest et al., who have discussed it in detail<sup>51</sup>. However, it should be noted that Cameron and co-workers<sup>52</sup> suggest that intermolecular crosslinks are more likely to involve solvated-cation-free anion/solvated-cation links rather than direct polymer/cation/polymer groupings.

### 1.3 Electrolyte theory and conductivity studies in polymer/salt complexes

#### 1.3.1 The origin of electrolyte theory

A true solid electrolyte, similar to an aqueous electrolyte, is a phase which has electric conductance wholly due to ionic motions within the solid lattice. The electronic contribution, by definition, should be negligible. It is the transport of ions which distinguishes electrolytes from electronic conductors where the current is carried entirely by electrons and this involves no transport of matter<sup>52, 53</sup>. Considering initially aqueous electrolytes, it is known that on addition of an acid, base or salt to water, they become spontaneously dissociated into positive and

negative ions



The degree of dissociation ( $k$ ) is the fraction of the total electrolyte which is split into ions and is almost constant at unity in strong electrolytes throughout the concentration range. In a weak electrolyte, the proportion of the molecules which dissociate into ions varies with the concentration of the solution only at infinite dilution.

In the absence of an electric field, the ions in solution are free to move independently, but during electrical conduction the ions are attracted to the electrode of opposite charge by the applied field. Consequently, the passage of current in an electrolyte is accompanied by a transport of matter due to the motion of positive and negative ions<sup>33</sup>.

The conductivity of an electrolyte at a particular temperature may be written as:

$$\sigma(T) = \sum_i n_i q_i \mu_i \quad (3)$$

where  $n_i$  is the number of charge carriers of type  $i$  in unit volume,  $q_i$  is the charge on each and  $\mu_i$  is the ionic mobility (i.e. the net velocity in unit field).

For a monovalent salt, the assumption that the

charge carriers in the electrolyte are generated only from the incorporated salt, equation (3), can be written as follows<sup>34</sup>:

$$\sigma = n_+ e\mu_+ + n_- e\mu_- = ne(\mu_+ + \mu_-) \quad (4)$$

where  $n_+$  and  $n_-$  are the number of cations and anions respectively solvated in the system and equal  $n$ , and  $\mu_+$  and  $\mu_-$  are the ionic mobilities of these charged species respectively. The ionic mobility  $\mu$  is related to the ionic diffusion coefficient  $D$  by the Nernst-Einstein equation<sup>34</sup> as shown below:

$$\mu = \frac{zeD}{KT} \quad (5)$$

where  $K$  is the Boltzman constant.

Assuming that the electronic conductivity is negligible, transport numbers are used to define the fraction of the total ionic current that is carried by particular ionic species. The cationic transport number ( $t_+$ ) and anionic transport number ( $t_-$ ) should add together to give unity and  $t_+$  and  $t_-$  are related to  $\mu$  and  $D$ <sup>35</sup> since

$$t_+ = \frac{\mu_+}{(\mu_+ + \mu_-)} = \frac{D_+}{(D_+ + D_-)} \quad (6)$$

### 1.3.2 The measurement of ionic conductivity and other transport properties

In electrochemistry, conductivity is a very important property, especially of an isolated electrolyte. It is not possible to measure the conductivity of an isolated electrolyte. Instead, a test cell has to be used, in which the electrolyte is sandwiched between a pair of contacting electrodes. The property that is then measured pertains to the whole assembly, i.e., to the electrolyte plus the attendant instrument leads, electrodes and interphases.

The electrodes can be blocking, i.e., incapable of acting as source or sink for the ions that traverse the electrolyte, or non-blocking, in which case ions can cross the interphase. For blocking electrodes, the current is carried by electrons along the leads to and from the instrument into the electrodes: through the electrolyte, the charge is carried by ions. The link at the interphases, between the two types of separated charge carrier is double layer capacitance.

In practice, direct current measurements are rarely used because the influence of a constant applied potential sets up a concentration gradient of ions. When equilibrium is reached, the chemical potential caused by this gradient is exactly sufficient to nullify the effect of the applied voltage and no current flows. The

test cell is said to be concentration polarised.

Two types of a.c. techniques are normally employed. Most older studies used a constant frequency technique to overcome the effect of concentration polarisation. The problem with this approach is that there is no real means of separating the contributions of the electrolyte from those of the other components in the test cell. In consequence, it is now more common to carry out measurements at variable frequency which has been described elsewhere<sup>56,57</sup>. However, for the purposes of this work, it is adequate to note that the current passing through the test cell and the voltage across it are both measured as a function of frequency. Since the test cell contains capacitance (and perhaps also inductive) components as well as resistance, the impedance,  $Z$ , rather than resistance,  $R$ , is obtained. The impedance is given by

$$Z = R - [j/(\omega C)] + j\omega L \quad (7)$$

where  $C$  is the capacitance and  $L$  is the inductance,  $\omega$  is angular frequency and  $j$  is the square root of  $-1$ .

The measurements are obtained at a series of frequencies which typically may range as low as  $10^{-4}$  to as high as 10 MHz. From the data it is possible to extract the conductivity and dielectric constant of the bulk electrolyte sample.

Information on the resistance to interfacial charge



transport can also be determined. This analysis follows on the lines originally proposed by Cole<sup>56</sup> and developed in detail by MacDonald<sup>57, 58</sup>.

### 1.3.3 Identity of charge carriers

The identity of the charge carriers and the fraction of the current carried by each is a more subtle issue that is still not resolved in most studies of solvent free polymer electrolytes. This issue was addressed by physical chemists around the turn of the century for liquid electrolytes. They devised simple but elegant methods for the determination of transference numbers, which are generally designated as  $t_+$  or  $t_-$  for the fraction of current carried by the cation and anion respectively<sup>59</sup>.

The measurement of transference numbers, or transport numbers as they are also called, is experimentally more difficult with the solid electrolytes than their solution counterparts<sup>15</sup>, but measurements of fair quality have been made and the general picture for a variety of polymer electrolytes is that somewhat over half of the current is carried by the anion and therefore less than half by the cation.

A major issue that is not yet well understood is the nature of the mobile species. With monovalent ions in

dilute aqueous solution the isolated cation and anion are the charge carriers. But the much lower dielectric constant of the polymer host in the solvent-free polymer electrolytes should be conducive to strong coulombic interaction between ions.

In the salt concentration range generally studied, the primary charge carriers may well be ion triplets, quintets and so on. A number of detailed studies of ion transport in fluid solutions of short chain PEO, provides a strong evidence for the importance of ion clusters in the solid electrolytes<sup>60-69</sup>.

#### 1.3.4 Conductivity studies in polymer salt complexes

Undoubtedly, the most studied characteristics of polymer electrolytes is ionic mobility in general and the net transport of ions in an electric field in particular. Conductivities have been measured as a function of salt type, concentration and temperature in most of the systems studied.

Originally, the ionic induction observed for PEO-salt complexes was explained by means of a model based first on the helical channel structure and the conduction mechanism in crystalline solids<sup>19</sup>. Specific cation conduction by a hopping mechanism within the

helical solvating structure was postulated. The model as such is no longer used to explain the conductivity of PEO-salt complexes, since the classic study of Berthier et al<sup>6</sup> which established that significant ionic mobility in polymer electrolytes is a property of an amorphous phase above the glass transition temperature. It has been recognised that for such phases the temperature dependence of the ionic conductivity roughly obeys a Vogel-Tannan-Fulcher(VTF)<sup>148-150</sup>/William-Landel-(WLF)<sup>70-72</sup> type of relationship and that the overall charge transport process is closely correlated with the visco-elastic properties of the host polymer. It is important to realise that the equations of the form

$$\sigma(T) = AT^{-1/2} \exp \left[ \frac{E_a}{R(T - T_0)} \right] \quad (7)$$

or

$$\sigma(T) = A \exp \left[ \frac{B}{(T - T_0)} \right] \quad (8)$$

or the mathematically equivalent

$$\ln [\sigma(T)/\sigma(T_0)] = \frac{C_1 (T - T_0)}{C_2 + (T - T_0)} \quad (9)$$

where A, E<sub>a</sub>, B, C<sub>1</sub> and C<sub>2</sub> are fitted constants and T<sub>0</sub> is a temperature related to the T<sub>g</sub>, and are essentially empirical in nature.

It is almost always straight forward to obtain a

reasonable fit to experimental data for amorphous phases, especially if the temperature range examined is relatively small. However, significant discrepancies can arise when analysis is carried out over different temperature ranges, as has been pointed out by Greenbaum<sup>73</sup>. Careful inspection of the data reveals that conductivity values are more Arrhenius-like at temperatures considerably above  $T_g$  than is predicted by VTF-type equations<sup>73-75</sup>. This implies that high temperature measurements tend to give relatively high values of  $E_a$  or  $B$  and low values of  $T_0$ .

The inclusion of  $T^{-1/2}$  term in the pre-exponential is a consequence of the takeover of the original VTF viscosity equation: for the temperature range accessible for polymer electrolytes, it is generally impossible to distinguish between equation (7) and (8), in terms of statistical significance, so that equation (8) or (9) seem preferable on the grounds of simplicity.

Most workers fit the equation to their data using 3 independent parameters (e.g.  $A$ ,  $B$  and  $T_0$ ) but  $T_0$  is sometimes treated differently. This parameter is given particular significance in theoretical treatments: for instance, in the configurational entropy model it refers to the temperature at which the probability of configurational transition tends to zero, as defined by Gibbs and di-Marzio<sup>71</sup>. This can be related to the experimental  $T_g$ , which can normally be substituted for

$T_g$  in the equations (7), (8) or (9).

The VTF representation of the conductivity data offers the advantage of emphasising the role played by  $T_g$  in conductivity and suggesting ways to optimise the conductivity by decreasing  $T_g$ . Meanwhile, several approaches are known for modifying the  $T_g$  of an electrolyte and thus improving its conductivity. The nature and concentration of salt, for example, have a considerable effect on  $T_g^{6,60}$  while various chemical and physical modifications to the solvating polymer are also possible.

Several other parameters strongly influence the conductivity of PEO-based electrolytes. For example, the real degrees of dissociation of the salt and the nature of the different species formed have an effect on  $\lambda$ , the term corresponding to the carrier concentration. The coexistence of amorphous and crystalline phases also affect the conductivity.

#### 1.4 Improvement of conductivity by polymer modification

Studies of PEO-LiX complexes demonstrate very clearly that ionic conductivity is present in the amorphous phase, not in the crystalline phases. On the one hand, conductivity in the electrolyte seems to

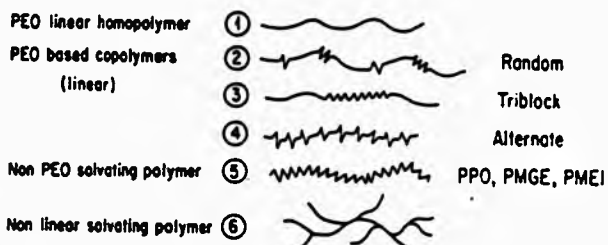
depend on the mobility of the polymer chain segments, as characterised by low Tg. On the other hand, the ion carrier concentration depends not only on the salt concentration but also on its degree of dissociation which is related to the dielectric constant of the polymer.

Optimization of Li-conducting polymer electrolytes for room temperature applications can, therefore, be achieved by modifying the solvating polymers in the electrolytes.

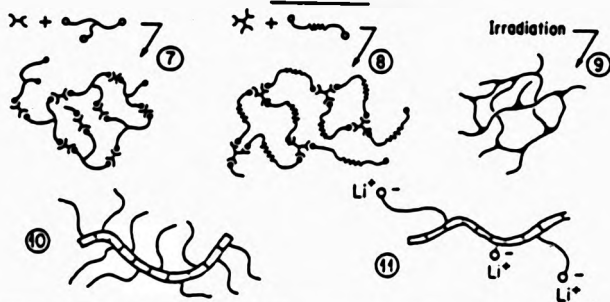
Considering the outstanding redox windows of PEO complexes and the high solvating power of the basic monomeric units ( $\text{CH}_2\text{CH}_2\text{O}$ ) (EO), it seemed that the first modification step would be to try to improve this electrolyte family by changing the properties of the EO chain. However, the changes envisaged should not jeopardise the electrochemical stability of the ether functions nor the solvating power of the EO segments. A rough classification of the modifications proposed for polyethers is presented in Figure 1.4.1.

#### 1.4.1 Crystallinity reduction

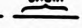

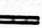
The stereo-regularity of the linear PEO chain means it has a high degree of crystallinity (80%). The melting



**NETWORKS**



**CHAIN UNITS**

CHAIN UNITS	Polymer chain	
a) EO solvating unit		a = Ethyl. oxide -CH <sub>2</sub> CH <sub>2</sub> O
b) Non EO solv. unit		b = Prop. oxide, aziridine, ester...
c) Non solvating unit		c = -CH <sub>2</sub> O-, -CH <sub>2</sub> -C(=O)-, -Si-O-, -P(=N)-COOR

**LINKAGES**


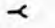


LINKAGES	Chemical formation	Polycondensation, vulcanization
Physical formation		1 <sup>st</sup> reactive endgroup (CH, insaturation)
-C-C- bond		+
Thermosetting, R <sup>+</sup>		2 <sup>nd</sup> reactive group (-NCO, -COCl, -Al-R)
Irradiation.....		↓
		Result linkage (urethan, ester, alumoxane...)

Fig. 4 | Examples of polymer derived from ethylene oxide (EO) configurations:

F.3.141 (Continued)

1. PEO = good solvation, high conductivity at  $>80^{\circ}\text{C}$ , room-temperature crystallization
2. Crystallinity reduction due to chemical disturbance
3. Crystallinity reduction due to chemical disturbance
4. Crystallinity reduction due to chemical disturbance
5. Less crystallizable monomer unit resulting in amorphous (but less solvating) polymer at room temperature
6. Structural disturbance: reduced crystallinity
7. PEO-based triol + diisocyanate polyurethane network
8. Triblock OE.OP.OE diol + triisocyanate (or + AIR3) polyurethane (or alumoxane network)
9. Physical crosslinking (gamma-radiation, free radicals)
10. Nonsolvating (low  $T_g$  ?) backbone ( $-\text{SiO}-$ ,  $-\text{P}=\text{N}$ , butadiene) with solvating sidechains (comb-like polymers)
11. Autoionizable polymers:  $-\text{O}^-$  strong anionic groups;  $\text{Li}^+$  associated lithium ion



point for high molecular weight ( $>10^6$ ) is 338 K,  $T_g$  is 213 K, and the density is 1.15. The high crystalline nature of pure or complexed PEO can be observed by the naked eye in the form of spherulites, which sometimes reach up to 1-3 mm on thin films (see ref. 77, as an example).

Crystallinity can be reduced in various ways; chemically, structurally and by combination of these methods, as explained below:

i) **Chemical approach:** It is possible to create disorder in EO chains by introducing one or several monomers or different sequences of the EO. These defects can be solvating or not, and can be distributed statistically, alternately or sequentially. This is the very basis of copolymers, examples of which are given in the literature<sup>49,77-80</sup>, and schematically illustrated in Figure 1.4.1.

The positive effects of reduced crystallinity usually become visible at temperatures below 333 K, and the published data tend to give room temperature conductivities of the order  $1-5 \times 10^{-5}$  compared to  $10^{-7} - 10^{-8} \text{ Scm}^{-1}$  for equivalent PEO-complexes.

ii) **Structural approach - non-linear structures**

PEO crystallinity can be reduced if the polymer has side chains or if it corresponds to a starlike structure. In these cases, the side chains remain free and the polymer is theoretically soluble (non-reticulated). A few examples can be found in the literature<sup>2,3</sup> while Figure 1.4.1 presents some conceptual possibilities.

### iii) Structural approach - crosslinked structure

Chemical or physical crosslinking represents a powerful means of preventing the crystallisation of PEO chains. From a practical point of view, it gives the network elastomeric properties which oppose the tendency of the electrolyte to creepage, as is the case for polymers with low T<sub>g</sub>s. Electrolytes consisting of polyether (PEO or PPO) networks and alkali metal salts have been studied systematically by Cheradame et al<sup>52,63,65,66,84</sup> and by Watanabe et al<sup>59,85-87</sup>.

The linkage agents employed are usually multifunctional isocyanates and substituted silanes. In these studies, the starting polyethers (PEO, PPO) have low molecular weight (400-10,000) and are present as homogeneous block type diols, or triols (see fig. 1.4.1).

Other chemically prepared polyethers have been proposed, sometimes with the purpose of reducing the

volumetric fraction of the reticulation nodes to improve conductivity. Fig.1.4, presents an example of the crosslinking of linear PEO by physical means. In ref. 88, gamma irradiation is performed at high temperature in order to fix the amorphous state which favours conductivity at low temperatures.

#### 1.4.2 Reduction of Tg

**Chemical Approach:** The relationship established between conductivity and Tg suggests that research would be worthwhile now on solvating polymers with very low Tg. Polyoxanes and polyphosphazenes have chains that offer very high flexibility, allowing cooperative polymer conformation fluctuations as needed for cation solvation and mobility. However, these chains do not have the required solvating power to form conducting complexes with salts. Oligomeric oxyethylene or oxypropylene groups are therefore attached to the polymer which acts as an inert backbone. Blonsky et al.<sup>41,89,90</sup> have described amorphous polymer electrolytes, based on substituted poly(dichlorophosphazene)s. The best known of these, poly[bis(methoxy ethoxy oxide)]phosphazene is known as MEEP.

Siloxane based comb-branched block copolymers have

been described by Shriver et al., Ward et al. and more extensively by Smid et al.<sup>92,93</sup>.

Methacrylate-based systems have been described by Zia et al<sup>93,94</sup>, by Bannister et al<sup>95</sup>, and by Tsuchida et al<sup>95</sup>. A related system, but with higher side chain density, based on poly(itaconic acid) has been studied by Cowie and Martin<sup>96,97,100</sup>. The latter workers have also studied the analogous comb branched system with PPO side chains<sup>102</sup> and the comb shaped polymers based on ethylene oxide macromers prepared from a vinyl ether monomer consisting of three oxyethylene units with a terminal methoxy group<sup>102</sup>.

For all the oxyethylene-based comb structures,  $n$ , the number of repeat units in the branches, is important. Studies have been undertaken in which this number has been varied from 2 to 20. For high values of  $n$ , a crystallisation exotherm is generally noted for the polymer host itself; crystalline salt complexes are also observed for higher values of  $n$ , depending on the salt used and its concentration. On the other hand, the  $T_g$  decreases (with subsequent increase in ionic mobility) as  $n$  is raised<sup>96</sup>.

Optimum behaviour, therefore, requires a compromise value for  $n$  which will provide adequate segmental mobility without an undue tendency to form crystalline phases.

Vincent and co-workers<sup>103,104</sup> have studied polymer

electrolytes based on structural variation on the comb-branched copolymer architecture derived from a long-block ABA copolymer with side chains polyoxy-ethylene sequences grafted on the B block to provide the ion solvating medium.

### 1.5 self-ionisable polymer electrolytes

Conductivity criteria : Marked anion mobility in electrolytes made from a charged polymer salt complex, similar to those described above has a negative effect on the energy efficiency of a battery. Various attempts have been made to curtail such mobility by increasing the size of the anions<sup>33,34</sup> , their chain length<sup>33,33,105</sup> or their electric charge<sup>33,34</sup> . But most results are disappointing; either the anion still has a high mobility, independent of it's chain length<sup>105</sup> , or the electrical conductivity obtained is too low because the salt dissociation is insufficient<sup>33,34,83</sup>.

The best way to immobilise the anion is to fix it on the polymer chain as is the case of the polyelectrolytes. The basic criteria to be fulfilled by polyelectrolytes in order to constitute dry solid electrolytes that are good conductors are:

1. Simultaneous presence of ionic groups with a fixed anion, along with cation-solvating groups.

2. Choice of dissociable ion pairs for enhanced ionisation of the salt (anionic groups derived from acids).

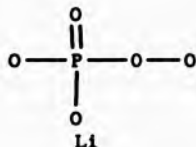
3. Sufficiently large number of ionisable groups and solvating functions to encourage cation displacement and conductivity values of the order of  $10^{-5} \text{ Scm}^{-1}$  at room temperature.

4. Suitable flexible solvating chains for cation solvation and migration at fairly low Tg.

5. Chemical and electrochemical stability of the various elements of the electrolyte for the intended applications.

Very few results have been published on self-ionising lithium conductors. LeNest<sup>106</sup> and Leveque<sup>83, 107</sup> have synthesised polyelectrolyte networks that use the ether functions (EO) as solvating groups. The ionic groups proposed are of the type:

Phosphate



Lewis acid lithium alcoholate complexes  
(e.g.  $\text{R}-\text{SbCl}_2\text{Li}^+$ ), perfluorocarboxylates  
(e.g.  $-(\text{CF}_2)_n-\text{COOM}$ )

Banister<sup>33</sup> has described a somewhat different approach, which involves mixing a polyether (solvating part) with the lithium salts of anionic polymers. Providing that molecular weights are sufficiently high and anions are derived from strongly acidic polymers, the mixture with PEO yields an entirely cationic conducting electrolyte. A comb-like polyether characterised by a methacrylate chain coreculated with sodium methacrylate has also been proposed specifically for cationic polymers<sup>108</sup>.

A specific cationic conductivity can be obtained with these electrolytes, but applications are limited, either because the conductivity is low or because the electrolytes are not electrochemically stable. The compatibility of the chemical reactions involved together with the difficulty in matching the various factors needed to reach the required conductivity, donor numbers, chain flexibility and cation mobility between sites, must nevertheless be assessed in terms of the advantages to be gained (in terms of battery performance, for example).

These types of electrolytes seem to present the ultimate as far as the future generations are concerned.

## 1.6 Increased solvating capability and polymer polarity

The solvating power of the polymer chain unit (CH<sub>2</sub>-CH<sub>2</sub>-O) and the degree of dissociation of the dissolved salt can be increased by replacing the oxygen by other donor heteroatoms such as Nitrogen or Sulphur. At the limit, other organic groups can be used instead of the ether functions.

### 1.6.1 Polyimines

The use of Nitrogen on a solvating monomeric unit of the type (CH<sub>2</sub>-CH<sub>2</sub>-NR) favours cation coordination because of the high donor number of amine functions: DN=61 for triethylamine as compared to DN=20 for the THF or 22 for PEO. The use of (CH<sub>2</sub>-CH<sub>2</sub>-NR) monomeric units in Lithium-conducting polymer electrolytes has been envisaged<sup>109,110</sup>, but the conductivity values reported so far are disappointing.

### 1.6.2 Poly(alkylene) sulphides

These sulphides, including the (CH<sub>2</sub>-CH<sub>2</sub>-S) monomeric unit, do not form complexes with Lithium salts<sup>111</sup>. Shriver et al. attribute these results to differences in



the conformation of PES and PEO chains due to the C-O and C-S bonds, and to the van den Waals radii of Oxygen Sulphur.

### 1.6.3 Polyesters and other solvating polymers

The formation of polymer-salt complexes has been demonstrated using poly(ethylene succinate) and poly(ethylene adipate) with Lithium salts<sup>88,112,113</sup>. These complexes have a strong concentration of polar groups, but their Tg values are equivalent to or higher than that of PEO. Crystalline complexes exist but, as with PEO, the conductivity is limited to the amorphous phase and is significantly lower than the value observed for PEO-containing electrolytes.

The dielectric constant, which is probably higher for these polar polymers than for PEO, should have a favourable effect on both the degree of salt dissociation and the conductivity. However, this is not observed because it seems to be masked by the effect of high Tg values on conductivity as well as the high cohesive energy of these polymers.

### 1.7 Application of solid polymer electrolytes

Research on lithium-conducting polymer electrolytes began in the context of 1970 world energy problems. For this reason, it's main goal from the outset was the development of rechargeable high-energy density batteries particularly for transportation purposes (electrical vehicles). The orientation was to determine the technical objectives and the materials selection criteria. Polymer electrolytes obviously had to meet fundamental basic and technological requirements if these objectives and criteria were to be fulfilled.

The initial focus of research on polymer electrolytes was on commercially available PEO. At high temperature, the conductivity of PEO complexes seems adequate to meet the power density requirements of electrical vehicles. This approach was adopted both by the Anglo-Danish group coordinated by Harwell Laboratories and by the France-Canada Group (ACED project), and it resulted in a first systematic study of the feasibility of polymer electrolyte batteries<sup>114, 115</sup>.

A number of polymer electrolytes now have conductivities within the target range of  $10^{-5}$  to  $10^{-4}$   $\text{Scm}^{-1}$ . However, a number of problems remain to be solved before expectation can be fulfilled. One is the transport number of the electrode reversible ion, with which the commonly quoted total conductivity must be

multiplied to obtain the operational value. Another, more severe, problem is the electrochemical environment. Some encouraging long-term results have appeared<sup>116</sup>.

A particular disadvantage of the elastomeric electrolyte is in the fabrication of on-chip power sources, in which thin film structures similar to those described above can be deposited directly as components on an integrated circuit. This technology has been demonstrated in principle<sup>117</sup> but encapsulation problems have yet to be overcome due to the extreme reactivity of alkali metals.

#### 1.7.2 Additives to battery electrodes

A less demanding role for the polymer electrolyte is an aid to ion-transport within an electrode structure<sup>118</sup>. In this case, mechanical stability is not necessarily required, as the electrode particles themselves act as a filler. The stability, however, remains a critical issue.

#### 1.7.3 Electrochemical displays

Another interesting device is the electrochromic display or window, i.e., a device which changes its visual appearance in response to an electrical signal.

Such devices can be made by laminating two electrolytes<sup>119</sup>. Here at least one of the electrodes should be an electrochromic material-i.e. one whose optical absorbance changes with the insertion of ions from the electrolyte and from the external circuit.

The electrochemical stability of the polymer may not be such a demanding requirement as the cell potential need not be high. However, a high conductivity is required to minimise the switching time.

#### 1.7.4 Chemical sensors

A number of sensor designs based on electrochemical cells can benefit from miniaturisation and mass production by use of polymer electrolytes. In this application a high conductivity is not required but, depending on the type of sensor, selectivity to one ion may or may not be required.

#### 1.7.4 Fuel cells

The cell



is the basis of many commercial fuel cells<sup>120</sup>. Liquid

electrolyte fuel cells operating below 100°C are limited in power output by slow electrode kinetics. The use of proton-conducting polymer electrolytes with a high thermal stability allows a higher operating temperature. Nafion-based membranes are currently in use, although PEO can also be made into a proton conductor by addition of phosphoric or sulphuric acids<sup>121</sup>.

CHAPTER TWO

AIMS AND OBJECTIVES

## 2.1 Polymer electrolyte network structures

By far the majority of investigations of polymer electrolytes so far reported have used commercial high molecular weight PEO as the host coordinating material. This has a number of disadvantages. First, the material is not well characterised, and some of its properties are age dependent (e.g. peroxide content, MW distribution etc.). It is known to contain variable amounts of catalyst residue and as a result has a rather high residual conductivity. Second, PEO and its complexes crystallise to varying extents (and rates which are history dependent).

Formation of crosslinked network structures has been extensively used to inhibit or reduce crystallinity and improve mechanical properties of linear PEO.

However, the problem of crystallinity in PEO-electrolytes was later eliminated by synthesising totally amorphous polymers with low T<sub>g</sub> values capable of dissolving salts. This was generally achieved by preparing comb-branched polymers with oligomeric ethylene oxide units attached to another polymer which acts as the inert backbone carrying the short EO chains. This has led to the synthesis of polysiloxanes, polyitaconates, polyphosphazenes and many other comb polymers, some of which are cited in the previous chapter. Most of these polymers were found to have

higher conductivities at room temperature than PEO-based electrolytes.

The majority of these polymers, however, have poor mechanical properties: at room temperature they resemble viscous melts and tend to flow at elevated temperatures. This is a serious drawback for potential commercial applications where long term dimensional stability is required. Crosslinking, in principle, can be used to eliminate flow or creep, but if carried out to excess, it may raise the  $T_g$  and be harmful. However, such levels of crosslinking should be unnecessary if a rubbery behaviour is acceptable.

In short, crosslinked polymer electrolytes have been prepared in order to : i) eliminate crystallinity in PEO, and ii) eliminate flow or creep in comb-polymer electrolytes. In the former case, the problem of crystallinity was substantially reduced, but conductivity levels were not all that high, and the materials had a number of major problems associated with them. For example, Polyurethane-based networks reported by Cheradame and coworkers cited in the previous chapter, were found to have the following problems:

- (i) Not very good film forming compositions
- (ii) Polyurethane linkage tends to increase  $T_g$  i.e. to decrease the segmental mobility and hence conductivity (the strong influence of urethane linkage



on the  $T_g$  is due to the existence of strong hydrogen bonding between the crosslinks and the surrounding polyether)

(iii) The electrochemical stability of the crosslinked materials suggest that unreacted or end linked isocyanates could disturb the electrochemical reaction on the lithium electrode.

Comb-shaped polymer electrolyte network systems have been prepared by a number of workers. For example, Cheradame and Dalard have synthesised a totally amorphous poly(dimethyl siloxane)-poly(ethylene oxide)-based polyurethane network, and Fontanella<sup>122, 123</sup> have reported ionic conductivity in solid, cross linked dimethyl siloxane-ethylene oxide copolymer networks containing sodium (triacetoxo and triethoxy silanes were employed as crosslinking agents). The synthetic procedure employed by these workers are complicated and the solid electrolytes offer no clear advantage over the previously discussed materials.

Ward et al.<sup>124</sup> and Smid et al.<sup>125</sup> have independently prepared network electrolytes of polysiloxane comb-polymers with EO teeth. In both cases linear polymers were initially synthesised and then thermally crosslinked at high temperatures. The conductivity levels reported for the salt complexes of these materials are substantially lower than the linear

polymers from which they were derived.

A different but very stable complex network system has been described by LeMehaut et al.<sup>126</sup>, which involves thermal treatment or irradiation of a styrene-butadiene-acrylonitrile copolymer. Hamaide et al.<sup>127</sup> have described more detailed studies on such composite materials which were formed from a mixture of styrene based macromer, poly(butadiene-co-acrylonitrile) elastomer., PEO and salt.

Generally, there are few examples in the literature where crosslinking procedures have been used to improve the mechanical integrity of the comb-shaped polymer electrolytes and in some cases, cited above, the crosslinking results in significant loss in conductivity due to large restrictions imposed on chain motion by the crosslink sites.

In principle, if the degree of crosslinking is kept low or if flexible crosslinkers are employed, segmental chain motion should not be seriously affected, leading to no or little sacrifice in conductivity.

Bearing these points in mind, there is now a need for facile crosslinking procedures to be developed, where physical properties as well as ionic conductivity of polymer electrolytes could be investigated.

## 2.2 Synthesis and characterization of a new type of polymer electrolytes

In the first chapter, the important role played by  $T_g$  in obtaining good conductivity levels in solid polymer electrolytes was discussed and several approaches for lowering the  $T_g$  of an electrolyte was highlighted. Whilst the  $T_g$  of these types of polymers are low, addition of salts leads to a somewhat monotonic increase in  $T_g$ . This restricts the conductivity when the  $T_g$  approaches room temperature and so it is an advantage to limit this effect as much as possible. But since the solvation of the ions is necessary for good conductivity, it is not possible to eliminate the effect completely. Since ion mobility is restricted as a result of the coordination of ions by polymer chain, a compromise must be reached as no coordination results in existence of salts in tight ion pairs, which means low conductivity.

To obtain maximum chain flexibility we must use a polymer chain with low  $T_g$ . Even though the  $T_g$  will increase when salts are added, the problem can be lessened because the relative increase will be lower if the initial value of the  $T_g$  is lower.

This line of approach is based on the concept that ion mobility in polymer electrolytes is assisted by large segmental motion of the polymer chain,

characteristic of that observed above  $T_g$ . It is then thought that the ions move by motion of the chain segment, to which they are coordinated, into the vicinity of new coordinating sites on the next chain. During the process new complexing bonds are formed and old ones broken, allowing the ions to change their spatial position. This implies that ionic conductivity is related to relaxation processes in the polymer but does not tell us much about the transport mechanisms although it has led to the use of free-volume and configurational entropy models<sup>71</sup> to describe ion transport in polymer electrolytes.

These approaches suffer certain limitations since variation in conductivity with ion size or frequency can not be explained. Therefore dissociation processes, the nature of ionic species, in polymer-salt complexes at molecular level needs to be understood firmly in order to comprehend ionic conductivity.

In a closed packed system migration of ions would be difficult although it would be enhanced by a temperature increase. To assist ion transportation, a polymer matrix could be formed which would allow pathways for the movement of ions.

Bearing these points in mind, the objective of this work is the synthesis and study of ion conduction using specifically designed polymers which are composed of crown ethers, chemically attached by spacer units of

varying lengths, to a highly flexible polymer backbone. The crown ether rings should then not only provide an in built free volume in the polymer matrix but may also form diffusion channels to encourage ion migration.

One point to investigate is whether the provision of these pathways counteracts any adverse T<sub>g</sub> effects which could limit ion mobility. Developing these polymers with salts allows us to investigate a) the possibility of creating preferable migration channels for ion transport or b), the restriction of cation-anion interaction due to the firm complexation of alkali metal ions by crown ethers, therefore reducing anion coordination with complexed cations. This may be achieved by the formation of complexes of salts with appropriately sized crown ethers with higher stability constants than their open chain polyether analogues.

By obtaining information from these systems it was hoped that a clearer picture of the mechanism of ion mobility would emerge in which one would establish the validity of the free volume approach which is also related to the dynamic percolation theory<sup>128</sup>.

CHAPTER THREE

EXPERIMENTAL

### 3.1 Instrumentation

#### 3.1.1 General notes

The  $^1\text{H}$ ,  $^{13}\text{H}$  n.m.r spectra were obtained on a Perkin-Elmer R32 ( $^1\text{H}$  resonance frequency = 90 MHz), and Bruker WP80 ( $^1\text{H}$  resonance frequency = 80 MHz;  $^{13}\text{C}$  resonance frequency = 20.15 MHz), Fourier transform spectrometer respectively.

Tetramethylsilane (TMS) was used as a reference and frequency locked on  $^2\text{H}$  of the deuterated solvents. The deuterated solvents were chloroform ( $\text{CDCl}_3$ ) and water ( $\text{D}_2\text{O}$ ). The following notation is used in reporting  $^1\text{H}$  and  $^{13}\text{C}$  n.m.r data : s = singlet; d = doublet; t = triplet; m = multiplet; q = quartet. The scale is quoted in parts per million (ppm) chemical shift ( $\delta$ ) scale.

The  $^{31}\text{P}$  n.m.r spectra of the polyphosphazenes reported in this work were obtained on a Bruker WP80 Fourier transform spectrometer at 32 MHz. All spectra were recorded in deuterated methanol ( $\text{CD}_3\text{OD}$ ). The isotropic hyperfine shift was measured as the difference of the observed position from the resonance position of 0.1 mM phosphoric acid solution in the inner compartment of a coaxial tube (5 mm internal and 10 mm external diameter). Shifts to the lower frequency are defined as positive.

Infrared analysis (Ir) was carried out using a Perkin-Elmer 557 grating Infrared spectrometer, a Shimadzu I.R. 435 infrared spectrometer or a Perkin-Elmer 197 infrared spectrometer. Samples were examined as thin films cast on sodium chloride plates. Elemental analyses were carried out using a Carlo Erba elemental analyser (C, H and N), model 1106.

All reagents used were distilled prior to use. Tetrahydrofuran (THF) and diethyl ether were refluxed over calcium hydride, stirred over lithium aluminium hydride and then distilled prior to use. Pyridine was stored over KOH pellets and then distilled prior to use. 1,4-Dioxane was refluxed in the presence of metallic sodium for 12 hours then distilled prior to use. Methanol was dried by conventional methods for obtaining the dry solvent then stored over 4A molecular sieves.

### 3.1.2 Differential Scanning Calorimetry (D.S.C)

D.S.C. is a technique used to detect any phenomena that are accompanied by an enthalpic change. Details of the theory and design of differential scanning calorimeters have been described by Watson and O'Neil<sup>129, 130</sup>.

D.S.C. is a technique in which the heat flow into or



from a sample and an inert reference is measured as a linear function of temperature. In the equipment the heat flow is measured by keeping the sample and inert reference thermally balanced by changing a current passing through the heaters under the two chambers. The variation in power required to maintain this level during a transition is measured. A signal,  $(dH/dt)$  proportional to the power difference is plotted on one of axis of an X-Y recorder and temperature is plotted on the other.

The instrument used for the analysis in this study was a Perkin-Elmer model D.S.C.-2 equipped with a low temperature mode accessory. Measurements were therefore possible in the temperature range 100-1000 K. Operation of the instrument was normally carried out in the subambient mode where dry helium was used as the purge gas and liquid nitrogen was used as the cooling fluid. Analysis of samples in the above ambient mode was carried out using oxygen free nitrogen as the purge gas. The scan rate used was  $20 \text{ K min}^{-1}$  for all the samples.

The  $T_g$  is manifest by a step change or a baseline shift in the output voltage as a function of scanning temperature. It is possible to define  $T_g$  as either the temperature of onset of the step change or the midpoint of the resulting inflection of the recorder trace. In this work both definitions were used.

### 3.1.3 Conductivity Instrumentation

Conductivity measurements were carried out as a function of increasing temperature using a PT1 digital conductivity meter which generated a low a.c. voltage (< 1 volt) at 1.59 KHz.

The conductivity meter operates basically on the Ohm's law principle

$$I = V/R$$

where R is the resistance (in ohms), I is the current (in amperes) and V is the electromotive force (emf, in volts). The resistance of the material between the cell plates is proportional to the distance between the plates (l cm) and inversely proportional to the cross-sectional area (A, cm<sup>2</sup>) of the plates. By introducing a proportionality constant ( $\rho$ ), the specific resistance of the material, it is possible to write

$$R = \rho \cdot l/A$$

where  $\rho$  has the units ohm-centimeters. The specific conductance or conductivity ( $\sigma$ ) of the material is the reciprocal of the specific resistance.

$$\sigma = 1/\rho = 1/R \cdot 1/A$$

For a given cell the distance between the plates and the cross-sectional area does not change and a cell constant (C) can be introduced :

$$\sigma = C / R$$

Electrode blocks were prepared using an inert insulating material (tuffnall). Silver discs were cut (1 cm<sup>2</sup>) and silver soldered to a metal block. This complete assembly was inserted into the tuffnall block so that the electrode surface was coplanar with the machined surface of the block.

A schematic diagram of the half cell block is shown in the Figure 2. Spacer shims were used to separate a pair of matched electrode blocks by a known distance (0.1 cm), and the complete cell block arrangement was clamped together firmly during measurements. Using a solution of potassium chloride ( $1 \times 10^{-3}$ , 298 K), cell constants of 0.097 and 0.092 were determined for two different assemblies used during this study. The conductivity meter was regularly calibrated using a standard resistance box. The meter compared the resistance of the test sample with the resistance of an accurate resistor in the circuit. The reciprocal resistance of the material was displayed in microsiemen

( $\mu\text{S}$ , where siemen is the unit corresponding to the reciprocal ohm or mho).

A thermostatically controlled oven was used to study the temperature variation on the conductivity of samples. Although the apparatus was equipped with a cooling mode, most conductivities were measured as a function of increasing temperature. A chromel-alumel thermocouple placed in the heating chamber, (with reference junction at 273 K), was used to determine the temperature of the sample during the experiments. After changing the temperature, a chart recorder was used to ensure that the system had stabilised before the temperature and conductance data were collected.

Conductivity measurements were carried out inside a dry glove box where the air was continuously circulated over fresh phosphorus pentoxide, and other drying agents, using a small compressor. The transfer compartment to the dry box was flushed with dry nitrogen gas during transfer operations, to maintain anhydrous conditions at all times.

To measure the conductivity of a material, the dry sample was loaded into the cell and rapidly transferred to the dry box. After connecting the cell block to the conductivity meter, the temperature was increased to about 353 K for several minutes. The polymer sample was then allowed to cool to room temperature and stabilise over a 12 hour period.

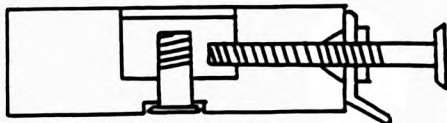


Figure 2 Schematic diagram of the half cell block used during conductivity measurements.

After noting the temperature and conductivity of the sample at room temperature, the temperature was increased and the new details were noted after about one hour. The data were generally collected from room temperature to about 410 K. Similar considerations were applied when collecting data as a function of decreasing temperature.

Using the conductance data in conjunction with the pertinent cell constant for the cell assembly used during the experiment it was possible to calculate the specific conductance or the conductivity of the sample.

#### 3.1.4 Preparation of polymer-salt complexes

All polymer samples and salts were dried under high vacuum at 333 K for at least 2-6 days prior to use and were then stored under anhydrous conditions. Methanol was used as the solvent in the preparation of polymer-salt complexes. Prior to use the solvent was dried according to standard procedures and stored over activated molecular sieves. Using *Karl Fischer* titration the moisture content of the solvent was determined as < 0.1%.

A wide range of polymer salt complexes were examined in this study. Salt concentrations in the complexes were

described using  $[M^+]/[EO]$ , i.e. the number of moles of the cations per mole of the solvating units. In general, complexes containing salts in the concentration range  $[M^+]/[EO] = 0.0125$  to  $0.25$  were examined.

For the uncrosslinked polymers, a known weight of the anhydrous polymer was added to the flask. A predetermined quantity of salt was weighed out and added to the polymer sample. Anhydrous methanol was added to the flask and the flask was sealed until the mixture had become homogeneous. The solvent was removed by evaporation and after complete loss of solvent all samples were dried under vacuum at  $333\text{ K}$  for 2-3 days prior to use. The *Karl Fischer* titration indicated that the moisture content of the dried material was  $< 0.01\%$ .

Using the technique to prepare the samples it was found that predominantly transparent, homogeneous products were formed. However, heterogeneous products were obtained from a limited number of samples.

As for the crosslinked materials, homogeneous amorphous solutions of the networks and salts were prepared by allowing the polymer to swell in a methanol solution of the salt. The mixtures were stirred and the methanol was evaporated slowly over a period of 48 hours. All samples were dried under high vacuum at  $333\text{ K}$  for 72 hours and the dry polymer-salt mixture was weighed to confirm the amount of the salt incorporated into the network. The concentration of the salt in the

polymer was varied by adjusting the weight of salt in methanol to that of the polymer.

For all the systems described in this work the different compositions are expressed as the cation concentration per ethylene oxide unit in the polymer. The ether oxygen adjacent to the main chain was not included in the calculations to allow comparison with other polymer-electrolytes previously studied<sup>96, 100-102</sup>.

#### 3.1.5 Network swelling

The polymer networks exhibited extensive swelling when exposed to water, methanol, ethanol, chloroform and hexane. A weighed sample of polymer was immersed in the swelling liquid for 48 hours at 292 K. It was then removed, placed in a weighed container and excess surface solvent removed by blowing nitrogen over the sample for about 30 seconds. The weight of liquid absorbed/g polymer was then estimated.

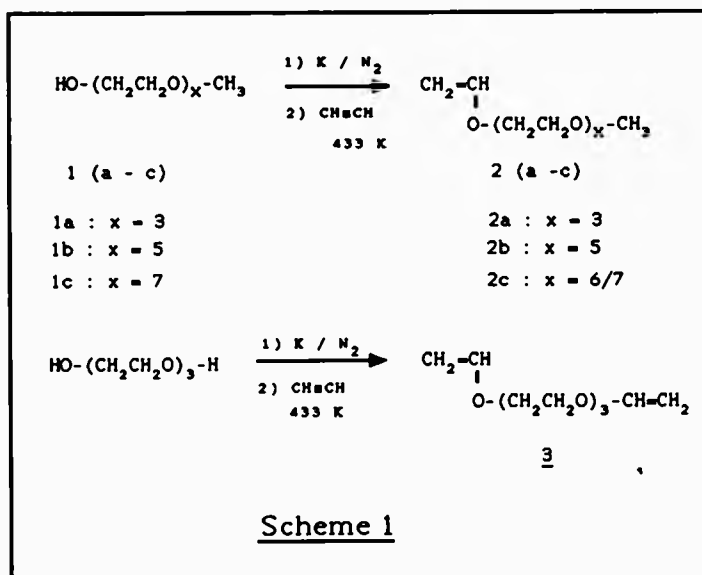


### 3.2 Synthesis and characterisation of vinyl ether

#### MONOMERS

#### 3.2.1 Synthesis of Mono- and divinyl ethers of oligo oxyethylenes

Vinyl ether formation procedure suggested by Mathias<sup>132</sup> were extended. This involved acetylene addition to alcohol groups catalysed by potassium salts. A number of monomethyl ethylene glycol vinyl ether macromonomers and a divinyl ether of triethylene glycol were synthesised according to the reaction scheme shown below:



### 3.2.1.1 Synthesis of triethylene glycol monomethyl vinyl ether

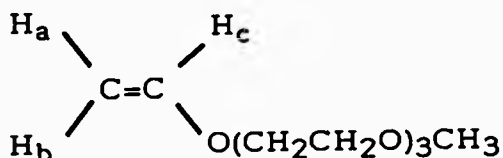
Triethylene glycol monomethyl ether (98.4g, 0.6 mol) was placed in a three necked flask, fitted with a fritted-glass inlet tube located near the bottom of the flask and an efficient condenser. The flask was placed in an oil bath and nitrogen was passed through it as the temperature of the bath was raised to 373 K. Potassium metal (2.73g, 0.07 mol) was added to the flask in small pieces to avoid vigorous evolution of hydrogen. The clear, colourless solution gradually turned dark brown. After complete addition of potassium, the temperature was raised to 433 K, the gas inlet tube was then switched to acetylene tank and rapid addition of the gas was begun. From this point on, at intervals of 30-60 minutes, small aliquots of the reaction mixture were removed for  $^{13}\text{C}$  n.m.r analysis. Acetylene addition was continued until the characteristic peaks due to the carbon atoms of the double bond showed no further enhancement with time.

Nitrogen was passed through the flask as the reaction mixture was allowed to cool to room temperature. The crude material was dissolved in 200 cm<sup>3</sup> of water and extracted several times with diethyl ether (4 x 400 cm<sup>3</sup>). The ether extracts were combined and dried over MgSO<sub>4</sub> and finally the organic solvent was

removed under reduced pressure.

The desired product was isolated as a colourless liquid at 331-333 K (0.01 mmHg) (48%). The reason for the rather low yield was found to be due to the chain shortening during the vinylation process which led to a mixture of products in which the highest homologue corresponded to that of the starting material alcohol (i.e.  $n = 3$ ).

$^1\text{H}$  n.m.r :



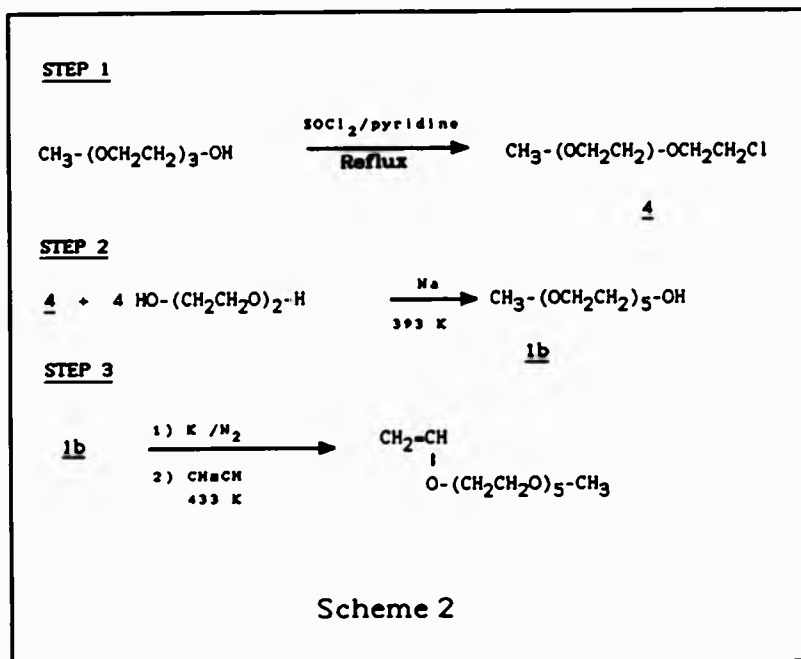
$\delta$  ppm ( $\text{CDCl}_3$ , 90 MHz), 3.39 (s, 1H) methyl  $\text{CH}_3$ , 3.5-3.9 (m, 12H) all the EO protons, 3.95-4.14 (m, 1H)  $\text{H}_a$ , 4.1-4.3 (m, 1H)  $\text{H}_b$ , 6.35-6.6 (q, 1H)  $\text{H}_c$ .

$^{13}\text{C}$  n.m.r :  $\delta$  ppm ( $\text{CDCl}_3$ , WP80 Bruker), 60.12 (t)  $\text{CH}_3$ , 68-77 (m) all the carbons of the EO units, 87.51 (t) and 153 (d) vinyl double bond carbons.

Ir :  $\otimes$  (thin film) , principle peaks at 3100 (=C-H stretch), 1630 (C=C stretch), 1150 (C-O stretch)  $\text{cm}^{-1}$ .

### 3.2.1.2 Synthesis of pentaethylene glycol monomethyl vinyl ether

The starting material pentaethylene glycol monomethyl ether was not commercially available, therefore the following reaction scheme was devised:



**STEP 1 : Synthesis of 2-[(2'-(2'-methoxy  
ethoxy)-ethoxy)ethyl chloride (4)**

To 102g (0.86 mol) of thionyl chloride in a 3 necked flask, fitted with a stirrer and a dropping funnel, and cooled in a mixture of salt and ice, was added a mixture of 9.2g (0.1) of dry pyridine and 82g (0.5 mol) of triethylene glycol monomethyl ether at such a rate that the temperature in the flask did not rise above 10°C. After all of the material was added, the mixture was refluxed for 8 hours then allowed to cool. Excess thionyl chloride was destroyed when 80 cm<sup>3</sup> of water was added to the mixture. The oily layer was separated and dried over calcium chloride.

Purification was performed by vacuum distillation (b.pt. 338 K, 0.01 mmHg). This gave a colourless liquid (74%).

<sup>1</sup>H n.m.r : δ ppm (CDCl<sub>3</sub>, 90 MHz), 3.37 (s, 3H) methyl protons, 3.5-3.9 (m, 12H) all of the EO protons.

**STEP 2: Synthesis of pentaethylene glycol monomethyl ether (1b)**

To 53g (0.5 mol) of freshly distilled diethylene glycol, which had been placed in a 3 necked flask, fitted with a stirrer, a condenser and a dropping

funnel, was added 2.87g (0.125 mol) of metallic sodium under nitrogen and heated to about 393 K. When all the sodium had reacted, 22.8g (0.125 mol) of compound (4), synthesised above was slowly added. The mixture was stirred at 393 K for 12 hours, and then allowed to cool. 60 cm<sup>3</sup> of water was added to the residue and the aqueous mixture was extracted several times with dichloromethane (4 x 70 cm<sup>3</sup>). The extracts were combined and dried over sodium sulphate. Finally the organic solvent was evaporated and the crude compound was purified by vacuum distillation (b.pt. 413 K, 0.01 mmHg).

<sup>1</sup>H n.m.r : 8 ppm (CDCl<sub>3</sub>, 90 MHz), 2.65 (s, 1H) hydroxy proton, 3.38 (s, 3H) methyl protons, 3.75 (m, 20H) all of the EO protons.

**Elemental analysis:**

calculated: C, 52.36 H, 9.59

found: C, 52.55 H, 9.48

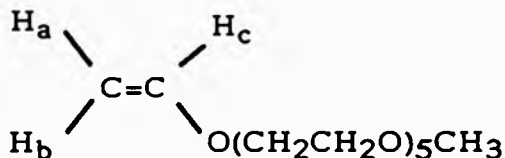
**STEP 3 : Pentaethylene glycol monomethyl vinyl ether  
(2b)**

A similar method as described for the preparation of (2a) was used. The starting materials were pentaethylene glycol monomethyl ether (60g, 0.24 mol), metallic

potassium (1g, 0.025 mol) and acetylene.

The crude material was purified by vacuum distillation which gave about 34g (56%) of the desired monomer (b.pt. 373-383, 0.01 mmHg).

<sup>1</sup>H n.m.r :



$\delta$  ppm (CDCl<sub>3</sub>, WP80 Bruker), 3.39 (s, 3H) methyl protons, 3.5-3.9 (m, 20H) all of the EO protons, 3.95-4.1 (m, H) =CH<sub>a</sub>, 4.1-4.3 (m, 1H) vinyl =CH<sub>b</sub>, 6.36-6.61 (q, 1H) vinyl =CH<sub>c</sub>.

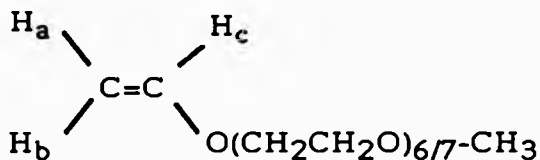
<sup>13</sup>C n.m.r :  $\delta$  (CDCl<sub>3</sub>, WP80 Bruker), 60 (t) methyl carbon, 67-77 (m) all the EO carbons, 87.5 (t) vinyl =CH<sub>2</sub>, 153 (d) vinyl =CH.

Ir :  $\delta$  (thin film), principle peaks at 3100 (=C-H stretch), 1630 (C-O stretch) cm<sup>-1</sup>.

3.2.1.3 Synthesis of a vinyl ether macromonomer with a mixed number of EO units (2c)

Poly(ethylene glycol methyl ether), average MW = 350 (Fluka) was vinylated according to the procedure used for the preparation of (2a). The pure product was isolated by vacuum distillation and the fraction collected between 393-408 K at 0.01 mmHg contained an average of 6/7 EO units per molecule as confirmed by n.m.r. This was further supported by elemental analysis.

<sup>1</sup>H n.m.r :



δ ppm (CDCl<sub>3</sub>, WP80 Bruker), 3.39 (s, 3H) methyl protons, 3.5-3.9 (m, 26H) all the EO protons, 3.93-4.1 (m, 1H) vinyl =CH<sub>a</sub>, 4.11-4.3 (m, 1H) vinyl =CH<sub>b</sub>, 6.36-6.60 (q, 1H) vinyl =CH<sub>c</sub>.

<sup>13</sup>C n.m.r : δ ppm (CDCl<sub>3</sub>, WP80), 60.21 (t) methyl carbon, 68-77 (m) all the carbons of EO units, 87.5 (t) vinyl =CH<sub>2</sub>, 155 (d) vinyl =CH.



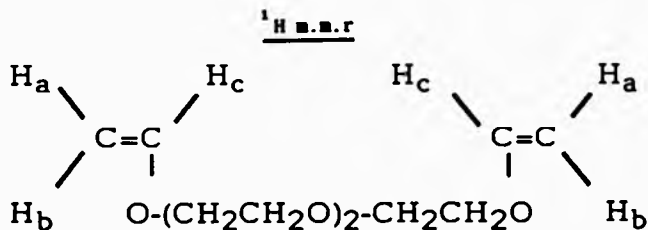
Ir :  $\theta$  (thin film), principle peaks at 3100 (=C-H stretch), 1630 (C=stretch) and 1150 (C-O stretch)  $\text{cm}^{-1}$ .

Elemental analysis :-

calculated:	C, 56.11	H, 9.27
found:	C, 55.88	H, 9.38

3.2.1.4 Synthesis of triethylene glycol divinyl ether (3)

Triethylene glycol was vinylated in a manner similar to that described previously (see 3.2.1). The purification was achieved by vacuum distillation. The fraction collected at 343 K (0.01 mmHg) was found to be the desired monomer (3).



$\delta$  ppm ( $\text{CDCl}_3$ , WP80 Bruker), 3.5-3.9 (m, 12H) all the EO protons, 3.95-4.40 (m, 4H) = $\text{CH}_a$  and = $\text{CH}_b$ , 6.35-6.62 (q, 2H) = $\text{CH}_c$ .

<sup>13</sup>C n.m.r :  $\delta$  ppm ( $\text{CDCl}_3$ , WP80 Bruker), 61.61-70.57 (m)

all the EO carbons, 86.55 (t)  $\text{-CH}_2$ , 151.55 (d)  $\text{-CH}$ .

**Elemental analysis:**

calculated: C, 59.39 H, 8.97

found: C, 59.34 H, 8.91

\*\*\*\*\*NOTE\*\*\*\*\*

i) In general, the impurities present in the crude vinyl ethers prepared above, were found to be acetaldehydes, carboxylic acid derivatives, acetals and acetylene.

For low molecular weight monomers with maximum 5 EO units per molecule, careful vacuum distillation of the crude product gave pure materials. The presence of small amounts of the mentioned impurities were found to affect the cationic polymerisation of these monomers, where only low molecular weight (oligomers) polymers could be obtained.

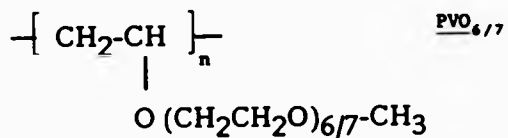
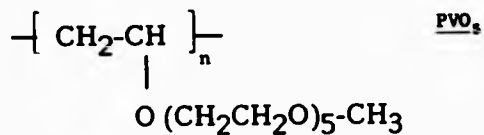
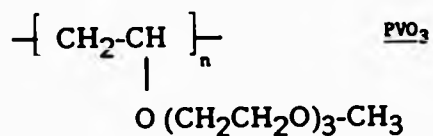
ii) The monomers, with a higher number of EO than 5 per molecule, have too high boiling points to be purified by vacuum distillation. Although, above we have described a successful purification of a vinyl ether with a mixed number of EO units(6/7) by vacuum distillation, but at least in more than one case it was found that a small amount of impurity caused an undesirable crosslinking of the monomer during cationic polymerisation.

Suzuki and Tomono<sup>133</sup> have reported a good but lengthy purification technique for vinyl ether macromonomers with 8, 12 and 20 EO units.

iii) Finally, it should be noted that vinyl ethers could be hydrolysed with various mineral and organic acids. The presence of small amounts of the hydrolysed matter has an adverse effect on the cationic polymerisation of these monomers. Therefore, if long term storage is required, the monomers should be kept in the presence of metallic sodium.

### 3.3 Preparation of linear and crosslinked polyvinyl ethers

Vinyl ether monomers synthesised according to the procedures described in the previous section were cationically polymerised using  $\text{BF}_3 \cdot \text{etherate}$  as catalyst. A series of linear polymers were prepared in which the length of the oxyethylene side chains were 3, 5 and 6/7:



In another set of experiments the vinyl ether monomer with 3 EO units was copolymerised with the divinyl monomer (3) in varying feed ratios, producing a series of network structures with a various number of crosslinking sites. The crosslink density was not measured in these systems and so apparent crosslink densities are only quoted here, which reflect the amount of divinyl monomer used in the feed mixture.

Following is a code named list of the network structures based on PVO<sub>3</sub>:

PVO <sub>3</sub> - 0.2% C-L,	PVO <sub>3</sub> - 1.2% C-L
PVO <sub>3</sub> - 2% C-L,	PVO <sub>3</sub> - 3.5% C-L
PVO <sub>3</sub> - 5% C-L,	PVO <sub>3</sub> - 11% C-L

Network structures based on the monomers with a higher number of EO units per repeat unit were also crosslinked with the divinyl monomer. Following are the code-names given to these polymers:

PVO<sub>5</sub> - 5% C-L  
PVO<sub>6/7</sub> - 5% C-L

The remainder of this section is devoted to the experimental procedures that describes polymerisation, purification and characterisation of the above polymers.

### 3.3.1 Preparation of uncrosslinked PVO,

The cationic polymerisation of monomer (2a) was achieved according to the procedure described below: The initiator solution was prepared using freshly dried and distilled  $\text{BF}_3 \cdot \text{etherate}$  (50 micro litre) and dry 1,2-dichloromethane (5  $\text{cm}^3$ ).

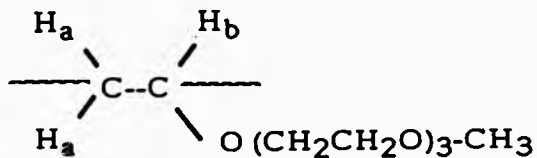
To a septum-sealed flask and magnetic stirrer which had been flame dried under vacuum, was added monomer (2a) (30g, 0.16 mol). After three freeze-evacuate-thaw cycles, nitrogen gas was then introduced into the system to 1 atmosphere pressure. The flask was cooled to about 233 K before 100 micro litre of the initiator solution was added slowly with a syringe. The temperature of the flask was allowed to increase gradually. At about 263 K the mixture suddenly became hot and viscous. After standing at room temperature for 2-3 hours the flask was opened and the polymer was dissolved in 50  $\text{cm}^3$  of dichloromethane and reprecipitated several times into hexane.

A highly viscous polymer was obtained in 75% yield. Using membrane osmometry the molecular weight of the polymer was determined as  $30000 \text{ gmol}^{-1}$ .

Using DSC the material was found to be totally amorphous with mid-point glass transition temperature ( $T_g$ ) of about 206 K.



<sup>1</sup>H n.m.r



δ ppm (CDCl<sub>3</sub>, WP80 Bruker), 1.4-2.1 (broad multiplet, 2H) main chain H<sub>a</sub>, 2.85-3.2 (broad multiplet, 1H) main chain H<sub>b</sub>, 3.39 (s, 3H) methyl, 3.46-4.1 (m, 12H) all of the EO protons.

Ir : 0 (thin film), principle peaks at 2950 (C-H stretch), 1630 (C=C stretch) and the monomer peaks absent at 3100 (=C-H stretch), 1630 (C=C stretch) cm<sup>-1</sup>.

### 3.3.2 Preparation of network polymers based on PVO,

Using a similar procedure as described above, monomer (2a) was copolymerised in varying feed ratios with the divinyl crosslinker (3). The crosslinked samples were swollen by the addition of chloroform, then washed repeatedly with acetone and methanol to remove

any unreacted monomer, or sol fraction and catalyst residue from the network polymers. The samples were dried under vacuum at 333 K for 72 hours. The materials obtained in this way were pale yellow, transparent, non sticky elastomers and easily handled.

Films could also be prepared by carrying out the polymerisation in a thin layer of reaction mixture spread on a petri dish under dry nitrogen. The product, at this stage could easily be peeled off the glass plate and formed a flexible elastomeric sheet.

Swelling of the film with chloroform and subsequent washings with acetone/methanol removed unreacted monomer and sol fraction from the crosslinked elastomers. Drying of the thin film was generally more difficult than those described above. In order to maintain the homogeneity of the film surface, the materials were partially dried by blowing nitrogen over them for 3-5 hours before drying in a vacuum oven for 72 hours at room temperature.

Initially, due to the crosslinked nature of the materials, obtaining N.M.R. spectral data was thought not to be possible. However, for the lightly crosslinked polymers (up to 5%), reasonably good quality  $^{13}\text{C}$  n.m.r spectra were obtained in  $\text{D}_2\text{O}$ . The spectra closely resembled that of the uncrosslinked PVO,. Unfortunately, proton n.m.r could not be obtained in this way due to narrowness of the proton n.m.r tube.

Glass transition temperature of the crosslinked

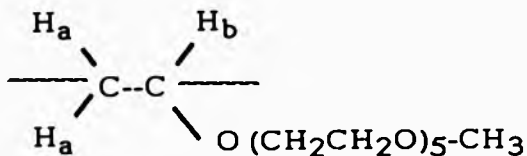
polymers were measured and are presented when discussing the variation of Tg as function of apparent crosslink density (see chapter 5).

### 3.3.3 Preparation of PVO<sub>5</sub>

Pentaethylene glycol monomethyl vinyl ether (2b) was cationically polymerised according to the procedure previously described.

The polymerisation mixture was dissolved in a minimum amount of chloroform and reprecipitated into hexane. A pale yellow viscous polymer was obtained which was dried in vacuum oven at 333 K for 72 hours. Using membrane osmometry the molecular weight of the polymer was determined as 41000 gmol<sup>-1</sup>. The material was found to be totally amorphous with a Tg of 208 K.

<sup>1</sup>H n.m.r



$\delta$  ppm (CDCl<sub>3</sub>, WP80 Bruker), 1.4-2.1 (broad multiplet, 2H) main chain H<sub>a</sub>, 2.85-3.2 (broad multiplet, 1H) main chain H<sub>b</sub>, 3.4 (s, 3H), methyl, 3.45-4.1 (m, 20H) protons of the EO units.

<sup>13</sup>C n.m.r :  $\delta$  ppm (CDCl<sub>3</sub>, WP80 Bruker), 33-40 (broad multiplet) main chain carbon attached to H<sub>a</sub>, 55.31 (t) Methyl carbon, 66.50-75.11 (m) main chain carbon attached to H<sub>b</sub> and all the carbons of EO units.

Ir :  $\delta$  (thin film) Principle peaks at 2950 (aliphatic C-H stretch), 1480 (-CH<sub>2</sub> stretch), 1375 (-CH<sub>3</sub> stretch), 1150 (C-O stretch) cm<sup>-1</sup>.

Principle monomer peaks absent at 3100 (=C-H stretch), 1630 (C=C stretch) cm<sup>-1</sup>.

#### 3.3.4 Preparation of PVO<sub>3</sub>- 5% C-L

A mixture of pentaethylene glycol monomethyl vinyl ether (2b) (10g, 0.036 mol) and the divinyl ether crosslinker (3) (0.335g, 0.0018 mol) were cationically copolymerised according to the procedure described earlier.

A network polymer was obtained which was purified by

repeated washing with chloroform, acetone and methanol. Finally the material was dried in a vacuum oven at 333K for 72 hours. The polymer was a pale yellow, transparent and non-sticky elastomer.

$^{13}\text{C}$  n.m.r of the swollen polymer in  $\text{D}_2\text{O}$  was found to be very similar to that of the uncrosslinked polymer  $\text{PVO}_3$ . The  $T_g$  of the material was measured as 211 K.

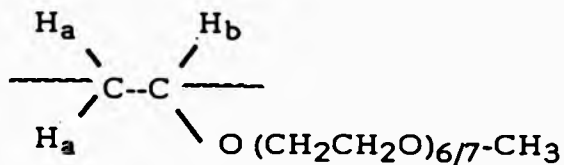
### 3.3.5 Preparation of $\text{PVO}_{6/7}$

The vinyl ether macromonomer (2c) was cationically polymerised according to the procedure described previously. Unreacted monomer and sol fractions were removed by repeated precipitation into hexane. Finally a viscous, pale yellow, transparent polymer was obtained which was dried in vacuum oven at 333 K for 72 hours.

The polymer contained an average of 6/7 EO units per side chain as determined by n.m.r. Using membrane osmometry, the average molecular weight of the polymer was found to be  $40,000 \text{ gmol}^{-1}$ .

The polymer was found to be totally amorphous with a glass transition temperature of 208 K.

<sup>1</sup>H n.m.r



δ ppm (CDCl<sub>3</sub>, 90 MHz R32), 1.4-2.1 (broad multiplet, 2H) main chain carbon attached to H<sub>a</sub>, 2.85-3.2 (broad multiplet, 1H) main chain carbon attached to H<sub>b</sub>, 3.41 (s, 3H) methyl, 3.45-4.10 (m, 26H) all of the EO protons.

<sup>13</sup>C n.m.r : δ ppm (CDCl<sub>3</sub>, WP80 Bruker), 33-40 (broad multiplet) main chain carbon attached to H<sub>a</sub>, 55.3 (t) methyl carbon, 66.55-75.15 (m) main chain carbon attached to H<sub>b</sub> and all of the carbons of EO units.

Ir : δ (thin film), principle peaks at 2950 (aliphatic stretch), 1470 ( -CH<sub>2</sub> stretch), 1150 (C-O stretch) cm<sup>-1</sup>. Principle monomer peaks absent at 3100 (=C-H stretch), 1630 (C=C stretch) cm<sup>-1</sup>.

**3.3.6 preparation of FVO<sub>6/7</sub> -5% C-L**

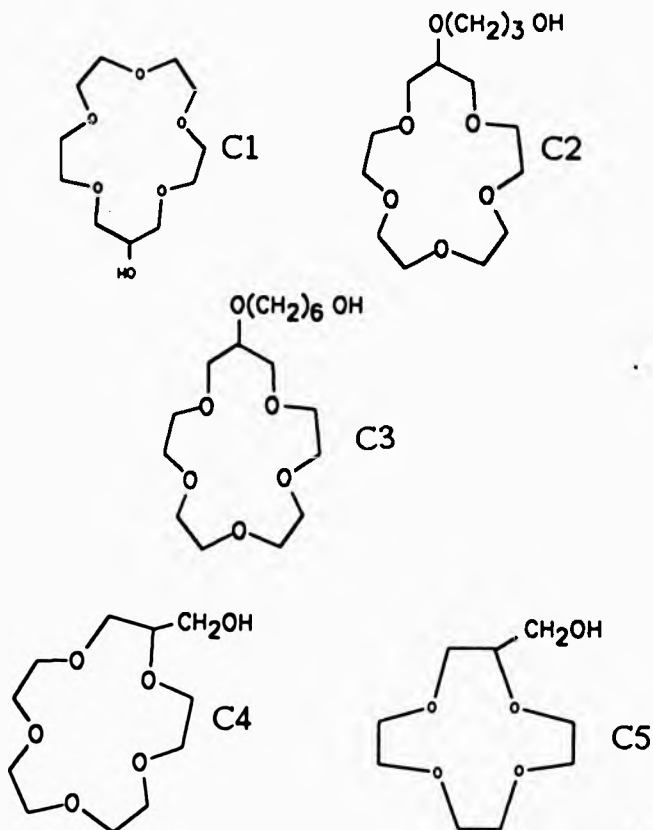
The vinyl ether macromonomer (2c) (10g , 0.03 mol)

and the divinyl ether crosslinker (3) (0.3g, 0.0015 mol) were cationically copolymerised, and purified according to the procedure described before.

$^{13}\text{C}$  n.m.r of the swollen polymer in  $\text{D}_2\text{O}$  was found to be similar to that of the uncrosslinked polymer  $\text{PVO}_{6/7}$ . The material was totally amorphous with  $T_g$  of 211.5 K.

### 3.4 Preparation of macrocyclic oligomers of ethylene oxide (Crown ethers)

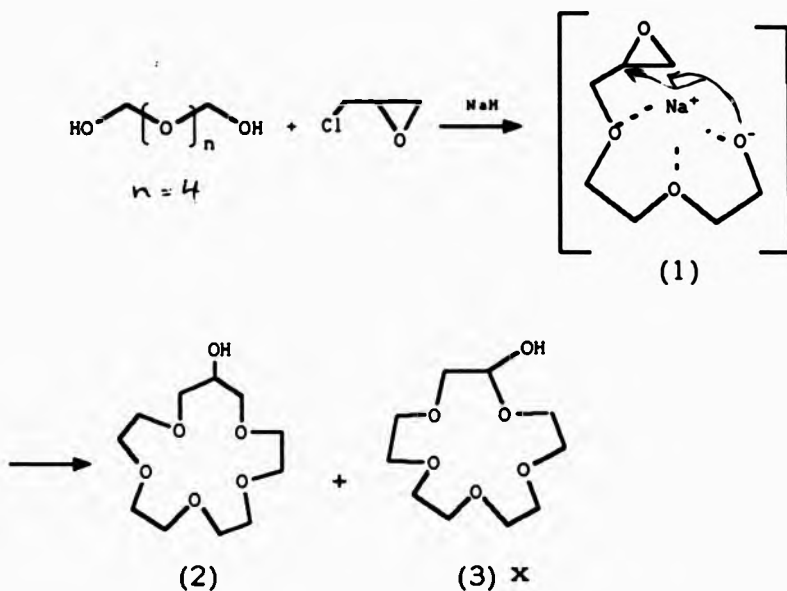
Hydroxy substituted crown ethers are versatile intermediates for further modification and for the formation of the polymer supported crown ethers. In this section, we describe synthetic procedures for a number of these crown ethers.





### 3.4.1 A facile one pot synthesis of hydroxy-substituted 16-crown-5 (C1)

This was achieved according to the synthetic route suggested by Okahara<sup>134</sup>. The reaction of tetraethylene glycol with epichlorohydrin in the presence of sodium afforded the intermediate (1) which under the reaction conditions cyclises to the hydroxy substituted crown ether (2) by the intermolecular attack of the alkoxide anion to the epoxy ring as shown below:



Following is a typical experimental procedure to prepare hydroxy-16-crown-5 :

Tetraethylene glycol (39g, 0.2 mol) was added dropwise to a suspension of dry sodium hydride (4.9g, 0.2 mol) in dioxane (anhydrous, 500 cm<sup>3</sup>), under nitrogen. After the evolution of hydrogen had ceased, epichlorohydrin (19g, 0.2 mol) was added in one lot and the mixture was stirred for one hour during which the temperature was carefully regulated not to exceed 313 K. Then the mixture was heated to reflux and stirred for an additional 10 hours at this temperature. Upon cooling NaCl was filtered off and dioxane was removed under reduced pressure. The resultant viscous liquid was dissolved in 70 cm<sup>3</sup> of water and extracted repeatedly with chloroform. The extracts were combined and dried over MgSO<sub>4</sub>. Chloroform was removed under reduced pressure and fractional distillation gave 25.3g of a pale yellow liquid (b.pt. 423 K, 0.01 mmHg).

The fractional distillation afforded the product, but it was usually difficult to remove a trace amount of contaminants, mainly tetraethylene glycol, from the objective compound. The material however, was freed of the last traces of the contaminant by extraction from aqueous solution with chloroform.

Two other methods of purifying the product also gave the pure compound:

i) Purification by an ion exchange column:

(Amberlite CG-120 type Na form)- where the contaminated distillate was dissolved in acetone, charged into the column packed with the activated resin, and eluted with acetone.

ii) Pyrolysis of  $MgBr_2$ .complex :

The acetone solution of the contaminated crown ether was added to a acetone solution saturated with  $MgBr_2 \cdot 6H_2O$  under stirring. The white precipitate which appeared was collected by filtration, washed with acetone, and dried under reduced pressure. The white crystalline solid was heated to 473 K in a distillation apparatus at 0.01 mmHg to release the pure hydroxy-16-crown-5 as a colourless liquid.

$^1H$  n.m.r :  $\delta$  ppm ( $CDCl_3$ , 90 MHz), 2.75 (s, 1H) hydroxyl -OH, 3.4-4.8 (m, 21H) protons of the crown ether ring.

Ir :  $\delta$  (thin film), Principle peaks at 3400-3200 (hydrogen bonded O-H stretch), 3000-2800 (aliphatic C-H stretch), 1120 (C-O stretch)  $cm^{-1}$ .

Accurate mass spectrum :

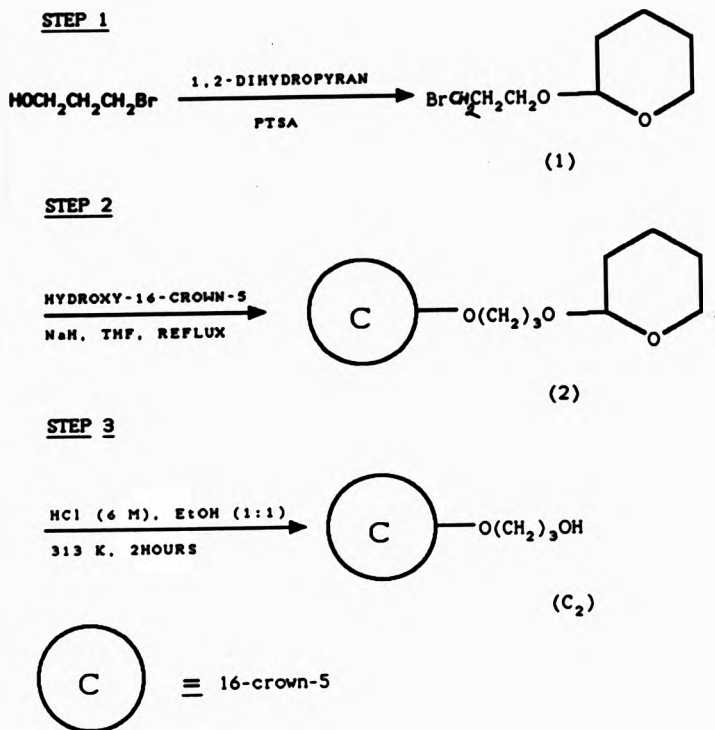
parent ion(m/e) observed: 250.2955  
calculated: 250.2912

**Elemental analysis :**

<b>found:</b>	<b>C; 52.78%</b>	<b>H; 8.80%</b>
<b>calculated:</b>	<b>C; 52.74%</b>	<b>H; 8.86%</b>

3.4.2 Preparation of hydroxy 16-crown-5 derivative  
with 3 methylene spacer units (C<sub>2</sub>)

The following reaction scheme was devised to prepare  
a derivative of hydroxy-16-crown-5 with 3 methylene  
spacer units:



Scheme 4

(PTSA = p-toluene sulphonic acid)

**STEP 1 : Tetrahydropyranyl ether of 3-Bromopropanol (1)**

To a stirred solution of freshly distilled 1,2-dihydropyran (8.4g, 100 mmol) at ice temperature was added a mixture of 3-bromopropanol (6.45g, 50 mmol) and p-toluene sulphonic acid (75 mg). The solution was stirred for an additional 12 hours at room temperature, after which aqueous NaHCO<sub>3</sub> (10%, 100 cm<sup>3</sup>) was added. The resulting mixture was extracted with dichloromethane (3x100 cm<sup>3</sup>), dried over MgSO<sub>4</sub>, and concentrated in vacuo to give an oil, which was distilled (9.87g, 91%) to give the protected alcohol as an oil (b.pt. 352 K, 0.1 mmHg).

Ir : Spectrum showed a total absence of hydrogen bonded O-H stretch and the appearance of C-O stretch at 1120 cm<sup>-1</sup>.

**STEP 2 : Tetrahydropyranyl ether - protected  
3-hydroxypropyl-16-crown5 (2)**

To a stirred suspension of dry NaH (1g, 0.04 mol) in dry THF (50 cm<sup>3</sup>) at room temperature under nitrogen gas was added hydroxy-16-crown-5 (Cl) (19g, 0.04 mol), and the mixture was heated to reflux for 20 minutes until the evolution of hydrogen had ceased. The protected 3-bromopropanol (1) (8.92g, 0.04 mol) was added dropwise

over a period of 30 minutes. The mixture was stirred for 12 hours. Upon cooling the solvent was removed under vacuum and 50 cm<sup>3</sup> of water was added to the crude reaction product. The aqueous mixture was extracted with chloroform (3x70 cm<sup>3</sup>), dried over MgSO<sub>4</sub>, and concentrated in vacuo to give a pale yellow oil which was used in the next step of the scheme without any further purification.

**STEP 3 : Acid catalysed deprotection of compound (2)**

A solution of (2) (10g), aqueous HCl (6M, 12 cm<sup>3</sup>), and methanol (45 cm<sup>3</sup>) was maintained at room temperature for 2 hours, and then solid Na<sub>2</sub>CO<sub>3</sub> (30g) was added, followed by concentration in vacuo, dissolution in water, and repeated extraction with chloroform. The combined organic layers were dried over MgSO<sub>4</sub>. After removal of solvent the crude product was column chromatographed to give 6g of a pale yellow oil which was identified as the desired product (2).

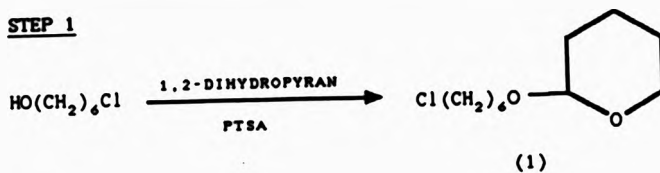
<sup>1</sup>H n.m.r :  $\delta$  ppm (CDCl<sub>3</sub>, 90 MHz), 1.4-2.1 (broad multiplet, 6H) methylene spacer units -CH<sub>2</sub>-, 2.565 (s, 1H) hydroxy OH, 3.45-4.1 (m, 21H) all the protons of the crown ring.

Ir :  $\nu$  (thin film), 3500-3400 (hydrogen bond O-H stretch), 3000-2800 (aliphatic C-H stretch), 1450 (-CH<sub>2</sub>-bend), 1150-1000 (C-O stretch) cm<sup>-1</sup>.

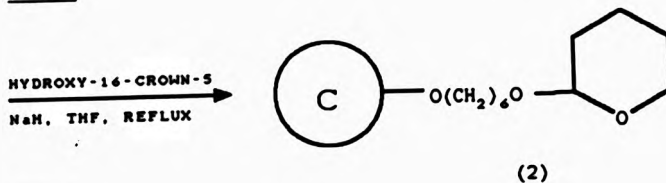


**3.4.3 Preparation of hydroxy-16-crown-5 derivative with  
6 methylene spacer units**

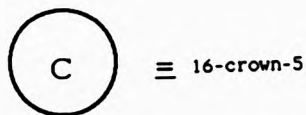
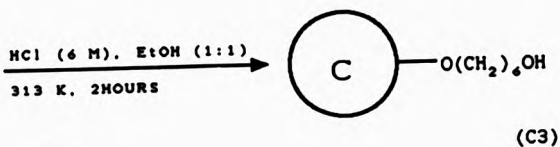
**STEP 1**



**STEP 2**



**STEP 3**



**Scheme 5**

(PTSA = p-toluene sulphonic acid)

**STEP 1: Tetrahydropyranyl ether of 6-chloro-hexan-1-ol**

To a stirred solution of freshly distilled 1,2-dihydropyran (20g, 238 mmol), at ice temperature, was added dropwise a mixture of 6-chloro-hexan-1-ol (13.65g, 100 mmol) and p-toluene sulphonic acid (85 mg). The solution was stirred for an additional 12 hours at room temperature after which aqueous NaHCO<sub>3</sub> (10% 100 cm<sup>3</sup>) was added. The resulting mixture was extracted with chloroform (3x100 cm<sup>3</sup>), dried over MgSO<sub>4</sub> and concentrated in vacuo to give an oil, which was vacuum distilled (b.pt. 69°C at 0.01 mmHg). This gave the protected chlorohydroxy alkane (1) (18.3g, 83%).

Ir spectrum showed a total absence of hydrogen bonded O-H stretch of the starting material and the appearance of C-O stretch at 1120 cm<sup>-1</sup> of the desired product.

**STEP 2 : Tetrahydropyranyl ether -protected 6-hydroxy  
hexyl-16-crown-5 (2)**

To a stirred suspension of dry NaH (1.44g, 0.06 mol) in dry THF (65 cm<sup>3</sup>) at room temperature under nitrogen gas was added hydroxy-16-crown-5 (Cl) (15g, 0.06 mol). The mixture was heated to reflux until evolution of

hydrogen gas had ceased. The protected alkane prepared above (1) (13.23g, 0.06 mol) was added dropwise (1/4 hour). The mixture was stirred under reflux condition for a further 12 hours. Upon cooling, the solvent was removed under vacuum and 80 cm<sup>3</sup> of water was added to the crude reaction mixture. The aqueous mixture was extracted several times with chloroform (3x100 cm<sup>3</sup>), dried over MgSO<sub>4</sub>, and concentrated in vacuo to give a viscous, pale yellow oil which was used in the next step without further purification.

**STEP 3 : Acid catalysed deprotection of compound (2)**

A solution of the above compound (12g), aqueous HCl (6M, 20 cm<sup>3</sup>), methanol (45 cm<sup>3</sup>) was maintained at room temperature for 2 hours, then solid Na<sub>2</sub>CO<sub>3</sub> (48g) was added followed by removal of water and methanol. This gave a solid which was dissolved in 100 cm<sup>3</sup> of water and extracted several times with chloroform (3x100 cm<sup>3</sup>). The combined extracts were dried and chloroform was removed under reduced pressure. The crude oil was column chromatographed to give a pale yellow oil which was characterised as the desired product (C3).

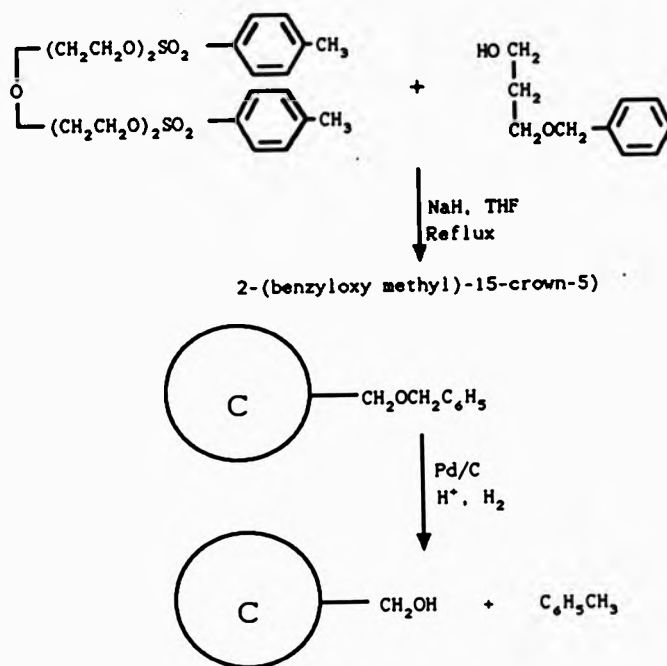
<sup>1</sup>H n.m.r :  $\delta$  ppm (CDCl<sub>3</sub>, 90 MHz R32), 1.4-2.1 (broad multiplet, 12H) methylene spacer units -CH<sub>2</sub>- , 2.6 (s,

1H) hydroxy OH, 3.45-4.1 (m, 21H) all of the protons of the crown ether.

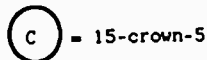
Ir :  $\nu$  (thin film), 3500-3400 (hydrogen bonded O-H stretch), 3000-2800 (aliphatic C-H stretch), 1450 ( $-\text{CH}_2$  bend), 1150-110 (C-O stretch)  $\text{cm}^{-1}$ .

### 3.4.4 Preparation of 2-hydroxy methyl-15-crown-5 (C4)

This was achieved according to the synthetic route suggested by Dishang et al.<sup>135</sup>. The cyclisation reaction leading to 2-(benzyloxy methyl)-15-crown-5, and subsequent hydrogenolysis applied to obtain the desired compound, are represented by the scheme shown below:



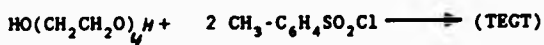
Scheme 6



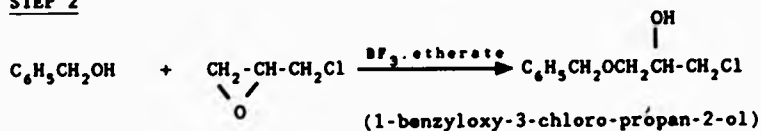
**3.4.4.1 Precursors for the preparation of 2-hydroxy methyl-15-crown-5**

The stepwise synthesis of the precursors to the cyclisation step is represented by the following equations:

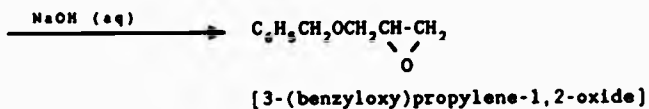
**STEP 1** Preparation of the ditosylate of tetraethylene glycol



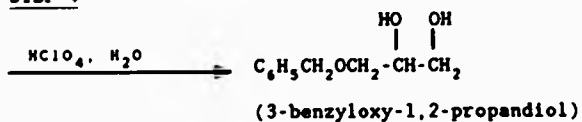
**STEP 2**



**STEP 3**



**STEP 4**



**Scheme 7**

### STEP 1: Tetraethylene glycol ditosylate (TEGT)

To a stirred solution of tetraethylene glycol (48g, 0.25 mol) and pyridine (40 cm<sup>3</sup>, two equivalents), p-toluene-sulphonyl chloride (152g, 0.8 mol) was added in portions, over a period of 1 hour, keeping the temperature below 293K. The mixture was left at room temperature for 24 hours. Sufficient water was added to dissolve the precipitated pyridinium chloride and to hydrolyse the excess p-toluene-sulphonyl chloride. The organic and aqueous layers were separated.

The aqueous phase was extracted repeatedly with diethyl ether (3 x 250 cm<sup>3</sup>). The organic layer was washed with water and sufficient ether was added to completely dissolve the organic material. The ether layer was collected and added to the accumulated extracts. This was further extracted from an aqueous solution of 75 cm<sup>3</sup> concentrated HCl in 250 cm<sup>3</sup>. The ether extracts were then washed with brine and dried over MgSO<sub>4</sub> until clear. The ether was removed on a rotary evaporator to afford 98g crude TEGT. Purification was achieved by extracting the impurities into boiling petroleum ether (40/60) to leave 50g of pure TEGT.

<sup>1</sup>H n.m.r. :  $\delta$  ppm (CDCl<sub>3</sub>, 90 MHz) 2.4 (s, 6H) the two methyl groups, 3.5 (m, 8H) ethylene protons of centre groups, 3.55-3.57 (m, 4H) S-O-CH<sub>2</sub>CH<sub>2</sub>, 4.05-4.25 (t, 4H)

S-O-CH<sub>2</sub>, 7.25-7.85 (m, 8H) aromatic protons.

Ir : 0 (thin film), 3050 (aromatic C-H stretch), 2950-2850 (aliphatic C-H stretch), 1925 and 1820 (overtones of the para substituted benzene ring 0, 1600 and 1500 (aromatic C=C), 1450 (-CH<sub>2</sub> bend), 1350 (S=O asym. stretch), 1175 (S=O stretch) cm<sup>-1</sup>.

**STEP 2: 1-Chloro-3-(benzyloxy)-propan-2-ol**

Benzyl alcohol (162.61g, 1.5 mol) was added to a stirred solution of 4.4 cm<sup>3</sup> freshly distilled BF<sub>3</sub>.Et<sub>2</sub>O (0.01 equiv.) under nitrogen. The temperature of the mixture was raised to 353K in an oil bath. Epichlorohydrin (138.80g, 1.5 mol) was added over a period of 1-2 hours and the reaction conditions were maintained for 20 hours. The mixture was cooled to room temperature, then 200 cm<sup>3</sup> of water was added and the mixture was repeatedly extracted with dichloromethane (3x250 cm<sup>3</sup>). The extracts were washed with brine and dried on a rotary evaporator and the crude product was purified by vacuum distillation (b.pt. 368-393 K, 0.09 mmHg).

<sup>1</sup>H n.m.r. : 8 ppm (CDCl<sub>3</sub>, 90 MHz), 2.9(broad singlet, 1H) proton of the asymmetric carbon, 3.4-3.7 (double



doublets, 4H)  $-\text{CH}_2-\text{CHOH}-\text{CH}_2$ , 3.9 (s, 1H) hydroxyl proton, 4.5 (s, 2H) benzylic protons, 7.3 (s, 5H) aromatic protons.

Ir :  $\delta$  (thin film), 3600-3150 (hydrogen bonded O-H stretch), 3100-3000 (aromatic C-H stretch), 2900-2850 (aliphatic C-H) 1950, 1875, 1815, 1600 and 1500 (overtones of the mono-substituted benzene ring), 1450 ( $-\text{CH}_2-$  bend), 1100 (C-O stretch), 750 (C-Cl stretch)  $\text{cm}^{-1}$ .

### STEP 3 : 3-(Benzoyloxy)propylene-1,2-oxide

153g of the halohydrin prepared above were cooled to about 278 K under nitrogen. Sodium hydroxide (76.26g of 50% aqueous NaOH solution, 0.95 mol) was added over a one hour period. The mixture was stirred for a further hour after addition until TLC analysis indicated the reaction to be complete. Water was added and the lower organic layer collected. The aqueous layer was extracted with dichloromethane (3 x 300  $\text{cm}^3$ ) and the combined extracts added to the organic phase. The mixture was washed with water until neutral and then washed with brine and finally dried over  $\text{MgSO}_4$ . The solvent was removed on a rotary evaporator to give 139g of the epoxide.

The crude material was used in the next step without any further purification.

**STEP 4 : 3-(benzyloxy)-1,2-propanediol**

The epoxide prepared above (135g, 0.83 mol), 750 cm<sup>3</sup> of water and 0.7 cm<sup>3</sup> of 74% HClO<sub>4</sub> solution were stirred for 15 hours at about 353 K. The solution was neutralised using a 5% solution of sodium carbonate and water was removed under reduced pressure. The crude oil was purified by vacuum distillation (b.pt. 120-136°C, 0.06 mmHg).

<sup>1</sup>H n.m.r : δ ppm (CDCl<sub>3</sub>, 90 MHz R32), 3-4 (m, 7H) (s, 5H), -O-CH<sub>2</sub>-CH-OHCH<sub>2</sub>OH, 4.5 (s, 2H) benzylic protons, 7.3 (s, 5H) aromatic protons.

Ir : δ (thin film), 3600-3100 (hydrogen bonded O-H stretch), 3100-3000 (aromatic C-H stretch), 2920-2860 (aliphatic C-H stretch), 1950, 1875 and 1800 (overtone due to mono-substituted benzene ring), 1600 and 1500 (aromatic C=C stretch), 1450 (-CH<sub>2</sub>- bend), 1125-1025 (C-O stretch) cm<sup>-1</sup>.

#### 3.4.4.2 Cyclisation to produce

##### 2-[benzyloxy(methyl)]-15-crown-5

4.16g of sodium hydroxide in oil (0.104 mol) were washed with 25 cm<sup>3</sup> petroleum ether (60/80) and with a similar amount of dry THF. The NaH was suspended in approximately 100 cm<sup>3</sup> dry THF under nitrogen. The suspension was heated to reflux. 3-(benzyloxy)-1,2-propanediol (4g, 0.023 mol) and TEGT (11.81g, 0.023 mol) were dissolved in about 35 cm<sup>3</sup> of THF and added to the refluxing suspension with vigorous stirring (over a period of 2-3 hours). Reflux and stirring were maintained for 24 hours. After cooling the precipitated salt was filtered off. The solvent was removed under reduced pressure leaving a pale yellow oil behind. A TLC analysis confirmed that the reaction had taken place with a mixture of products being achieved. The crude product was chromatographed. This gave 2.37g (33%) of the pure product.

<sup>1</sup>H n.m.r :  $\delta$  ppm (CDCl<sub>3</sub>, 90 MHz), 3.65 (m, 21H) crown protons plus the adjacent -CH<sub>2</sub>-, 4.55 (s, 2H) benzylic protons, 7.3 (s, 5H) aromatic protons.

Ir :  $\delta$  (thin film), 2850 (aliphatic stretch), 1950, 1875 (overtones of the mono-substituted benzene ring, 1600 and 1500 (aromatic C=C stretch), 1450 (-CH<sub>2</sub>- bend), 1150

(C-O stretch)  $\text{cm}^{-1}$ .

#### 3.4.4.3 2-(hydroxymethyl)-15-crown-5

2g of the compound prepared above were dissolved in approximately 150  $\text{cm}^3$  of ethanol and 0.11g of 10% Pd/C catalyst was added. Three drops of concentrated HCl were added and the mixture was stirred under 15 atm hydrogen for 48 hours.

The mixture was filtered through a thin bed of sollica gel and the solvent was then removed under reduced pressure. The product was purified by vacuum distillation (423 K, 0.01 mmHg) (yield > 90%).

$^1\text{H}$  n.m.r :  $\delta$  ppm ( $\text{CDCl}_3$ , 90 MHz), 2.45 (broad singlet, 1H) hydroxyl proton, 3.65 (m, 21H) crown ether and the adjacent  $-\text{CH}_2-$  protons.

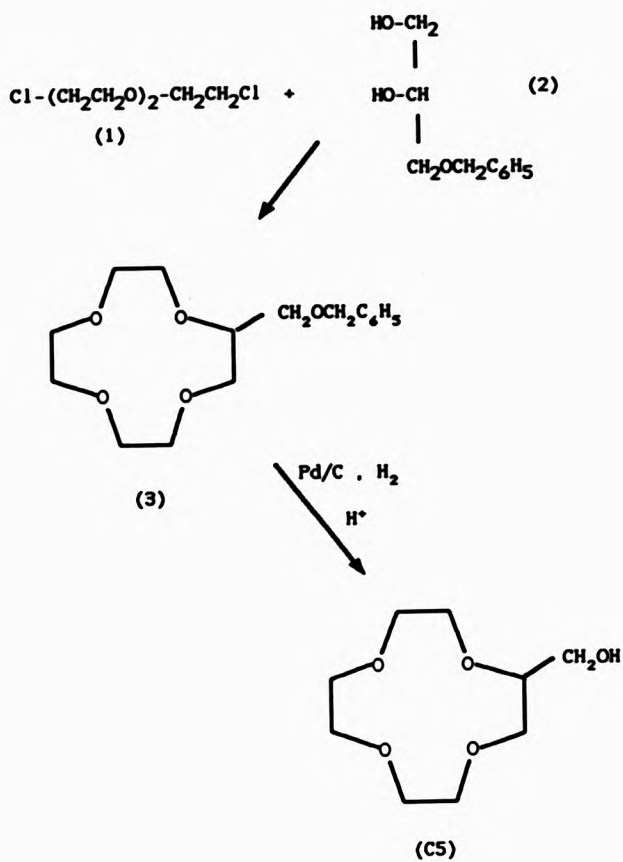
$^{13}\text{C}$  n.m.r :  $\delta$  ppm ( $\text{CDCl}_3$ , WP80 Bruker), 68.15 (t) methoxy carbon, 69.9-72 (m) all the secondary carbons in the crown ether ring, 79.85 (d) tertiary carbon coupled to the single proton.

Ir :  $\delta$  (thin film) , 3500-3000 (hydrogen bonded O-H stretch), 3000-2800 (aliphatic C-H stretch), 1450 ( $-\text{CH}_2-$

bend), 1350, 1300 and 1250 (C-C stretch), 1150 (C-O stretch)  $\text{cm}^{-1}$ .

### 3.4.5 Preparation of 2-hydroxymethyl-12-crown-4 (C5)

As a route to compound (C5) the reactions shown in scheme 5 were used according to the method suggested by Miyazaki et al.<sup>136</sup>.



The synthetic route to compound (2) was described in the previous section and the starting material (1) is commercially available (Aldrich).

Following is a typical procedure for the synthesis of 2-hydroxy-methyl-12-Crown-4.

#### 3.3.5.1 Preparation of benzyloxy methyl-12-Crown-4

A three necked flask equipped with a reflux condenser, a dropping funnel and a magnetic stirrer was charged with t-butyl alcohol (dry, 150 cm<sup>3</sup>) and metallic lithium (0.57g, 0.82 mol). After refluxing for an hour under stirring, 3-benzyloxy 1,2-propandiol (5g, 0.027 mol) was added dropwise, causing the solution to become cloudy because of the precipitation of the lithium salts of 3-benzyloxy-1,2-propandiol (2). To the above heterogeneous solution was added 1,8-dichloro-3,6-dioxanate (1) (5.14g, 0.027 mol) and LiBr.H<sub>2</sub>O (2.88g, 0.027 mol) successively. The heterogeneous reaction mixture was refluxed and stirred until the dichloride almost disappeared completely (as indicated by TLC). This usually took about 10-12 days. After the bulk of t-butyl alcohol had been evaporated under reduced pressure, a 10 cm<sup>3</sup> portion of water was added to the residue and extracted three times with a 10cm<sup>3</sup> portion of dichloromethane. The combined extracts

were dried over MgSO<sub>4</sub> (anhydrous). The solvent was removed under reduced pressure. The resulting pale yellow liquid was vacuum distilled giving 5.7g (70%): b.pt. 393-403K at 0.03 mmHg.

Spectral and elemental analysis confirmed the structure to be that of the desired compound.

<sup>1</sup>H n.m.r. :  $\delta$  ppm (CDCl<sub>3</sub>, 90 MHz), 3.48-3.90 (m, 17H) crown ether plus adjacent protons, 4.55 (s, 2H) benzylic protons, 7.25 (s, 5H) aromatic protons.

Ir :  $\nu$  (thin film) 3035 (aromatic C-C stretch), 2930-2870 (aliphatic C-H stretch), 1600 and 1500 (aromatic C=C stretch), 1100 (C-O stretch) cm<sup>-1</sup>.

**Elemental analysis:**

Found:	C, 64.70;	H, 8.22%
Calculated:	C, 64.86;	H, 8.16%

**3.4.5.2 Preparation of 2-hydroxy methyl-12-Crown-4 (C5)**

5g of the compound prepared above were hydrogenolysed according to the procedure previously described. After filtration and removal of solvent, the residue was vacuum distilled to yield 89% of the desired



product (b.pt. 383-385K, 0.01 mmHg).

Spectral and elemental analysis confirmed the successful synthesis and purity of the desired product.

$^1\text{H}$  n.m.r :  $\delta$  ppm ( $\text{CDCl}_3$ , 90 MHz), 3.05 (s, 1H) hydroxyl proton, 3.45-3.90 (m, 19H) crown ether protons plus adjacent methylene group.

$^{13}\text{C}$  n.m.r :  $\delta$  ppm ( $\text{CDCl}_3$ , WP80 Bruker), 68 (t) methoxy carbon, 60.9 72 (m) all the secondary carbons of the crown ether, 80 (d) tertiary carbon attached to a single proton.

Ir :  $\theta$  (thin film), 3500-3000 (hydrogen bonded O-H stretch), 3000-2800 (aliphatic stretch), 1450 ( $-\text{CH}_2-$  bend), 1150 (C-O stretch)  $\text{cm}^{-1}$ .

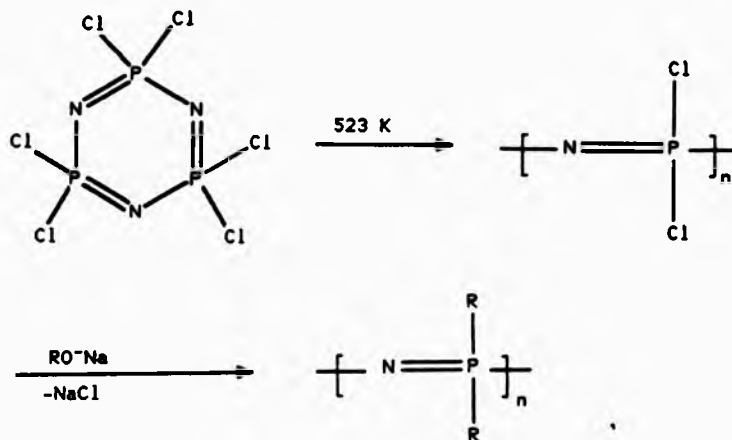
**Elemental analysis :**

found:	C, 52.21;	H, 9.08
calculated:	C, 52.41;	H, 8.80

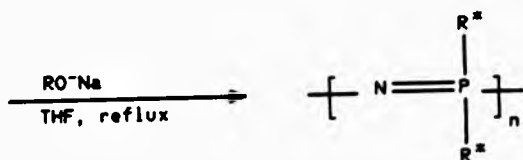
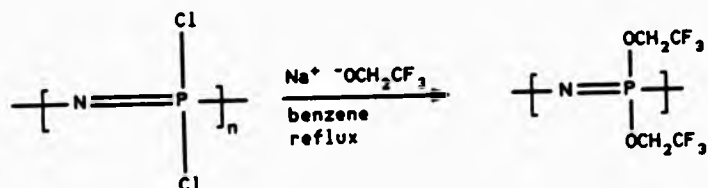
### 3.5 Preparation of polyphosphazenes with crown ether side chains

One of the main characteristics of the poly(organo phosphazene) systems is the ease with which different organic side groups can be attached into the macromolecular structure. This is the consequence of the substitutive mode of synthesis used for these polymers, as described by Allcock et al.<sup>137, 138</sup>.

Poly(organo phosphazene)s have been prepared generally, by the prior synthesis of a reactive high polymer namely poly(dichloro phosphazene) intermediate (2). This is achieved by thermal ring opening polymerisation of the corresponding cyclic trimer hexachlorocyclotriphosphazene (1), followed by nucleophilic replacement of the chlorine atoms by organic nucleophiles.



Poly(dichlorophosphazene) is susceptible to extensive hydrolysis and it has a tendency to crosslink in solution which seriously complicates its handling and storage. To overcome this problem we chose to prepare poly[bis(trifluoroethoxy)phosphazene]<sup>138</sup> (3) and by chemical modification, obtain the crown ether derivatives reported in this work. Polymer (3) is soluble in a variety of organic solvents; it is unaffected by water, and it can be kept at room temperature over a long period without change.



R\* = crown ether rings

### 3.5.1 Poly[bis(trifluoroethoxy)phosphazene] (3)

Hexachlorocyclotriphosphazene (Aldrich 99%) was used to prepare (3) as described by Allcock<sup>131</sup>.

The above trimer (30g) was placed in a glass tube which was evacuated for 30 minutes at a pressure of  $10^{-3}$  mmHg and then isolated from the vacuum line. The material was melted by applying heat and allowed to cool to solidify for 30 minutes. The degassing procedure was repeated 3 times before the tube was sealed and placed in a thermoregulated oven at 523 K for 24 hours after which it was cooled to room temperature. The tube was opened in a glove box and the sample was dissolved in 50 cm<sup>3</sup> of dry benzene. No attempt was made to purify the polymer from residual trimer and other oligomeric contaminants.

This solution was added over a period of 2 hours to a stirred solution of trifluoro ethoxide which was prepared from sodium (23g, ca. 1 mol) and dry trifluoroethanol (150g, 1.5 mol). When addition was complete, the mixture was refluxed for 24 hours. The cooled reaction mixture was acidified with HCl and filtered to remove polymer and NaCl. The salt was removed by repeated washing with boiling water. Finally the polymer was isolated by repeated reprecipitation from acetone into benzene.

A white elastic polymer was obtained (25g) which was

dried under vacuum at 333 K for 48 hours. The material was found to be soluble in THF, ethyl acetate, ethylene glycol, acetone, but not soluble in diethyl ether, dioxane, ethanol, and in aromatic hydrocarbons. It was also unaffected by water, strong acids or bases.

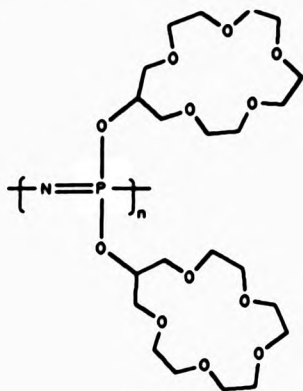
Ir :  $\epsilon$  (thin film),  $1280\text{ cm}^{-1}$  (N=P peak)

$^{31}\text{P}$  n.m.r : a single peak at 7.5 ppm

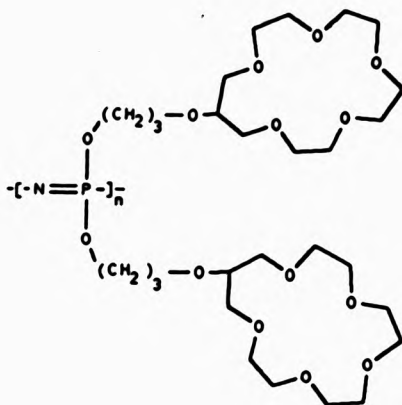
$T_g = 339\text{ K}$  and  $T_m = 515\text{ K}$

Literature molecular weight  $1,700,000\text{ gmol}^{-1}$

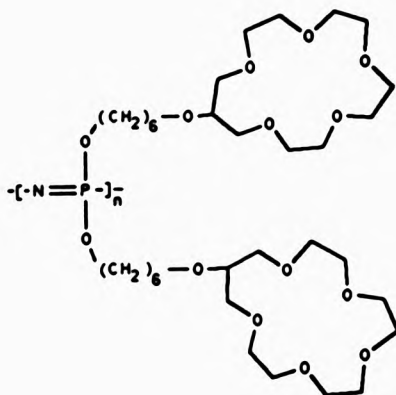
The following polymers were made according to the scheme outlined above:



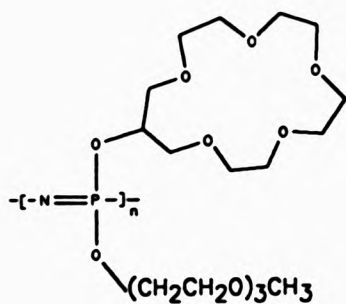
PPC1



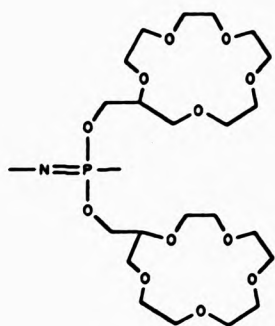
PPC2



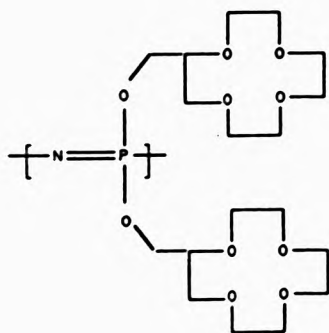
PPC3



PPC4



PPC5



PPC6

### 3.5.2 Preparation of polymers PPCl, PG2 and PPCl

All the polymeric compounds were prepared in the same manner. The following procedure is typical :

A solution of poly[bis(trifluoro ethoxy)phosphazene] (5g, 0.02 mol of monomeric unit) in 35 cm<sup>3</sup> of dry THF was added over a period of 2-3 hours at 333 K, under argon to a stirred solution of the sodium salt of the hydroxy-16-crown-5 (Cl) prepared from dry sodium hydride (1.68g, 0.07 mol) and the crown ether (20g, 0.08 mol) in 35 cm<sup>3</sup> of THF and 0.1g of tetrabutyl ammonium bromide. Heating under reflux was maintained for 4 days after which the mixture was cooled to room temperature and the solvent was evaporated under reduced pressure.

The high polymer was recovered by repeated extraction from acetone into hexane and further purified by dialysis against deionised water (5 litre) for 72 hours (water was changed every 12-15 hours). Finally water was removed on a rotary evaporator with toluene, and dried further under high vacuum at 343 K for 4 days.

The polymer obtained in this way was a pale yellow, highly viscous, transparent and sticky material which would flow only at elevated temperatures ( >383 K).

The material was found to be readily soluble in THF, ethyl acetate, methanol, water, but insoluble in aromatic and aliphatic hydrocarbons.



Polymers PFC2 and PFC3 were also prepared according to the procedure described above. The polymers had similar physical appearance and solubilities as that of PFC1.

Characterisation of PFC1:

$^1\text{H}$  n.m.r :  $\delta$  ppm ( $\text{CDCl}_3$ , WP80 Bruker), 3.8-4.8 (broad multiplet) protons of the crown ether rings.

$^{31}\text{P}$  n.m.r : a single peak at 7.7 ppm.

Ir :  $\nu$  (thin film), principle peaks observed at 3000-2800 (aliphatic C-H stretch), 1280 (N=P stretch), 1120 (C-O stretch)  $\text{cm}^{-1}$ .

Tg = 233 K

Characterisation of PFC2:

$^1\text{H}$  n.m.r :  $\delta$  ppm ( $\text{CDCl}_3$ , WP80, Bruker), 1.37-2.15 (broad multiplet, 12H) all the methylene spacer units, 3.45-4.2 (m, 42H) all the protons of the two crown ether rings.

$^{31}\text{P}$  : a single peak at 7.65 ppm

Ir :  $\nu$  (thin film), 3000-2800 (aliphatic C-H stretch),  
1450 ( $-\text{CH}_2-$  bend), 1280 (N=P stretch), 1150 (C-O

stretch),  $\text{cm}^{-1}$ .

$T_g = 226 \text{ K}$

#### Characterisation of PFC3:

$^1\text{H}$  n.m.r :  $\delta$  ppm ( $\text{CDCl}_3$ , WP80 Bruker), 1.4-2.4 (broad multiplet, 24H) methylene spacer units, 3.35-4.15 (m, 42H) all the protons of the crown ether rings.

$^{31}\text{P}$  : a single peak at 7.7 ppm

Ir :  $\theta$  (thin film), principle peaks at 3000-2800 (aliphatic C-H stretch), 1450 ( $-\text{CH}_2-$  bend), 1280 (N-P stretch), 1150 (C-O stretch)  $\text{cm}^{-1}$ .

$T_g = 224.5 \text{ K}$

#### 3.5.3 Preparation of the polymer PFC4

A mixture of freshly distilled triethylene glycol monomethyl ether (2.13g, 0.013 mol) and hydroxy-16-crown-5 (10g, 0.04 mol) (Cl) in 20  $\text{cm}^3$  of dry THF was gradually added to a suspension of dry NaH (1.3g, 0.053 mol) in 15  $\text{cm}^3$  of THF under nitrogen. The mixture was refluxed for approximately 1 hour with continuous stirring before poly[bis(trifluoro

ethaoxy)phosphazene] (5g, 0.02 moles of the monomeric unit) in 25 cm<sup>3</sup> of THF was added over a period of 2-3 hours. Finally 0.1g of tetrabutyl ammonium bromide was added and the mixture was left to reflux for 3 days after which the mixture was cooled to room temperature and solvent was evaporated.

The polymer was purified by using a similar procedure described for the other phosphazene polymers described in the previous section.

The polymer was found to be highly viscous, pale yellow and transparent material. Solubility of this material was found to be similar to the other phosphazene polymers described earlier.

<sup>1</sup>H n.m.r :  $\delta$  (CDCl<sub>3</sub>, WP80), 3.41 (s, 3H) methyl group protons, 4.45-4.2 (broad multiplet, 57H) all of the protons of EO units (linear and cyclic ether protons).

<sup>31</sup>P : a single peak at 7.7 ppm

Ir :  $\delta$  (thin film), principle peaks at 3000-2800 (aliphatic C-H stretch), 1285 (N-P stretch), 1120 (C-O stretch) cm<sup>-1</sup>.

Tg = 224 K.

#### 3.5.4 Preparation of the polymer PFC3

A similar experimental procedure described for the preparation of PFC1, PFC2, and PFC3 was used.

The polymer was a highly viscous material which was found to dissolve in a variety of organic solvents such as THF, chloroform, acetone methanol.

<sup>1</sup>H n.m.r :  $\delta$  ppm (CDCl<sub>3</sub>, WP80), 3.65 (m) crown ether and adjacent -CH<sub>2</sub>- protons.

<sup>13</sup>C n.m.r :  $\delta$  ppm (CDCl<sub>3</sub>, WP80 Bruker), 69.3 (t) methoxy carbon -CH<sub>2</sub>-, 69.9-73 (m) all secondary carbons in the crown ether rings, 80 (d) tertiary carbon coupled to the single proton.

<sup>31</sup>P : a single peak at 7,75 ppm.

Ir ;  $\theta$  (thin film), principle peaks at 3000-2800 (aliphatic C-H stretch), 1450 (-CH<sub>2</sub>- bend), 1350, 1300 and 1250 (C-C stretch), 1150 (C-O stretch), 1280 (N=P stretch), 1150 (C-O stretch) cm<sup>-1</sup>.

Tg = 228 K

### 3.5.5 Preparation of the polymer PFC6

The title polymer was prepared by the procedure described earlier. The material had a similar physical appearance to other phosphazene polymers reported in the previous sections. The polymer was characterised according to its physical properties.

$^1\text{H}$  n.m.r :  $\delta$  ppm ( $\text{CDCl}_3$ , WP80 Bruker), 3.45-3.9 (m) crown ether protons plus the adjacent methylene group.

$^{13}\text{C}$  :  $\delta$  ppm ( $\text{CDCl}_3$ , WP80 Bruker), 68.08 (t) methoxy carbon  $-\text{CH}_2-$ , 60-71.9 (m) all the secondary carbons of the polyether, 80 (d) tertiary carbon attached to a single proton.

CHAPTER FOUR

POLYVINYL ETHERS

#### 4.1 Polymer preparation

The first vinyl ether to be polymerised was reported over 100 years ago by Wislicenus<sup>159</sup> who treated ethyl vinyl ether with iodine and obtained a violent reaction giving a resinous material. Further studies<sup>160-163</sup> on this reaction indicated that I<sup>+</sup> is the active initiator and that carbonium ions are involved.

Reppe and co-workers<sup>164</sup> have described the polymerisation of a wide variety of vinyl ethers by acidic reagents used in small amounts. Some typical acidic reagents or catalysts used by Reppe are SnCl<sub>4</sub> , AlCl<sub>3</sub> , BF<sub>3</sub> , BF<sub>3</sub> complexes , FeCl<sub>3</sub> , ZnCl<sub>2</sub> , H<sub>2</sub>SO<sub>4</sub> , SO<sub>2</sub> , H<sub>3</sub>PO<sub>4</sub> , etc. The polymerisations were reported to be violent at room temperature and above, and afforded low molecular weight polymers.

Anionic catalysts fail to initiate polymerisation and free-radical initiators in bulk or solution give low molecular weight polymers.

Vinyl ethers copolymerise well with a wide variety of monomers (olefins, halo-olefins, alkoxy butadiene, acrylates, maleic anhydride, acrylonitrile, allyl, pyrrole, and vinyl carbazole, etc.) using free-radical ionic initiators or coordination-type catalysts<sup>165</sup>.

Vinyl ethers having oxyethylene chains  $[-(\text{CH}_2\text{CH}_2\text{O})_n-\text{CH}_2]$  as substituents, can readily be polymerised by various cationic initiators that were

mentioned above. Two common catalyst widely used are  $\text{BF}_3$ .etherate and  $\text{HI/I}_2$ . Polymerisation of these vinyl ethers by the former catalyst generally yields high molecular weight polymers with a broad molecular weight distribution (MWD), whereas  $\text{HI/I}_2$  leads to a very narrow distribution with  $M_w/M_n \leq 1.1^{18}$ .

The cationic polymerization of alkyl ethers is sensitive to oxygen containing impurities such as acetals, alcohols, aldehydes, and water in the monomer; removal of these impurities is largely effected by washing with water, drying over lime, and by distillation.<sup>19</sup>

The high reactivity of vinyl alkyl ethers is largely associated with the electron-donating properties of the alkoxy substituents, and it is not surprising that vinyl ethers with differing alkyl groups polymerize at different rates under given reaction conditions.

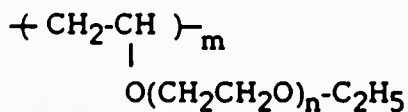
Apart from the binding properties of these materials with various metal ions, vinyl ether polymers are useful in lacquer resins, plasticizers, adhesives, paints, coatings, anticorrosion agents, thickening agents and many other applications.



#### 4.2 Formation of Polymer-salt complexes

Long before the discovery of crown ethers and their binding and transport of ionic solutes, non-cyclic poly(oxyethylenes) were known to bind cations of alkali metals and alkali earth metals<sup>140</sup>. Detailed knowledge is available for their ion binding properties as a function of the number of oxyethylene units per molecule and the structure of end groups<sup>141</sup>. Poly(oxyethylene)-containing compounds have been designed and examined as carriers for metal-ion transport and as phase transport catalysts; examples include a telechelic poly(oxyethylene) capped with strongly coordinating end groups ("non-cyclic crown ether")<sup>142</sup> and "polypod ligands" that carry 3-6 poly(oxyethylene) chains in one molecule<sup>143, 144</sup>.

Comb-like Poly(oxyethylenes) prepared by cationic polymerisation of vinyl ethers carrying a pendant poly(oxyethylene)<sup>132</sup>, have been shown to transport alkali metals across liquid membranes<sup>145</sup>.



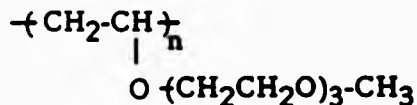
X : n = 0  
Y : n = 2  
Z : n = 4

Higashimura and co-workers<sup>145</sup> have clearly established that the polymer with four EO units per side chain (n=4) transports all of the alkali metal ions but shows particular selectivity for K<sup>+</sup>. Further more the material was more effective as an ion carrier than its non-polymeric counterpart (tetraglyme). The observed polymeric effect was thought to be due to enhancement of ion transport via a cooperative action of the neighbouring poly(oxyethylene) side chains. For all metal cations studied by the above authors, the ion transport increased in the order:



Z was reported to be more or less selective for K<sup>+</sup>, ca. 12 times more effective than Y, whereas Y and X showed almost no selectivity for ion size.

The ability of these materials to dissociate alkali metal salts and the possibility that these may actually form polymer-salt complexes with low glass transition temperatures, were utilised by Cowie and Martin<sup>101,102</sup> to obtain a highly ion-conducting system. The polymer electrolyte reported by the above workers consisted of three oxyethylene units with a terminal methoxy group:



In polymer-salt complexes prepared from EO substituted itaconic acid polymers<sup>94</sup>, and some other polymer electrolytes the conductivity levels have been reported to increase with the length of the sidechain. Generally the optimum chain length of seven EO units is understood to give the optimum conductivity level. For the values higher than seven, a crystallisation exotherm is generally noted for the polymer host itself. The glass transition temperature decreases (with subsequent increase in ion mobility) as the EO chain length increase to seven.

Bearing these points in mind, and in view of a high degree of conductivity exhibited by the above poly vinyl ether electrolyte, it was therefore possible to prepare a series of materials where the number of EO units were increased. The desirability of designing further flexibility in these polymer electrolyte mixtures also means that they would be predominately viscous liquids that will be mechanically weak. However, they can be transformed into rubber-like films by crosslinking (described in chapter 3).

The work presented in the following chapters 5, 6 and 7 discusses both the effect of crosslinking using a flexible divinyl ether, and sidechain extension on a.c. conductivity and other physical properties of poly(vinyl ether) electrolytes.

CHAPTER FIVE

EFFECT OF CROSSLINKING ON THE A.C.

CONDUCTIVITY OF POLYVINYL ETHERS

### 5.1 Swelling studies

The swelling behaviour of a sample with a nominal 5% crosslinking was examined in a selection of liquids and the effectiveness of each was estimated from the weight absorbed per g of polymer. The results obtained were an average of three measurements at 292 K and are shown in Table 5.1.1

Chloroform is clearly the best in the group and the non polar hexane is the least effective. While not the best swelling agent, methanol was selected for doping purposes because it was a good solvent for the salt (avoiding water) and , because it is relatively volatile, it can be removed easily from the polymer-salt mixture during sample preparation. The swelling characteristics of the networks in methanol with apparent per cent crosslinking varying from 0.2% to 11%, are also shown in the second columns of the Table 5.1.1. The amount of methanol absorbed decreases with increasing per cent crosslinking and appears to approach an asymptotic limit in this solvent around 11% crosslinking, as can be seen from Figure 5.1.1.

Liquid	Weight absorbed liquid /g 5% crosslinked polymer	Apparent % Crosslinking	Weight MeOH absorbed/g polymer
Hexane	0.25	0.2	6.95
Methanol	2.57	1.2	4.53
Ethanol	4.66	2.0	3.66
Water	6.46	5.0	2.57
Chloroform	14.67	11.0	1.99

TABLE 5.1.1 Swelling characteristics of the polymer as function of apparent % crosslinking and for a 5% crosslinked sample in several samples.

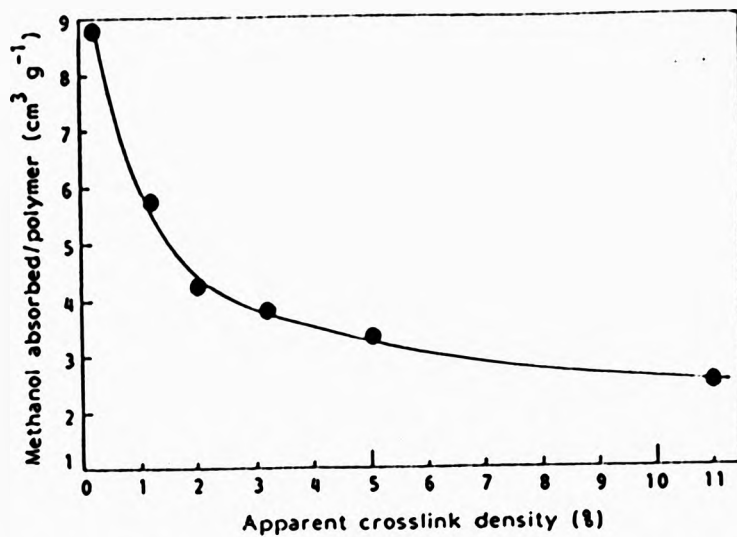


Figure 5.1.1 Volume of methanol absorbed by 1g of polymer measured at different levels of apparent per cent crosslinking.

## 5.2 Glass transition studies

When a polymeric material is progressively crosslinked the T<sub>g</sub> of the network increases because of the restrictions imposed by the crosslinks on the freedom of motion of the polymer backbone. Samples with apparent per cent crosslinking of up to about 100% were prepared and the values of T<sub>g</sub> rose steadily, but not uniformly, by about 125 K as can be seen in Table 5.2.1.

After an initial small increase of 5 K the T<sub>g</sub> seemed to remain constant between 1% and 5% crosslinking after which there was a sharper rise up to 11% which slowed down at higher crosslink densities. However, one can not read too much into these trends as the per cent crosslinking is only an apparent value and may not be particularly accurate.

## 5.3 Effect of salt addition on T<sub>g</sub>

The results shown above are for salt free polymers but the addition of salt to the network also introduces a second (non covalent) type of crosslink where the cations coordinate with ether oxygens of the side chains to form intermolecular interactions which lead to a more rigid structure. The effect can be seen in the data reported in Table 5.3.1 for samples with varying



crosslink densities and salt concentrations which can be compared with an uncrosslinked sample.

On addition of Lithium perchlorate to each of the polymers a non-linear increase in  $T_g$  occurs with increasing salt concentration. At high salt concentrations a plateau value of  $T_g$  begins to occur (see Figures 5.3.1 to 5.3.7). This effect is indicative of the solubility limit of the salt in the polymers. For the lightly crosslinked polymers (up to 5%) this solubility limit is reached at salt concentrations higher than  $[M^+]/[EO] = 0.25$ . However for the 11% crosslinked material this limit seems to be significantly lower ( $[M^+]/[EO] = 0.125$ ).

Unlike the other polymer salt complexes reported above the  $T_g$  versus salt concentration plot of the 11% crosslinked polymer salt complex showed a marked inflexion at about ( $[M^+] / [EO] = 0.025$ ). This behaviour may be indicative of two overlapping coordination processes occurring simultaneously. At a particular salt concentration it can be suggested that a transition from one dominant coordination process to another may occur. A changeover from a predominately crosslinking to a predominately sidechain stiffening coordination process can be suggested as the reason for the noted irregular enhancement of  $T_g$  with salt concentration exhibited by this complex.

It is difficult to envisage how it may be confirmed

Apparent per cent crosslinking	Tg / K	Apparent per cent crosslinking	Tg / K
0	206	7.0	215
0.2	206	9.0	219
2.0	210	11.0	226
3.0	211	40.0	241
5.0	211	100.0	331

TABLE 5.2.1 Variation of Tg with apparent percent crosslinking

which of these two processes occurs initially at low salt concentrations and which occurs on incorporation of high concentration of salt. From the work presented above the following generalisation can be made:

1. The networks swell extensively when exposed to variety of solvents and this feature was used to prepare polymer salt mixtures.
2. Due to progressive crosslinking the  $T_g$  of the networks rose steadily. After an initial small increase of 5 K the  $T_g$  seemed to remain constant up to 5% crosslinking after which there was a sharper rise up to 11% which slowed down at higher crosslink densities.
3. All of the polymeric materials discussed above have an ability to form complexes with  $LiClO_4$ .
4. A loss of flexibility is noted in each of the polymeric hosts on dissolution of salt. This effect is increased as the number of cations solvated by the polymer is increased until at the solubility limit of the salt in the polymer no loss of flexibility occurs.
5. The loss of flexibility noted in the polymer on addition of a particular concentration of salt was found to be similar for the lightly crosslinked materials (up to 5% crosslinked).
6. As the salt concentration was increased in the 11%

crosslinked polymer there appeared to be a transition from one predominant coordination process to another at a concentration of salt particular to that complex.

Apparent % Crosslinking	T <sub>g</sub> / K								
	$\frac{[Li^+]}{[EO]}$	0	0.0125	0.025	0.05	0.125	0.25		
0		206	216	224	238	260	280		
0.2		206	216	220	239	259	282		
3.25		210	220	223	236	263	285		
5.0		211	223	226	238	264	287		
11.0		226	236	239	264	274	-		

TABLE 5.3.1 The effect of added salt on the T<sub>g</sub> of uncrosslinked and crosslinked samples of PVO<sub>3</sub>.

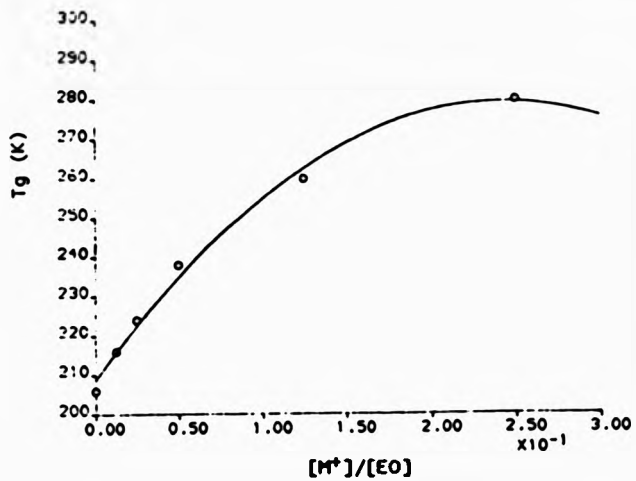


Figure 5.3.1 Plot of T<sub>g</sub> against salt concentration for the uncrosslinked PVO<sub>3</sub>/LiClO<sub>4</sub> mixtures.

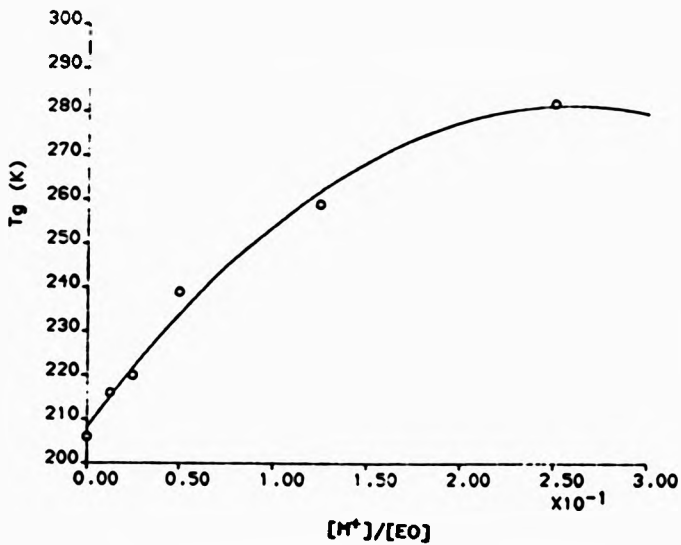


Figure 5.3.2 Plot of T<sub>g</sub> vs salt concentration for the 0.2% crosslinked PVO<sub>3</sub>/LiClO<sub>4</sub> mixtures.

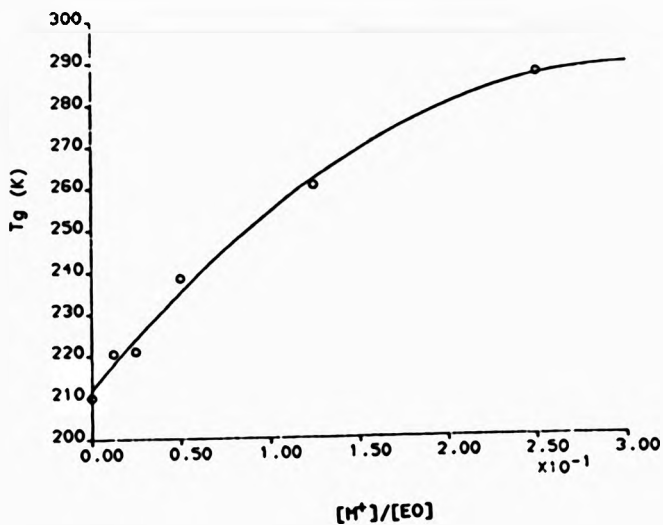


Figure 5.3.3 Plot of  $T_g$  vs salt concentration for the 1.2% crosslinked  $PVO_3/LiClO_4$  mixtures.

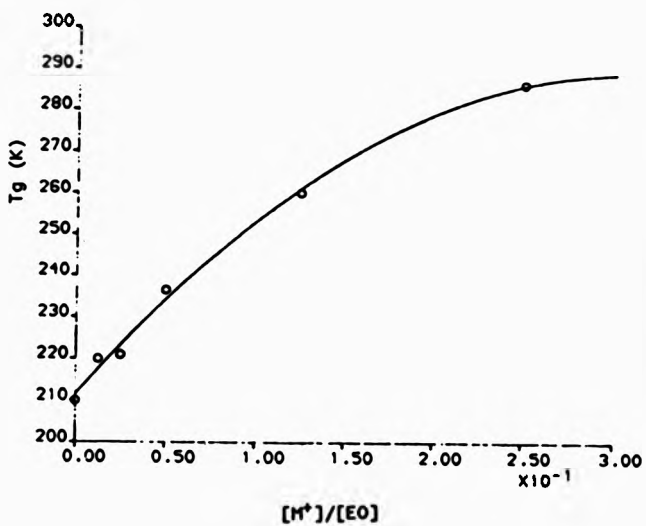


Figure 5.3.4 Plot of  $T_g$  vs salt concentration for the 2% crosslinked  $PVO_3/LiClO_4$  mixtures.

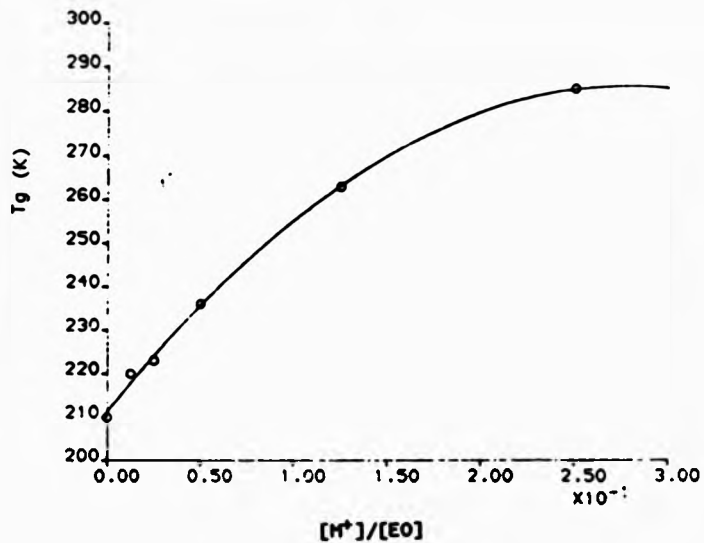


Figure 5.3.5 Plot of  $T_g$  vs salt concentration for the 3.25% crosslinked  $PVO_3/LiClO_4$  mixture.

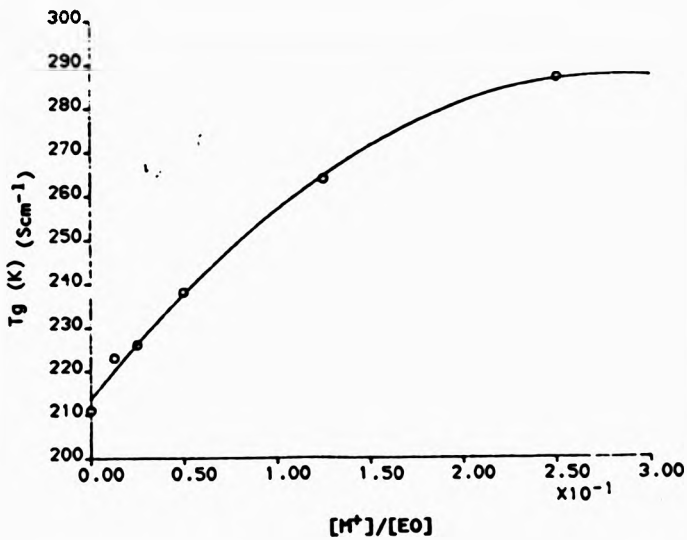
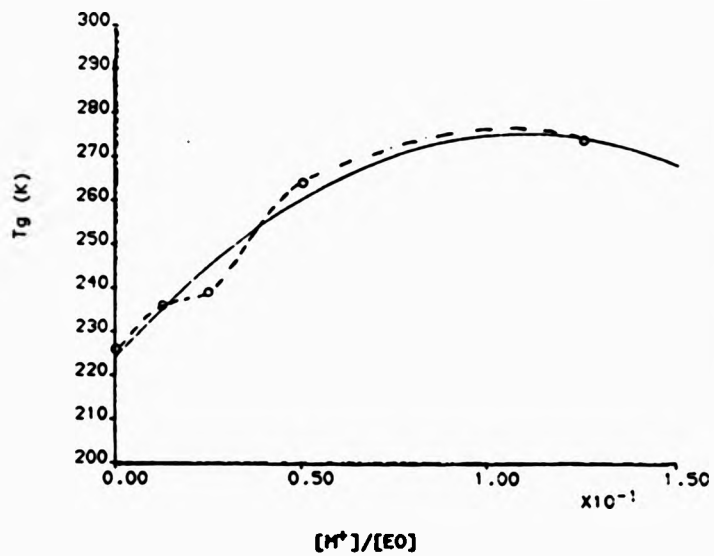


Figure 5.3.6 Plot of  $T_g$  vs salt concentration for the 5% crosslinked  $PVO_3/LiClO_4$  mixtures.





**Figure 5.3.7** Plot of  $T_g$  against salt concentration for the 11% crosslinked  $PVO_2/LiClO_4$  mixtures.

#### 5.4 Effect of crosslinking on conductivity

The conductivity levels measured for each of the undoped polymers were less than  $10^{-9} \text{ Scm}^{-1}$ , throughout the temperature range.

Since each of the polymeric hosts showed the ability to solvate metal cations the conductivities exhibited by the  $\text{LiClO}_4$  complexes of these materials were measured as a function of increasing temperature.

In Figures 5.4.1 to 5.4.5 log conductivity/reciprocal temperature data obtained for an uncrosslinked sample and networks with apparent crosslink densities of 0.2%, 1.2%, 2%, 5% and 11% are shown. The dependence of log  $\sigma$  on salt concentration is also apparent from the same figures.

From initial examination of the plots it can be seen that the conductivity of a particular complex increases as the temperature is increased but since curved lines were obtained the complexes do not exhibit Arrhenius behaviour in the temperature range studied. The only exception is for some of the data of the 11% crosslinking where there is an approach to Arrhenius behaviour. It can also be noted that at a particular temperature the most conductive materials are not always the richest in salt.

A comparison of the temperature dependence of the  $\log \sigma$  (conductivity) for an uncrosslinked sample and

networks with apparent crosslink densities of 2% , 5% , and 11% at a fixed value of  $[Li^+]/[EO] = 0.05$ , is shown in Figure 5.4.6. There is virtually no change in conductivity up to 5% crosslinking and only when this increases to 11% is there a noticeable decrease in  $\log \sigma$ .

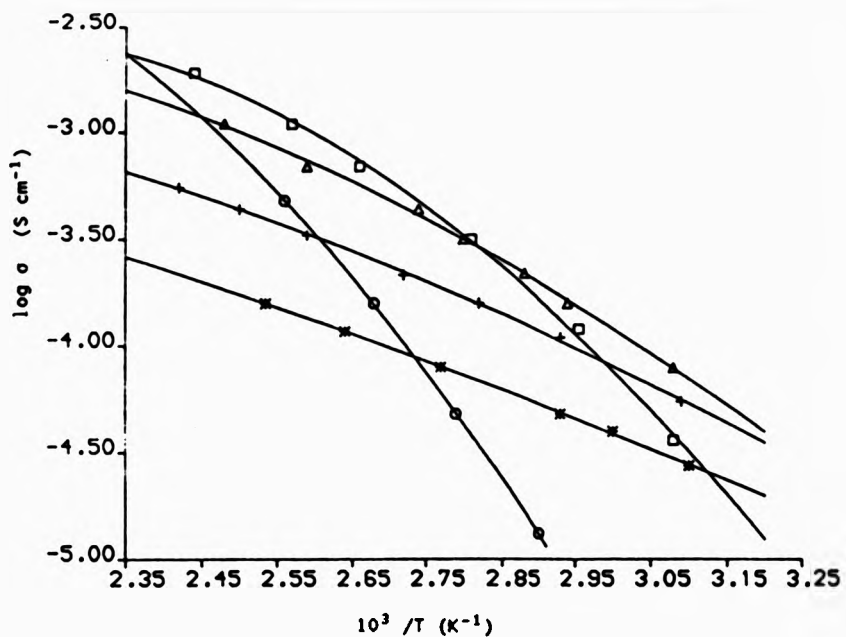


Figure 5.4.1 Arrhenius plot of log conductivity against reciprocal temperature for the uncrosslinked PVO<sub>3</sub>/LiClO<sub>4</sub> mixtures.

[M\*]/[EO] ratios: 0.0125 (\*)  
 0.0250 (x)  
 0.0500 (Δ)  
 0.0125 (□)  
 0.2500 (o)

5.4.2

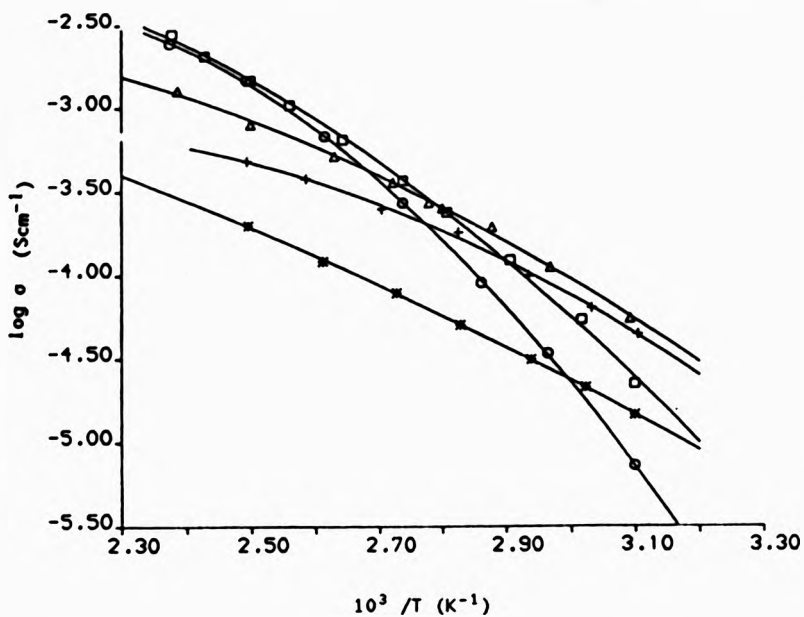


Figure 5.4.2 Arrhenius plot of log conductivity against reciprocal temperature for 0.2% crosslinked  $\text{PVO}_3/\text{LiClO}_4$  mixture.

$[\text{M}^+]/[\text{EO}]$  ratios: 0.0125 (\*),  
0.0250 (x),  
0.0500 (Δ),  
0.1250 (◻),  
0.2500 (○).

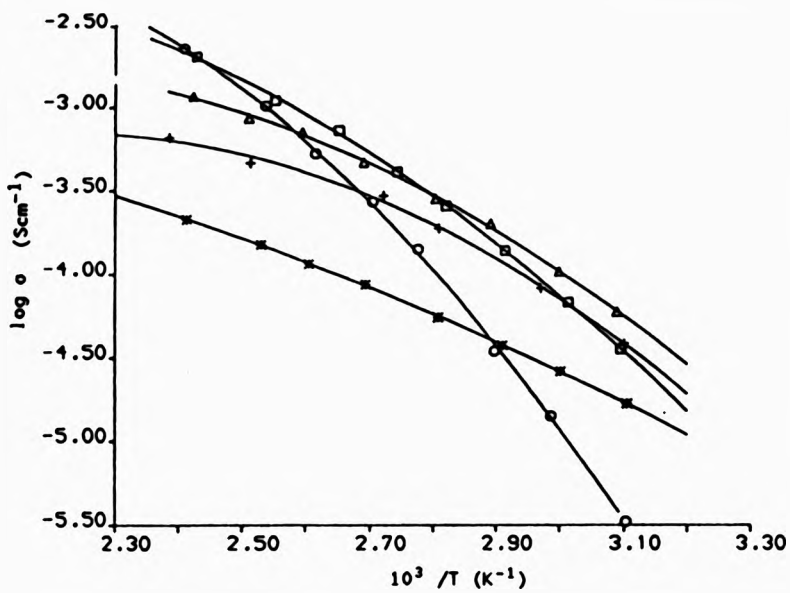


Figure 5.4.3 Arrhenius plot of log conductivity against reciprocal temperature for the 5% crosslinked  $\text{PVO}_3/\text{LiClO}_4$  mixtures.

$[\text{M}^+]/[\text{EO}]$  ratios: 0.0125 (\*)  
 0.0250 (x)  
 0.0500 (Δ)  
 0.0125 (□)  
 0.2500 (o)

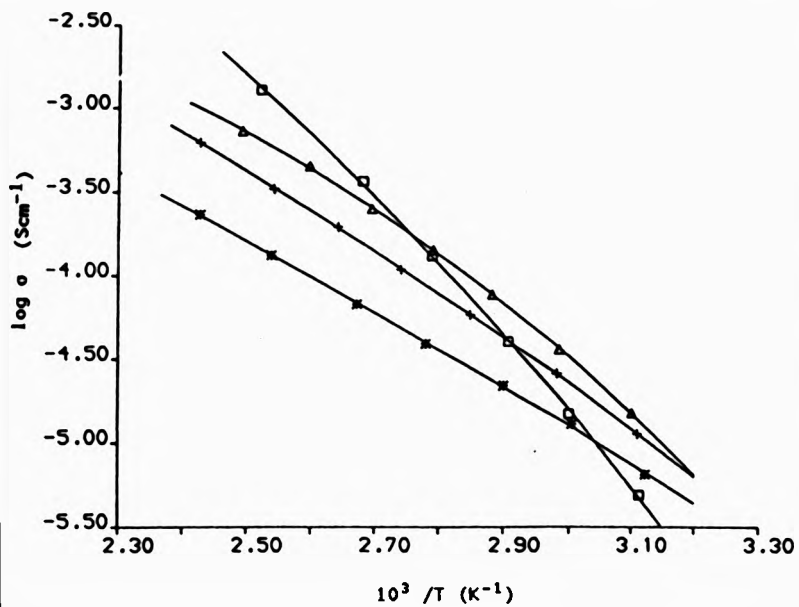


Figure 5.4.5 Arrhenius plot of log conductivity against reciprocal temperature for 11% crosslinked  $\text{PVO}_3/\text{LiClO}_4$  mixture.

$[\text{M}^+]/[\text{EO}]$  ratios:

0.0125 (\*),

0.0250 (x),

0.0500 ( $\Delta$ ),

0.1250 (O).

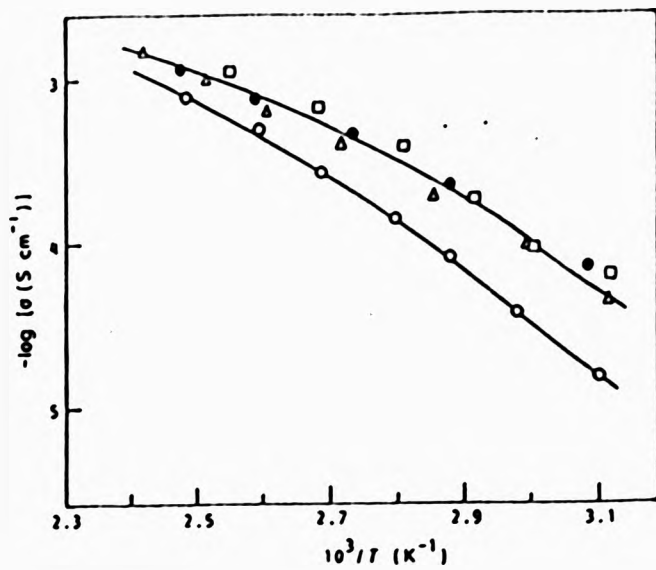


Figure 5.4.6 Temperature dependence of  $\log \sigma$  for networks at a fixed salt concentration of  $[Li^+]/[EO] = 0.05$ . Apparent per cent crosslinking:

( $\circ$ ), 0%; ( $\Delta$ ), 2%; ( $\square$ ), 5%; ( $\circ$ ), 11% .



### 5.5 Isothermal conductivity

It is clear from the Figures 5.4.1 to 5.4.5 conductivity varies with both temperature and salt concentration. The latter dependence is easily illustrated by examining isothermal sections of the log  $\sigma$  versus salt concentration data as shown in Figures 5.5.1 to 5.5.5. For all of the polymer complexes under study here a maximum in conductivity was observed which moves to higher concentrations as the temperature is increased.

Angell and Bressel<sup>146</sup> have rationalized this behaviour on the basis of an isothermal version of the VTF equation

$$\sigma = A X \exp \left[ \frac{K}{Q (X_0 - X)} \right] \quad (11)$$

where  $Q = (dT_g/dX)$ ,  $X$  is the mole fraction of salt and  $X_0$  is the mole fraction of salt at  $T_g = T$ . The dependence of conductivity on salt concentration can then be estimated from equation (11) and results have been shown in good agreement with the experimental data, but the significance of the parameter is less obvious. The pre exponential factor  $A$  is usually regarded as being inversely proportional to the number of charge carriers in the system and will decrease as the number of charge carriers increases.

Angell<sup>147</sup> has proposed that the maximum in conductivity is caused by two opposing effects. First there is a build up of charge carriers as more salt is added but this is eventually offset by the increase in  $T_g$  and the consequential reduction in ion mobility which will impede ion movement. As the temperature increases the chains will become more mobile and the maximum moves to higher salt concentration. While this explanation is reasonable, but it is not the whole answer.

The conductivity data can be plotted at constant chain flexibility as shown in Figures 5.5.6 to 5.5.8, where  $\log \sigma$  is presented as a function of constant  $(T - T_g)$  values for all of the samples. This eliminates the effect of  $T_g$  by comparing conductivities at different salt concentrations but at constant temperature above the  $T_g$  of each polymer/salt mixture. The maxima are still observed although they now appear to have moved to higher but essentially constant, salt concentrations.

By examining the complexes under conditions of constant reduced temperature, it is therefore possible to consider the conductivities exhibited when the mobility of the polymer is the same in each polymer-salt mixture. Due to the common salt ( $\text{LiClO}_4$ ) in the materials, if differences are noted in the conductivity then these will result from the differences in the number of charge carriers in the complex. Two isothermal plots at  $(T_g + 100)$  &  $(T_g + 150)$  are shown in Figure

5.5.9 which indicate that the response of the uncrosslinked and crosslinked samples including the 11% is essentially identical at comparable chain flexibilities. This indicates that the number of charge carriers in the 11% crosslinked polymer/salt mixture is comparable with those of the lightly crosslinked systems.

This also suggests that the dissociation of the salt and therefore the number of charge carriers in all the samples are very similar. It seems as if the mobility of the ethylene oxide sidechains has not been seriously affected despite extensive crosslinking. This is an interesting point which implies that the significant drop in bulk conductivity noted for the 11% crosslinked sample, under normal conditions, is basically due to the reduced flexibility of the polymer backbone.

The data presented here confirms the previous findings that in polymer-electrolytes the ionic conduction takes place through the disordered part of the polymer matrix and is assisted by large-amplitude segmental motion of the polymer backbone.

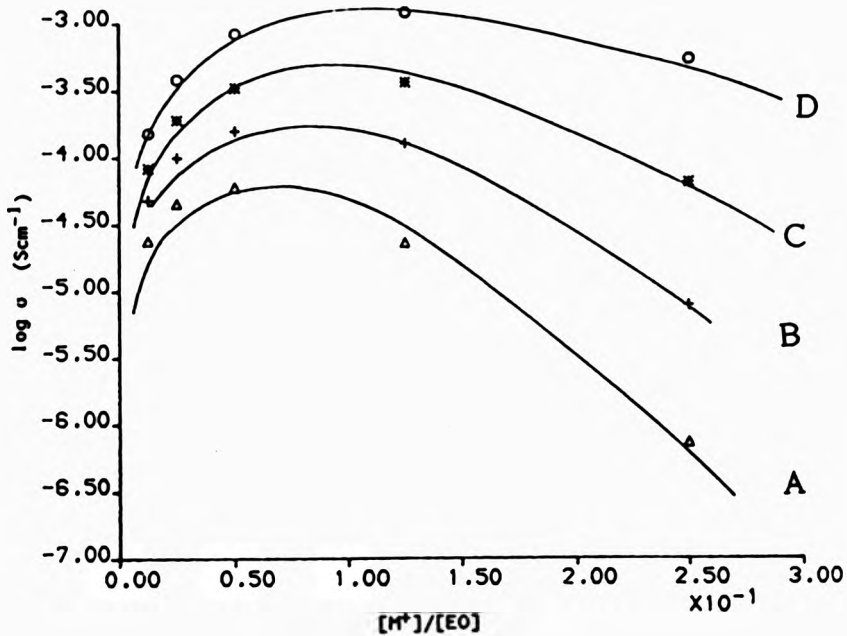


Figure 5.5.1

Isothermal variation of log conductivity with salt concentration ( $\text{LiClO}_4$ ) for uncrosslinked  $\text{PVO}_3$ , measured at temperatures of curve:

A, 320 K; B, 340 K; and C, 360 K, and D, 392.15 K.

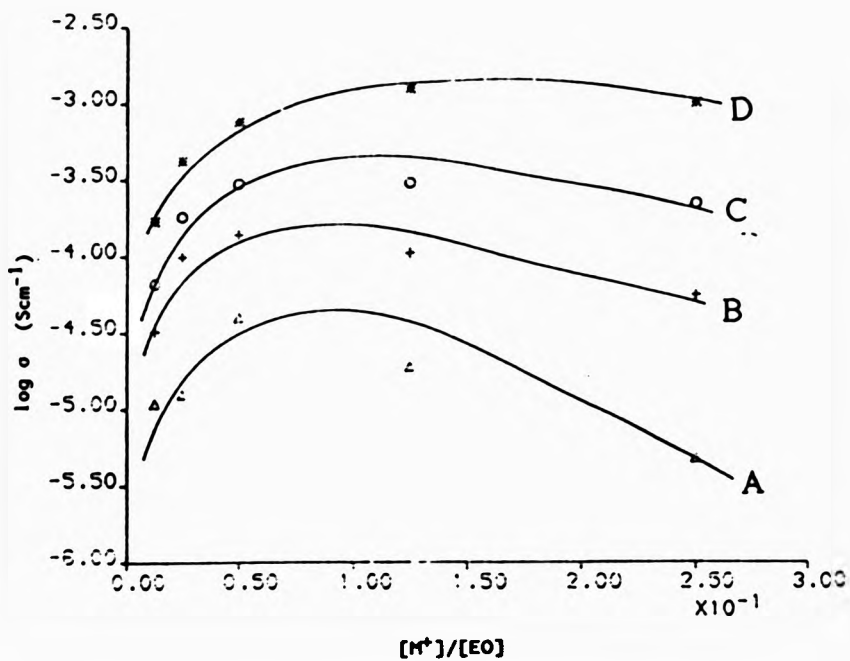
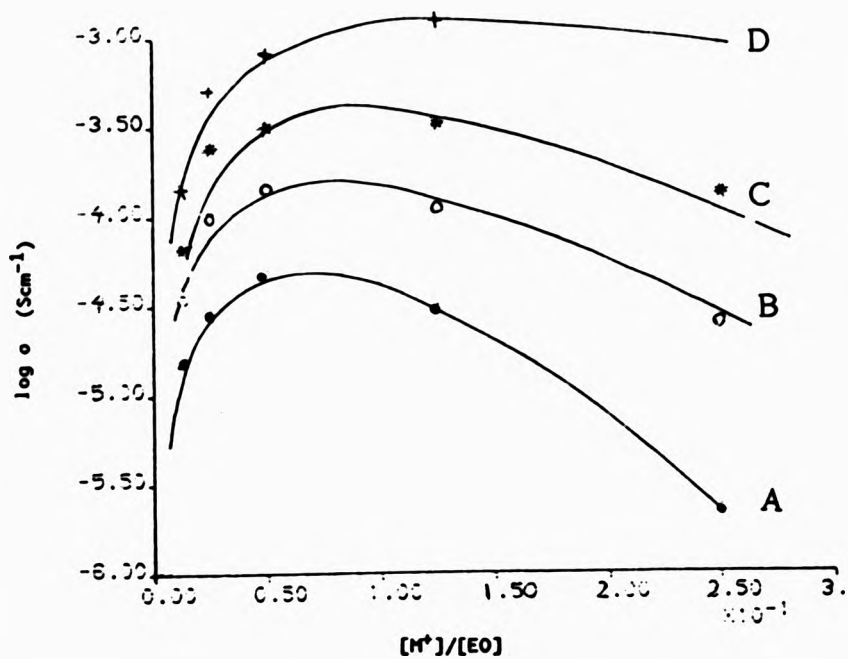


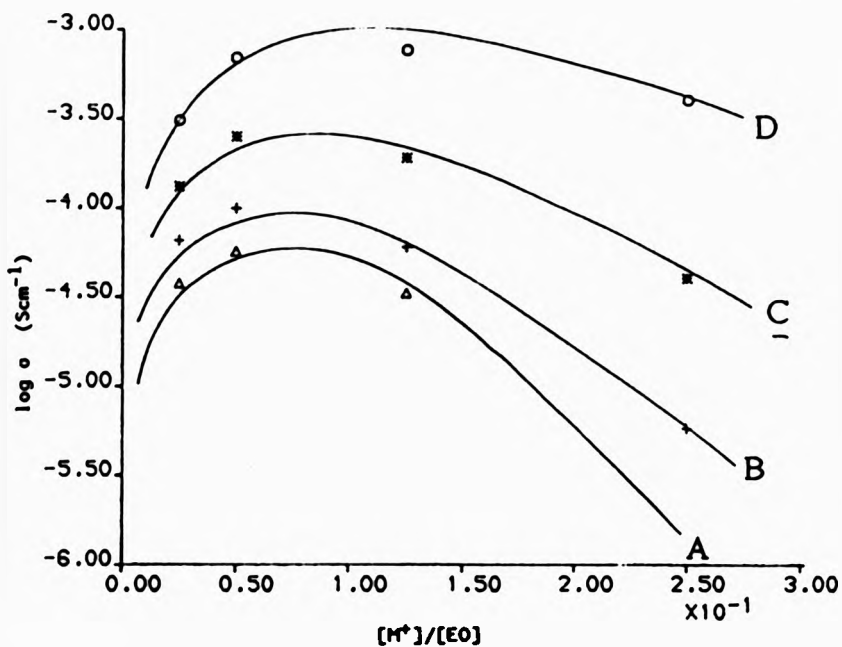
Figure 5.5.2

Isothermal variation of log conductivity with salt concentration ( $\text{LiClO}_4$ ) for 0.2% crosslinked  $\text{PVO}_3$ , measured at temperatures of curve:

A, 320 K; B, 340 K; and C, 360 K, and D, 392.15 K.



**Figure 5.5.3**  
 Isothermal variation of log conductivity with salt concentration ( $\text{LiClO}_4$ ) for 1.2% crosslinked  $\text{PVO}_2$ , measured at temperatures of curve: A, 320 K; B, 340 K; and C, 360 K, and D, 392.15 K.



**Figure 5.5.4**  
 Isothermal variation of log conductivity with salt concentration ( $\text{LiClO}_4$ ) for 5% crosslinked  $\text{PVO}_3$  measured at temperatures of curve: A, 320 K; B, 340 K; and C, 360 K, and D, 392.15 K.

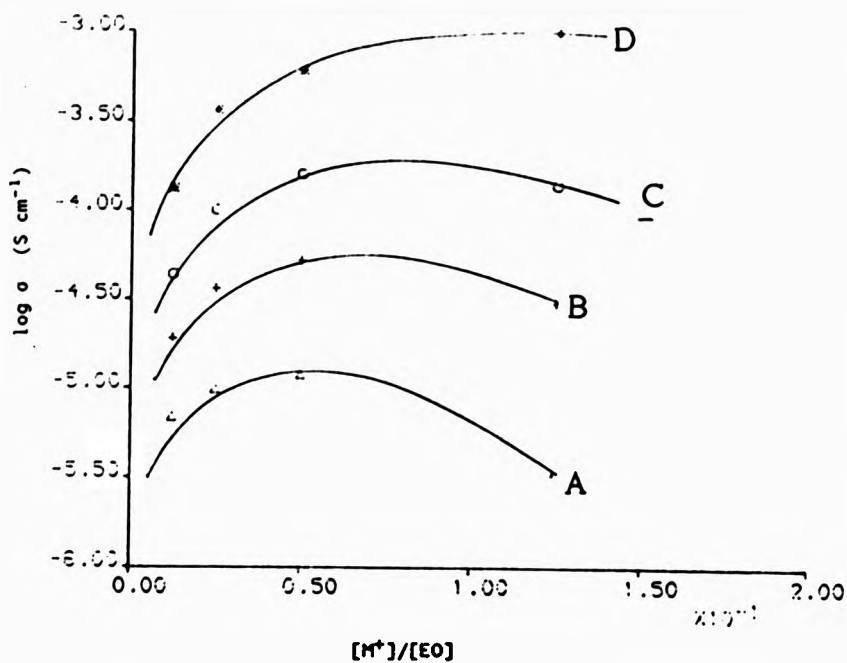


Figure 5.5.5

Isothermal variation of log conductivity with salt concentration ( $LiClO_4$ ) for 5% crosslinked  $PVO_3$ , measured at temperatures of curve:

A: 320 K, B: 340 K, C: 360 K, D: 392.15 K



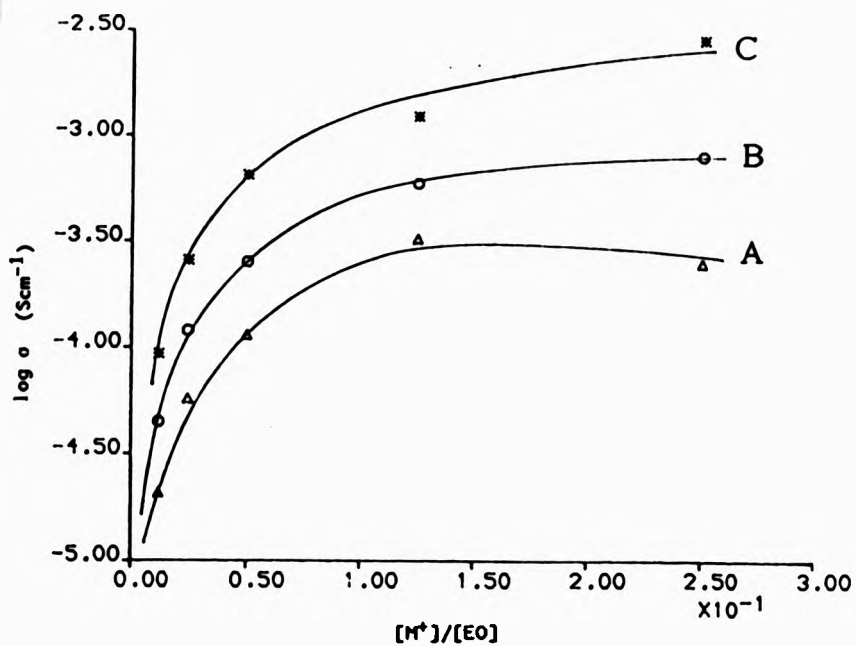


Figure 5.5.6 Plot of  $\log \sigma$  against salt concentration for uncrosslinked  $\text{PVO}_3/\text{LiClO}_4$  mixtures under various constant reduced temperature conditions.

A:  $T_g + 100 \text{ K}$       B:  $T_g + 130 \text{ K}$       C:  $T_g + 150 \text{ K}$

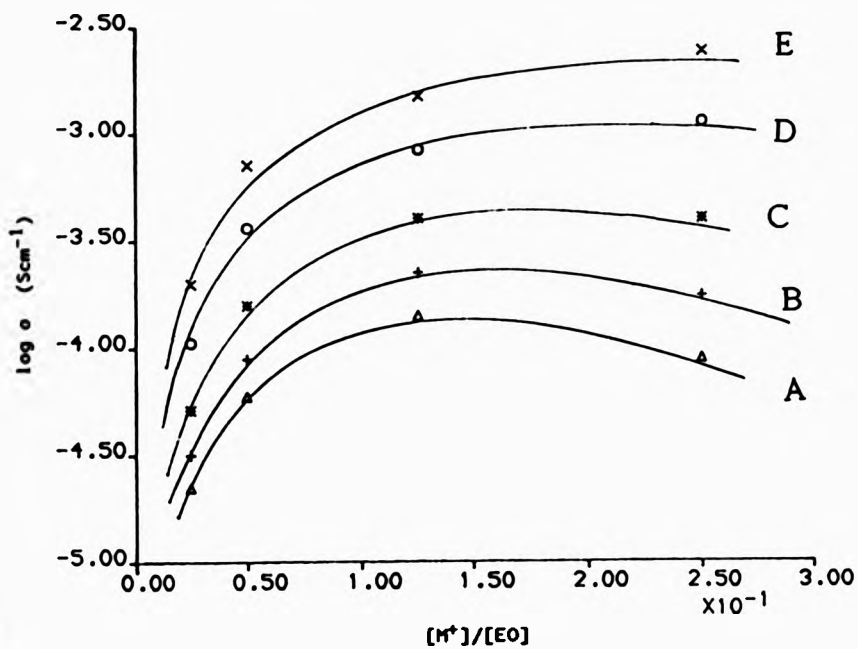


Figure 5.5.7 Plot of  $\log \sigma$  against salt concentration for 5% crosslinked  $\text{PVO}_3/\text{LiClO}_4$  mixtures under various constant reduced temperature conditions.

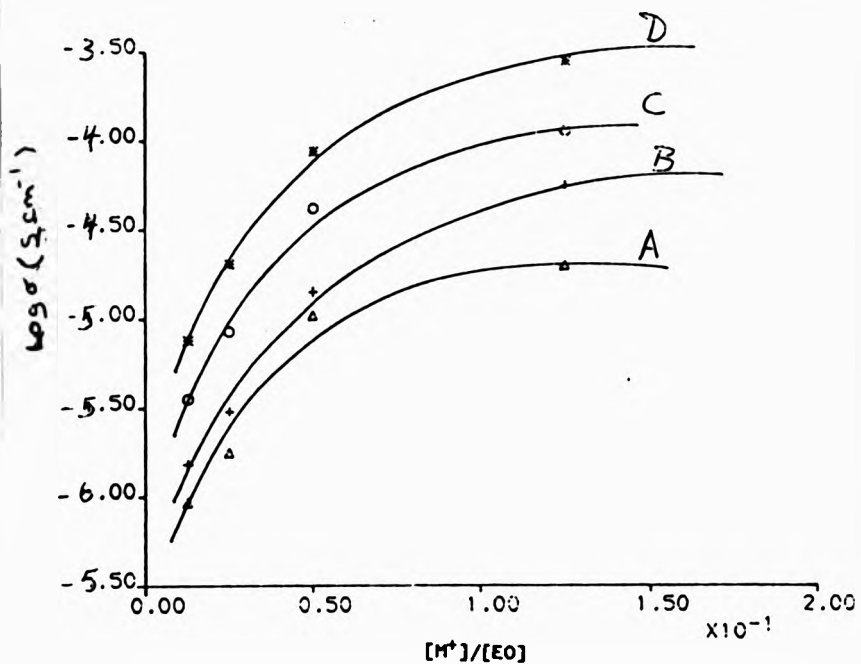
A:  $T_g + 80 \text{ K}$

B:  $T_g + 90 \text{ K}$

C:  $T_g + 100 \text{ K}$

D:  $T_g + 130 \text{ K}$

E:  $T_g + 150 \text{ K}$



5.5.8 Plot of  $\log \sigma$  against salt concentration for 11% crosslinked  $\text{PVO}_3/\text{LiClO}_4$  mixtures under various constant reduced temperature conditions.

A:  $T_g + 80 \text{ K}$       B:  $T_g + 100 \text{ K}$       C:  $T_g + 130 \text{ K}$   
 D:  $T_g + 150 \text{ K}$

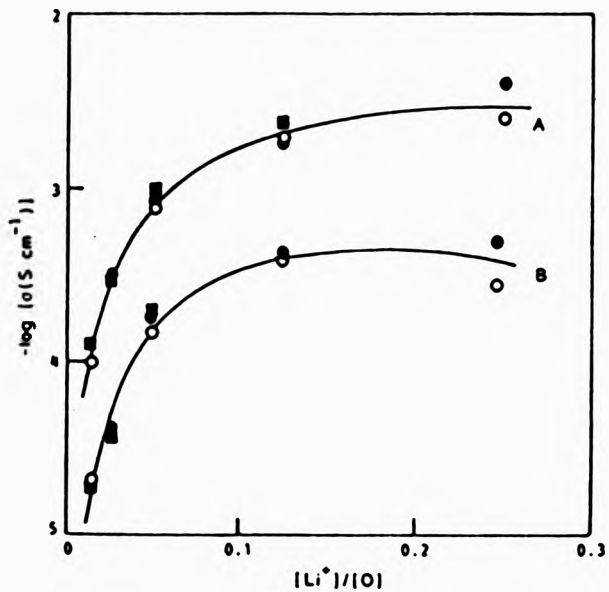


Figure 5.5.9 Variation of  $\log \sigma$  with salt concentration at curve A ( $T_g + 150\text{ K}$ ) and curve B ( $T_g + 100\text{ K}$ ) for (O), uncrosslinked; (◐), 5% crosslinked and (◑), 11% crosslinked samples.

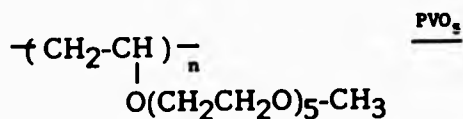
CHAPTER SIX  
CHAIN EXTENDED POLYVINYL ETHER  
ELECTROLYTES

### 4.1 Introduction

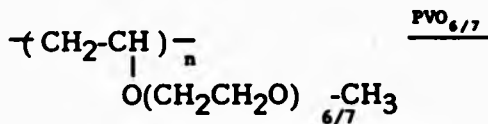
In view of high degrees of ionic conductivity exhibited by the poly(vinyl ether)-salt complexes discussed in the previous chapter, a natural follow up to this work is to determine if extension of the length of ethylene oxide sidechain in the polymeric host would result in higher levels of conductivity.

According to the previous studies<sup>9,6</sup> for long ethylene oxide sidechains, a crystallisation exotherm is generally noted for the polymer host itself. On the other hand, the glass transition decreases (with consequent increase in ion mobility) as the length of the ethylene oxide sidechain is increased. Optimum behaviour therefore requires a compromise value for the length of EO units which will provide adequate segmental mobility without an undue tendency to form crystalline phases.

In chapter three, preparation of two new types of polymeric host materials was reported:



and



For the latter material, 6/7, describes the number average of ethylene oxide units per sidechain of PVO<sub>6/7</sub> whereas in PVO<sub>5</sub>, all the sidechains contain 5 EO units.

The above polymers and their related 5% crosslinked network structures were subsequently studied as potential ion conducting materials. These materials were doped with various Lithium salts and sodium perchlorate, but the major salt of interest was LiClO<sub>4</sub>.

## 6.2 Swelling studies

The swelling behaviour of samples of 5% crosslinked PVO<sub>5</sub> and PVO<sub>6/7</sub> was examined in a selection of liquids similar to the PVO<sub>5</sub>-based structures discussed previously. The effectiveness of each solvent was estimated from the weight absorbed per g of polymer. The results obtained are compared with the swelling characteristics of the 5% crosslinked PVO<sub>5</sub>, and are shown in Table 6.2.1. Chloroform is clearly the best in the group and seem to cause similar swelling behaviour in all of the samples and the non-polar hexane is less effective. Longer ethylene oxide sidechains in PVO<sub>5</sub> and

PVO<sub>6,7</sub> samples seem to cause greater swelling in polar solvents. This can be seen from data shown in Table 6.2.1 where the amount of ethanol, methanol and water absorbed increased with increasing the sidechain length. On the other hand, the amount of hexane absorbed decreased with increasing the number of ethylene oxide units in the sidechain of the polymers. This is not a surprising effect since the increase in the number of EO units results in greater polarity of the polymers which is reflected in greater swelling of these polymers in polar solvents. The data in Table 6.2.1 also indicate that network structures based on PVO<sub>3</sub> and PVO<sub>6,7</sub> have very similar swelling properties.



Liquid	Weight absorbed liquid / g of 5% crosslinked polymer		
	PVO <sub>3</sub>	PVO <sub>5</sub>	PVO <sub>6/7</sub>
Hexane	0.25	0.11	0.17
Methanol	2.57	3.95	3.90
Ethanol	4.66	7.21	7.14
Water	6.46	10.88	10.95
Chloroform	14.67	15.51	14.84

TABLE 6.2.1 Swelling characteristics of the 5% crosslinked

PVO<sub>3</sub>, PVO<sub>5</sub> and PVO<sub>6/7</sub> samples in several solvents.

### 6.3 Glass transition temperature

The glass transition temperature of PVO<sub>3</sub>, PVO<sub>3</sub> , PVO<sub>6,7</sub> and their related 5% crosslinked polymer host materials are shown in Table 6.3.1. The D.S.C. also indicated that these polymers were totally amorphous.

According to these measurements, the T<sub>g</sub> of the PVO<sub>3</sub> is about 2 K higher than PVO<sub>3</sub>. In other words, no further flexibility is achieved when the number of EO units is raised to 5. It can also be noted that the polymer with a mixed number of EO units (6/7) have a similar T<sub>g</sub> to the mono-dispersed PVO<sub>3</sub> and the increase in T<sub>g</sub> due to 5% crosslinking of this polymer is also comparable to the 5% crosslinked PVO<sub>3</sub>.

Similar to PVO<sub>3</sub> and its related crosslinked forms addition of salt to the polymers under study here introduces a second (non-covalent) type of crosslink where the cations coordinate with ether oxygens of the sidechains to form intermolecular interactions which lead to a more rigid structure. The effect can be seen in the data presented in Table 6.3.2 for the uncrosslinked PVO<sub>3</sub> doped with LiClO<sub>4</sub> , Table 6.3.3 for the 5% crosslinked PVO<sub>3</sub> doped with several lithium salts, Table 6.3.4 for the 5% crosslinked PVO<sub>3</sub> doped with NaClO<sub>4</sub> and finally Table 6.3.5 for the 5% crosslinked PVO<sub>6,7</sub> doped with LiClO<sub>4</sub>.

On addition of various salts to each of these

Polymer	T <sub>g</sub> / K	
	Uncrosslinked	Crosslinked
PVO <sub>3</sub>	206	211
PV05	208	211.5
PVO <sub>6/7</sub>	208	211.5

TABLE 6.3.1 The glass transition temperature of various poly(vinyl ethers) and their related 5% crosslinked polymers.

polymers a non linear increase in  $T_g$  occurs with increasing salt concentration, as can be seen in Figures 6.3.1 to 6.3.6 . The non linearity in these systems have been illustrated by drawing a best fit curve through each set of data points. This might be a misleading representation of the observed trend in the data, as closer inspection of the data reveals some degree of inflexion which might be due to errors contained in the data or may suggest that at least two overlapping coordination processes occurring simultaneously where points of inflexion are observed in the data.

In most of the polymer-salt complexes studied in this chapter, at high concentration of the salt, a plateau value of  $T_g$  was observed which is indicative of the solubility limit of the salt. But the response of these polymers upon salt addition was not identical. The differences are generally due to the nature of the polymer and variation in the salt type, and can be observed when comparing the relative change in  $T_g$  ( $\Delta T_g$ ) upon salt addition for the above polymers as illustrated in Figures 6.3.7 to 6.3.9. Based on these Figures the following observations could be made:

- (i) For the crosslinked PVO<sub>2</sub> doped with LiClO<sub>4</sub>, the plateau value of  $T_g$  was observed to have moved to higher values than the uncrosslinked PVO<sub>2</sub> system. At Lower salt concentrations the relative

change in  $T_g$  was marginally smaller than the uncrosslinked PVO<sub>3</sub> (see Figure 6.3.7).

- (ii) For the crosslinked PVO<sub>3</sub> doped with LiSO<sub>3</sub>CF<sub>3</sub>, and LiBF<sub>4</sub>, the change in  $T_g$  at lower salt concentrations up to  $[M^+] / [EO] = 0.05$  is comparable to the crosslinked PVO<sub>3</sub>-LiClO<sub>4</sub> complex, whereas at concentrations above this, the increase in  $T_g$  for these complexes is markedly lower.
- (iii) For the crosslinked PVO<sub>3</sub> doped with NaClO<sub>4</sub>, the relative increase in  $T_g$  at lower salt concentrations up to  $[M^+] / [EO] = 0.05$  is almost similar to the LiClO<sub>4</sub> material but at higher concentrations the change in  $T_g$  is smaller (see Figure 6.3.8).
- (iv) Finally the response of the crosslinked PVO<sub>6,7</sub> doped with LiClO<sub>4</sub> is almost similar to the crosslinked PVO<sub>3</sub>/LiClO<sub>4</sub> complex except at high salt concentrations where a relatively lower solubility limit is observed.

In chapter three, the effect of crosslinking on the polymer with 3 ethylene oxide units in the sidechain (PVO<sub>3</sub>) was discussed, and it was noted that up on salt addition the relative change in  $T_g$  was similar for the polymers up to 5% crosslinking. According to the results outlined above, a similar behaviour is not observed for

the chain extended PVO<sub>3</sub> system up on salt addition. This difference can be observed in Figure 6.3.9. The comparison of the two uncrosslinked PVO<sub>3</sub> and PVO<sub>3</sub>/LiClO<sub>4</sub> complexes suggest that the relative rise in T<sub>g</sub> for the PVO<sub>3</sub> complex was significantly greater than the one observed in the PVO<sub>3</sub> case, especially at high salt concentrations.

This indicates that the dissociation of the salt and therefore the number of charge carriers, ion-polymer, ion-ion interactions, ionic mobility and other related effects may not be similar in these two types of polymer/salt mixtures. This is clearly reflected in the conductivity data obtained for the chain extended polymer/salt mixtures discussed in the following section.

$\frac{[Li^+]}{[EO]}$	Tg / K	$\Delta T_g$
0	208	0
0.0125	218.35	10.35
0.025	227	19
0.05	232.5	24
0.125	240	32
0.25	260	52

TABLE 6.3.2 The effect of added salt ( $LiClO_4$ ) on the Tg of uncrosslinked  $PVO_3$ .

Salt	T <sub>g</sub> / K					
	$\frac{[M^*]}{[EO]}$	0.0125	0.025	0.05	0.125	0.25
LiClO <sub>4</sub>		212	219	227	265	300
LiSO <sub>3</sub> CF <sub>3</sub>		-	220.5	233	246.75	270.5
LiBF <sub>4</sub>		-	215.5	228	244.25	262.5

TABLE 6.3.3 The effect of added salt on the glass transition temperature of 5 % crosslinked PVO<sub>3</sub>



$\frac{[Li^+]}{[EO]}$	T <sub>g</sub> / K	ΔT <sub>g</sub>
0	211	-
0.025	217	6
0.05	235	24
0.125	256.5	45.5
0.25	282.5	71.5

TABLE 6.3.4 The effect of added salt (NaClO<sub>4</sub>) on the T<sub>g</sub> of the 5% crosslinked PVO<sub>3</sub>.

$\frac{[Li^+]}{[EO]}$	T <sub>g</sub> / K	ΔT <sub>g</sub>
0	211.5	-
0.025	217.2	5.77
0.05	231.5	20
0.071	234.5	23
0.125	251.5	40
0.25	278.5	67

TABLE 6.3.5 The effect of added salt (LiClO<sub>4</sub>) on the T<sub>g</sub> of the 5% crosslinked PVO<sub>6/7</sub> .

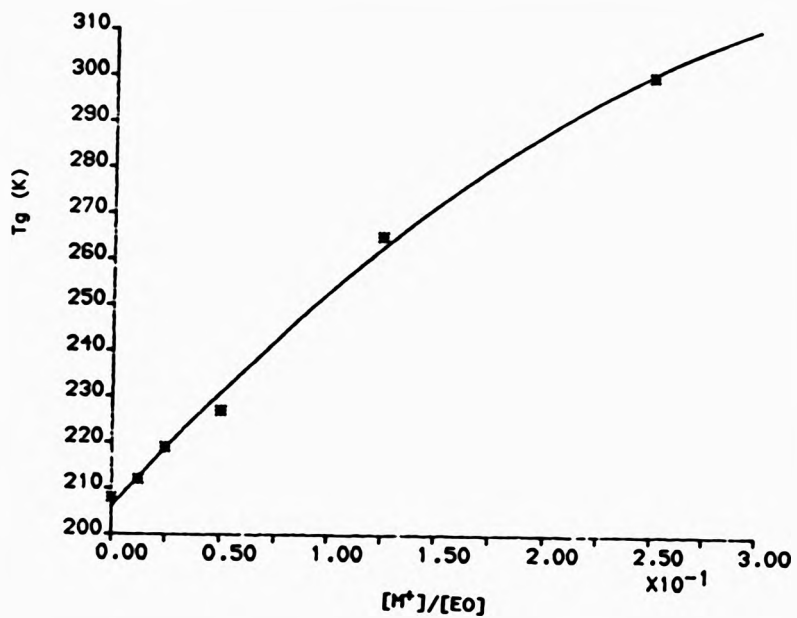


Figure 6.3.2 Plot of  $T_g$  vs salt concentration for 5% crosslinked  $PVO_3/LiClO_4$  salt mixtures.

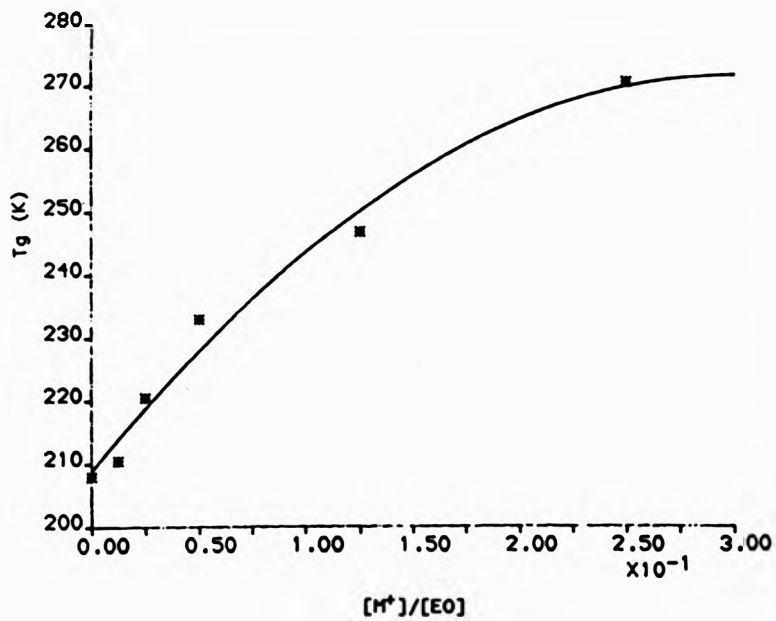


Figure 6.3.3 Plot of  $T_g$  vs salt concentration for 5% crosslinked  $PVO_3/LiSO_3CF_3$  salt mixtures.

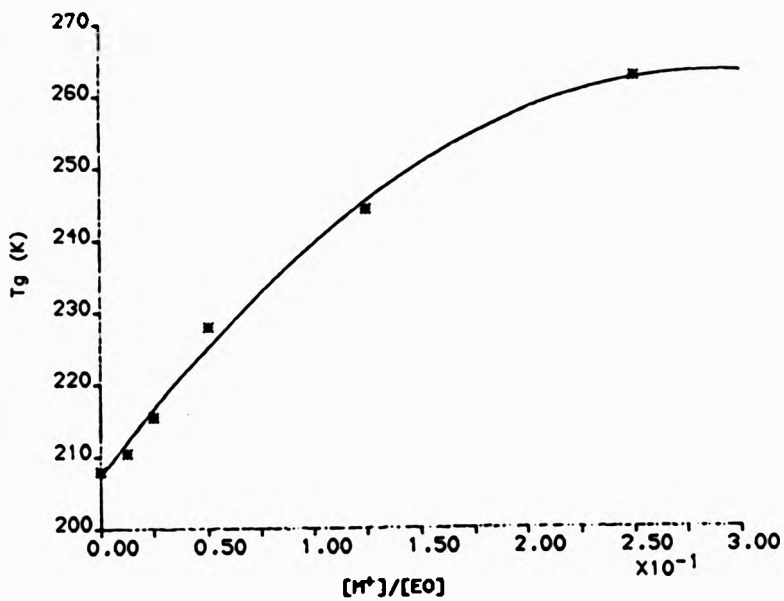


Figure 6.3.4 Plot of  $T_g$  vs salt concentration for 5% crosslinked  $PVO_3/LiBF_4$  salt mixtures.

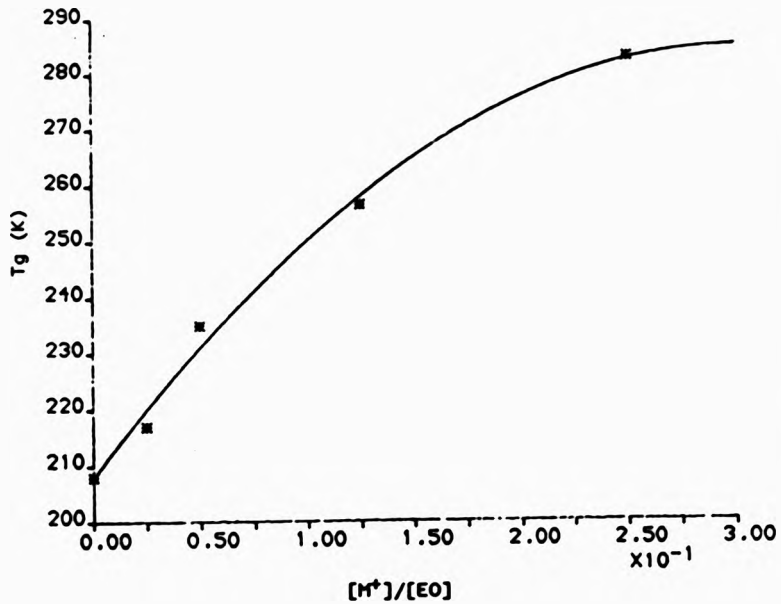


Figure 6.3.5 Plot of  $T_g$  vs salt concentration for 5% crosslinked  $PVO_3/NaClO_4$  salt mixtures.

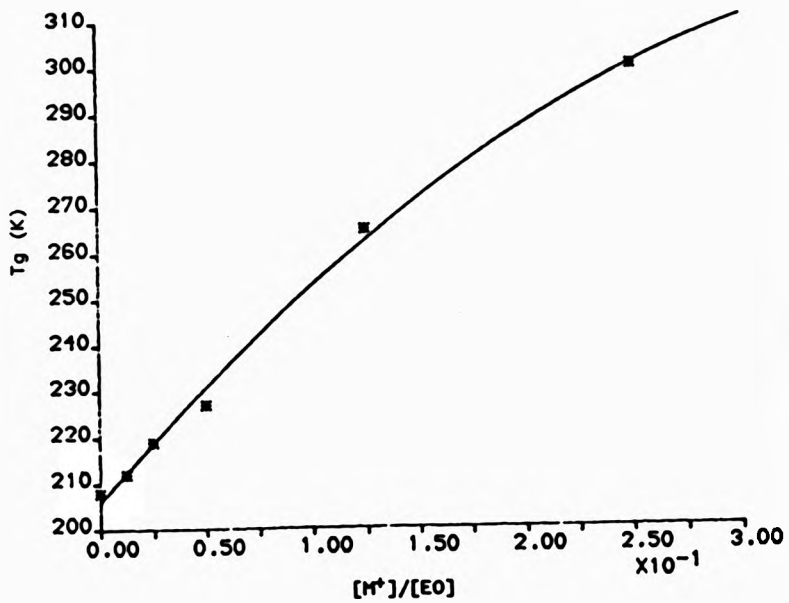


Figure 6.3.6 Plot of  $T_g$  vs salt concentration for 5% crosslinked PVO<sub>6,7</sub>/LiClO<sub>4</sub> salt mixtures.

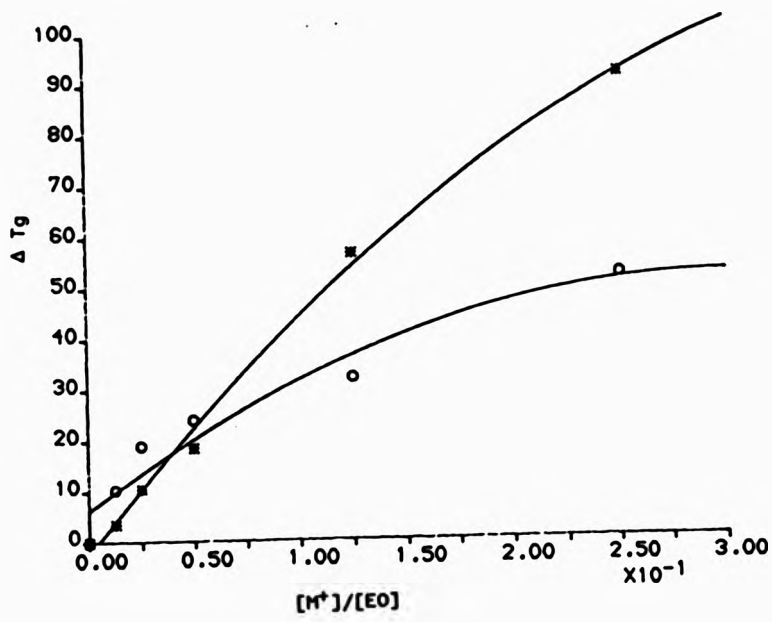


Figure 6.3.7 Comparison of relative change in  $T_g$  up on addition of  $\text{LiClO}_4$  for uncrosslinked (O) and 5% crosslinked (\*)  $\text{PVO}_3$ .



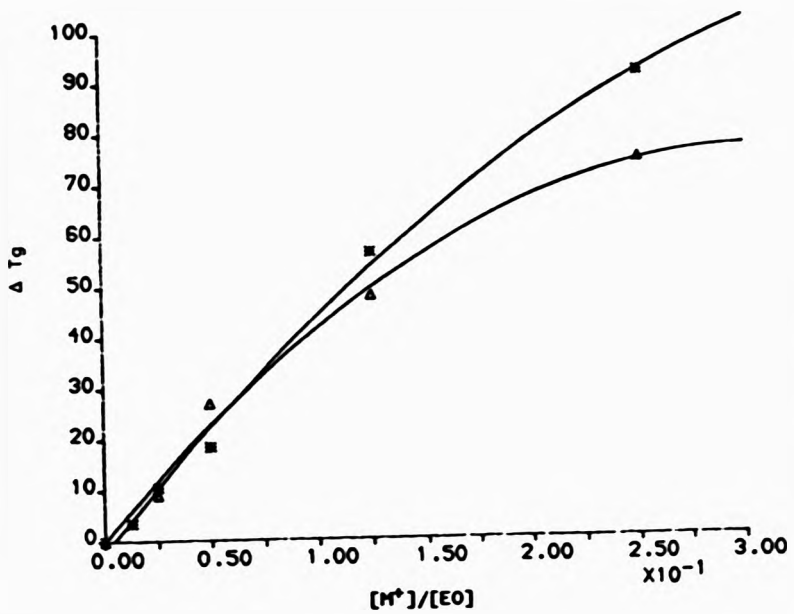


Figure 6.3.8 Comparison of relative change in  $T_g$  up on addition of  $\text{LiClO}_4$  (■) and  $\text{NaClO}_4$  (▲) to 5% crosslinked  $\text{PVO}_3$ .

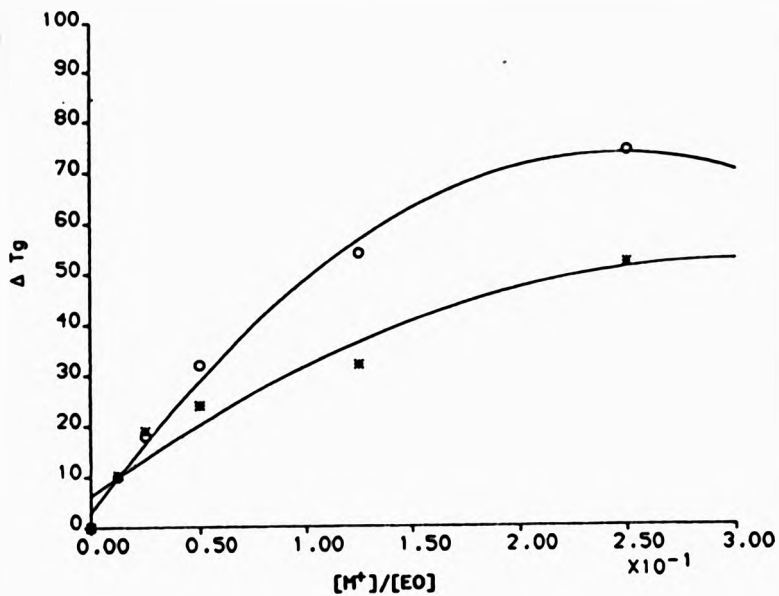


Figure 6.3.9 Comparison of relative change in  $T_g$  up on addition of  $\text{LiClO}_4$  to linear  $\text{PVO}_3$  (O) and  $\text{PVO}_3$  (\*).

#### 6.4 Conductivity Studies

The ionic conductivity of the polymer/salt mixtures were measured as function of increasing salt concentration and temperature.

In Figure 6.4.1 to 6.4.6 log conductivity-reciprocal temperature data obtained for the following systems are shown:

- (i) uncrosslinked PVO<sub>3</sub> doped with LiClO<sub>4</sub>
- (ii) 5% crosslinked PVO<sub>3</sub> " " "
- (iii) 5% crosslinked PVO<sub>3</sub> " LiSO<sub>3</sub>CF<sub>3</sub>
- (iv) 5% crosslinked PVO<sub>3</sub> " " LiBF<sub>4</sub>
- (v) 5% crosslinked PVO<sub>3</sub> " " NaClO<sub>4</sub>
- (vi) 5% crosslinked PVO<sub>6,7</sub> " " LiClO<sub>4</sub>

Similar to the PVO<sub>3</sub>/salt complexes discussed in the previous chapter, the examination of the plots reveal that conductivity of a particular complex increases as the temperature is increased. For most of the data curved lines were obtained indicating that the complexes do not exhibit Arrhenius behaviour in the temperature range studied. Generally, curvature in these complexes seem to be significantly less than the PVO<sub>3</sub>/salt complexes and at low salt concentrations there is an approach to Arrhenius behaviour. It can also be noted that at a particular temperature the most conductive

materials are not always the richest in salt.

It is clear from the Figure 6.4.1 to 6.4.6 that conductivity varies with both temperature and salt concentration but the response of the samples are not the same. From these Figures it is apparent that the differences observed in conductivity of these materials depend on salt type, crosslinking and sidechain length.

PVO<sub>5</sub>/NaClO<sub>4</sub> mixtures seem to give the most conducting materials at medium to low salt concentrations (  $[M^+]/[EO] = 0.05$  to  $0.025$  ) as can be seen in Figure 6.4.7, while the change in anion of the Lithium salts does not result in superior conductivity levels and these salts give conductivities that are slightly lower than the PVO<sub>5</sub>/LiClO<sub>4</sub> mixtures. Finally, the 5% crosslinked PVO<sub>5</sub>,-LiClO<sub>4</sub> mixtures do not exhibit an advantage (in terms of conductivity levels) over the mono-dispersed PVO<sub>5</sub>/LiClO<sub>4</sub> electrolyte (see Figure 6.4.2 and 6.4.6).

However, comparison of some of the data outlined above, with PVO<sub>3</sub>-based complexes reveal a substantial increase in conductivity levels for the chain extended poly(vinyl ether)/salt mixtures as shown in Figures 6.4.8 and 6.4.11. Also apparent from these Figures is the approach to Arrhenius behaviour at low salt concentrations for some of the chain extended samples.

### 6.5 Isothermal conductivity

Similar to the PVO<sub>3</sub>-based systems, if the log<sub>10</sub> data are plotted as a function of salt concentration at a series of fixed measuring temperatures, the expected maxima in conductivity are observed, as can be seen in Figures 6.5.1 to 6.5.6 for the different polymer/salt mixtures. These maxima were observed to move to higher salt concentrations with increasing temperature and the trend has been explained by assuming that the initial rise in conductivity is due to the increasing number of charge carriers being introduced into the system. This is ultimately offset by effects such as ion triplet formation, charge cloud effects and restriction to chain mobility which cause the conductivity to drop, thereby producing the observed maxima.

The observed maxima for the uncrosslinked and 5% crosslinked PVO<sub>3</sub>/LiClO<sub>4</sub> mixtures are more or less the same, and the variation in anion in the latter system does not seem to have caused a significant change in the observed trend. The only noticeable change is for PVO<sub>3</sub>/NaClO<sub>4</sub> mixtures where the maxima occur over a narrower range of salt concentration, and at high salt concentrations the drop in conductivity is greater than in the other systems. This observation is consistent with the effect noted in the previous section, where

upon salt addition,  $\text{NaClO}_4$ , at high salt concentrations the relative increase in  $T_g$  was smaller than the Li-based electrolytes.

As for the  $\text{PVO}_{6,7} / \text{LiClO}_4$  electrolytes the maxima tend to occur over a slightly broader range of salt concentration and no other change in trend can be detected.

The data were replotted on a reduced temperature scale where  $\log \sigma$  is presented as function of salt concentration at a fixed temperature above the  $T_g$  of each polymer-salt mixture. Such isothermal plots, at various temperature scales are shown in Figures 6.5.7 to 6.5.12. The maxima are now less defined and have moved to higher values but essentially constant salt concentrations.

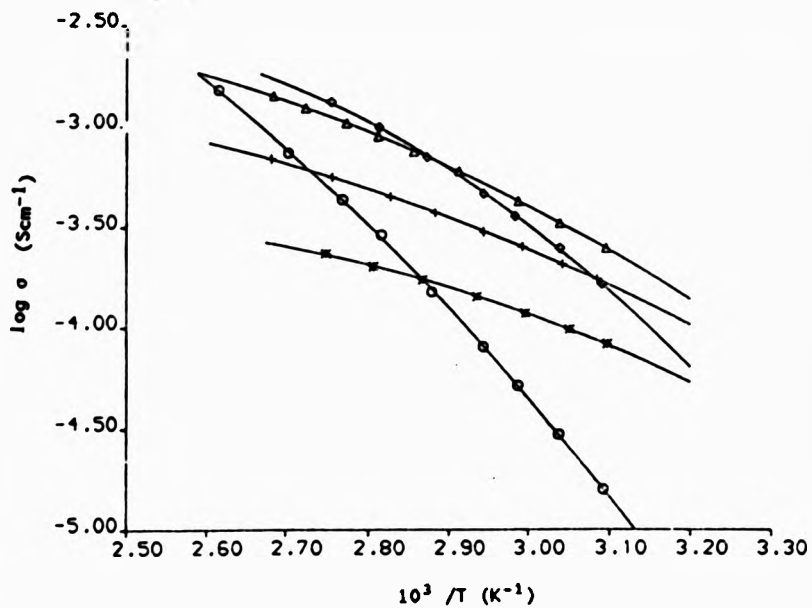


Figure 6.4.1 Arrhenius plot of  $\log \sigma$  against reciprocal temperature for linear  $\text{PVO}_5/\text{LiClO}_4$  complexes.

[M\*]/[EO] ratios: 0.0125 (■)  
 0.0250 (×)  
 0.0500 (▲)  
 0.1250 (◊)  
 0.2500 (○)

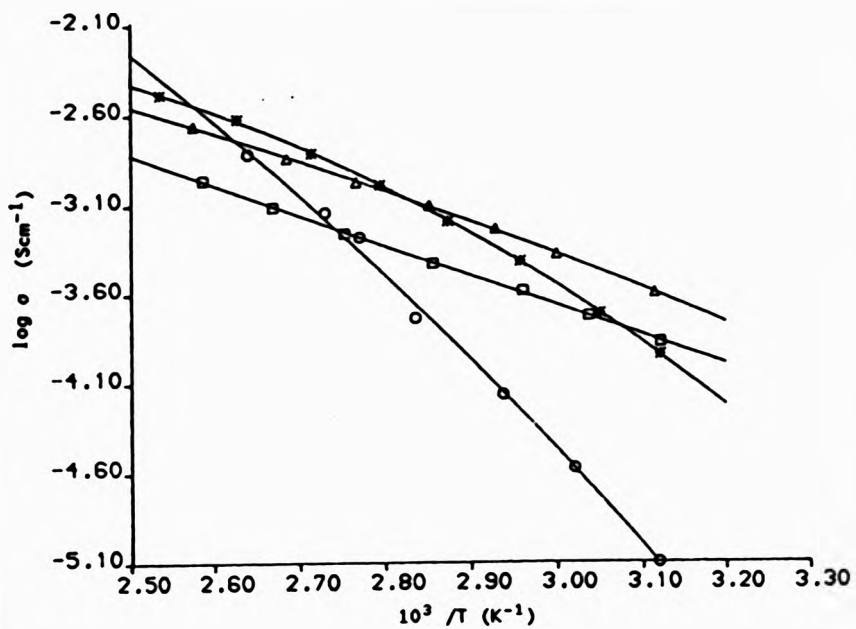


Figure 6.4.2 Arrhenius plot of  $\log \sigma$  against reciprocal temperature for 5% crosslinked  $\text{PVO}_3/\text{LiClO}_4$  complexes.

$[\text{H}^+]/[\text{EO}]$  ratios:

0.0250 (x)  
 0.0500 (Δ)  
 0.1250 (\* )  
 0.2500 (○)



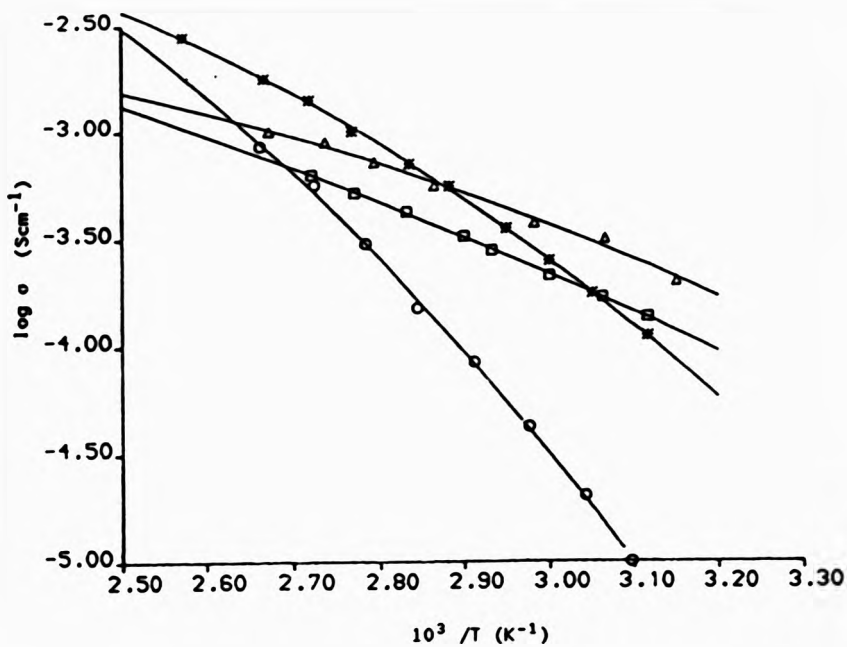


Figure 6.4.3 Arrhenius plot of  $\log \sigma$  against reciprocal temperature for SX crosslinked  $\text{PVO}_3/\text{LiSO}_3\text{CF}_3$  complexes.

$[\text{M}^*]/[\text{EO}]$  ratios:

- 0.0250 (x)
- 0.0500 (Δ)
- 0.1250 (□)
- 0.2500 (o)

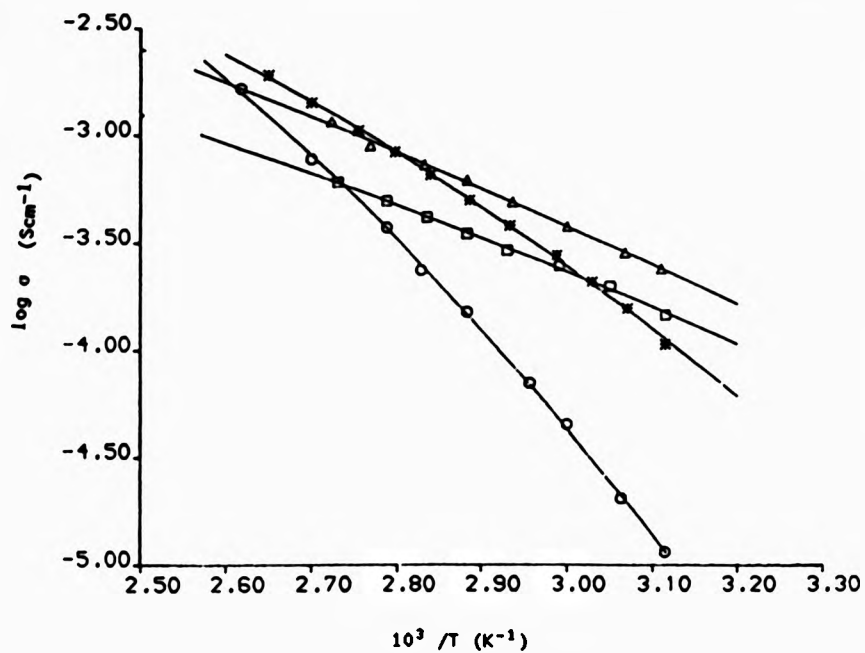


Figure 6.4.4 Arrhenius plot of  $\log \sigma$  against reciprocal temperature for 5% crosslinked  $\text{PVO}_3/\text{LiBF}_4$  complexes.

$[\text{M}^*]/[\text{EO}]$  ratios:

0.0250 (x)  
 0.0500 (Δ)  
 0.1250 (□)  
 0.2500 (o)

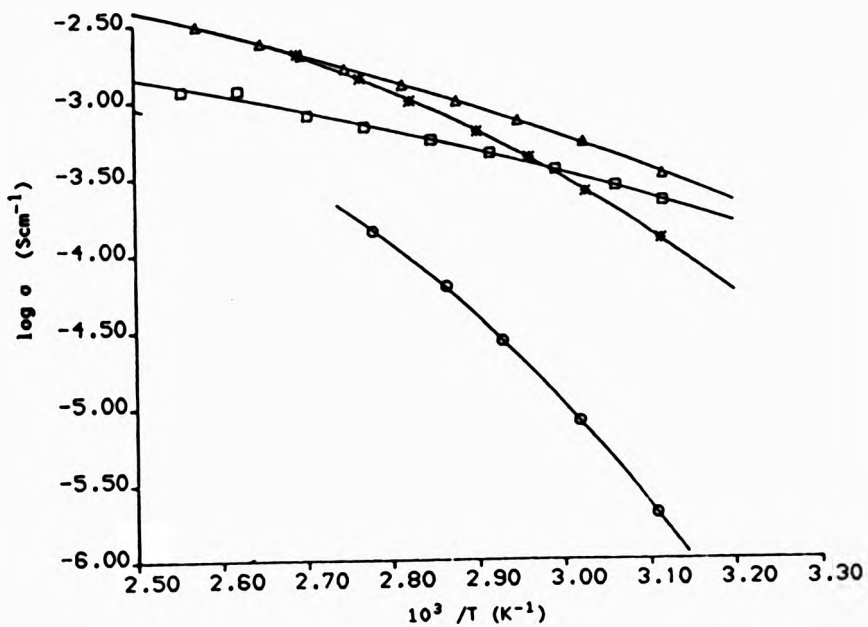


Figure 6.4.5 Arrhenius plot of  $\log \sigma$  against reciprocal temperature for 5% crosslinked  $\text{PVO}_3/\text{NaClO}_4$  complexes.

[M\*]/[EO] ratios:

- 0.0250 (x)
- 0.0500 (Δ)
- 0.1250 (□)
- 0.2500 (○)

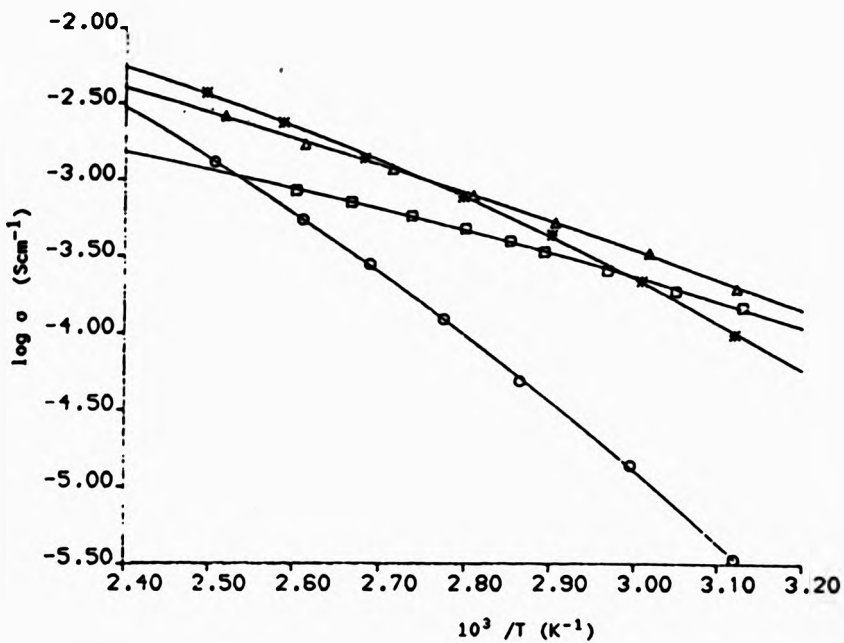


Figure 6.4.6 Arrhenius plot of  $\log a$  against reciprocal temperature for 5% crosslinked  $\text{PVO}_{9,7} / \text{LiClO}_4$  complexes.

$[\text{M}^*]/[\text{EO}]$  ratios:

- 0.0250 (x)
- 0.0500 ( $\Delta$ )
- 0.1250 ( $\blacksquare$ )
- 0.2500 ( $\circ$ )

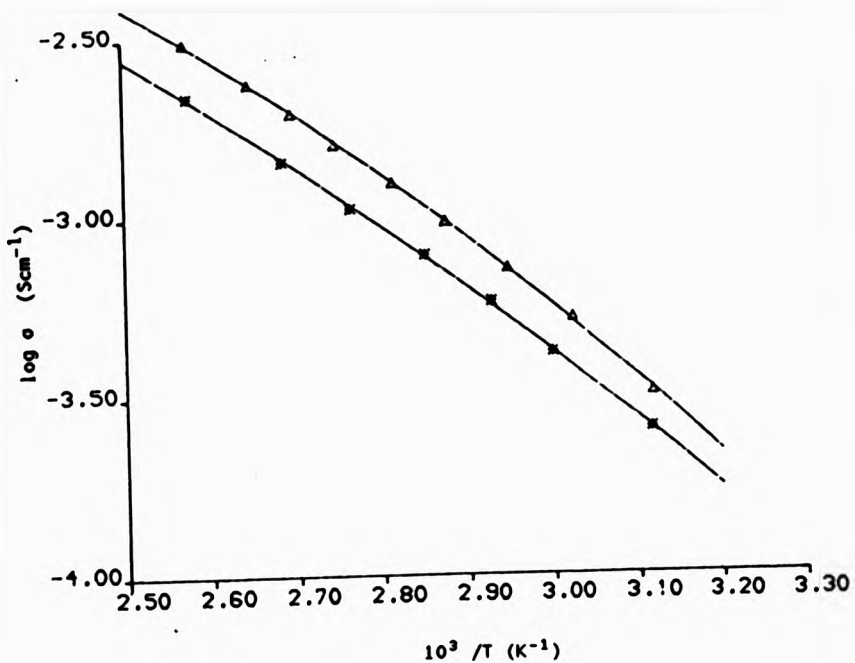


Figure 6.4.7 Comparison of  $\log \sigma$  against reciprocal temperature for 5% crosslinked PVO<sub>3</sub> lithium and sodium perchlorate at a fixed salt concentration  $[M^+]/[EO] = 0.05$ .

LiClO<sub>4</sub> (■)  
NaClO<sub>4</sub> (▲)

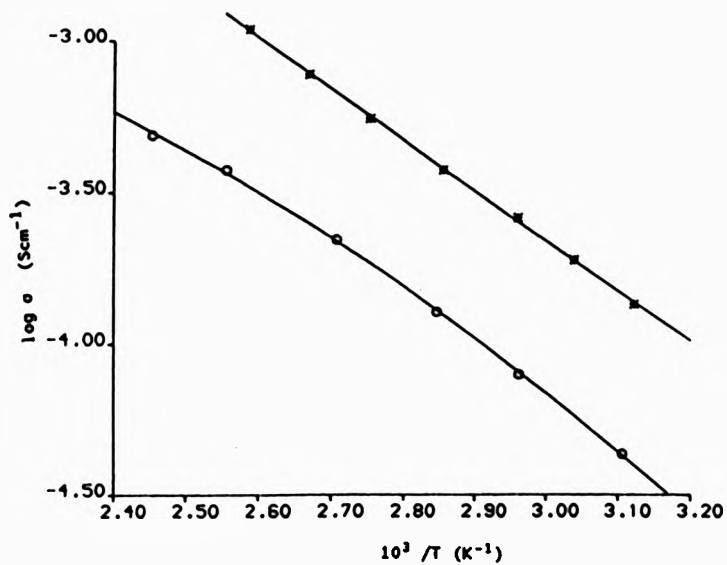


Figure 6.4.8 Comparison of  $\log \sigma$  against reciprocal temperature for 5% crosslinked  $PVO_3$  and  $PVO_3$  lithium perchlorate complexes at a fixed salt concentration  $[M^+]/[EO] = 0.025$ .

5%  $PVO_3/LiClO_4$  (○)

5%  $PVO_3/LiClO_4$  (■)

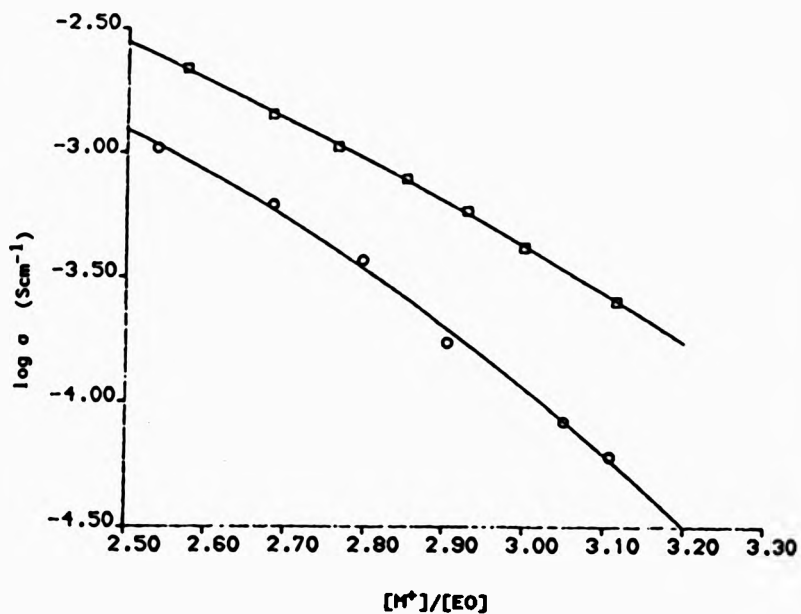


Figure 6.4.9 Comparison of  $\log \sigma$  against reciprocal temperature for 5% crosslinked  $PVO_3$  and  $PVO_3$  lithium perchlorate complexes at a fixed salt concentration  $[M^+]/[EO] = 0.05$ .

5% crosslinked  $PVO_3/LiClO_4$  (○)

5% crosslinked  $PVO_3/LiClO_4$  (□)

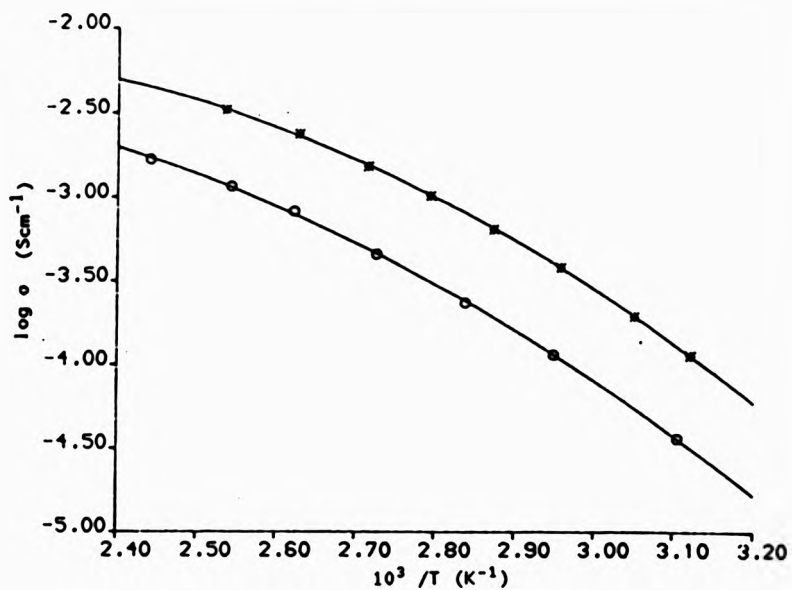


Figure 6.4.10 Comparison of  $\log \sigma$  against reciprocal temperature for 5% crosslinked  $\text{PVO}_3$  and  $\text{PVO}_3$  lithium perchlorate complexes at a fixed salt concentration  $[\text{M}^+]/[\text{EO}] = 0.125$

5% crosslinked  $\text{PVO}_3/\text{LiClO}_4$  (○)

5% crosslinked  $\text{PVO}_3/\text{LiClO}_4$  (■)



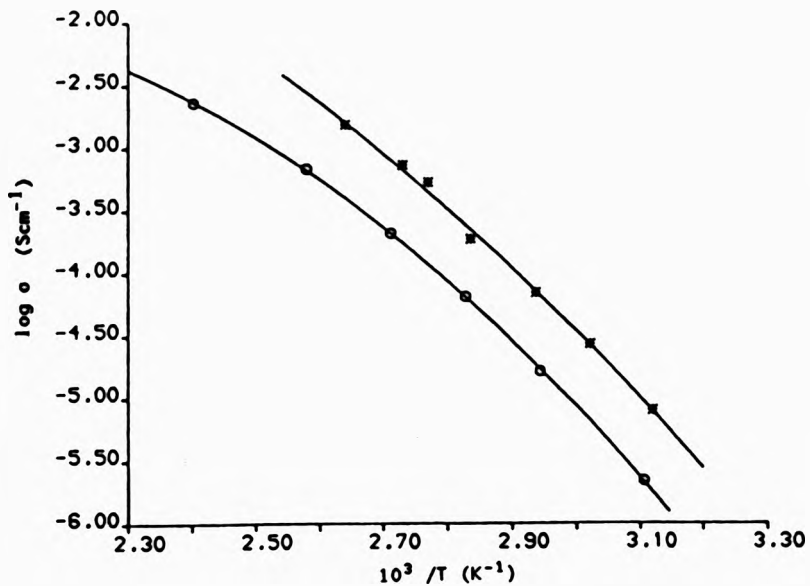
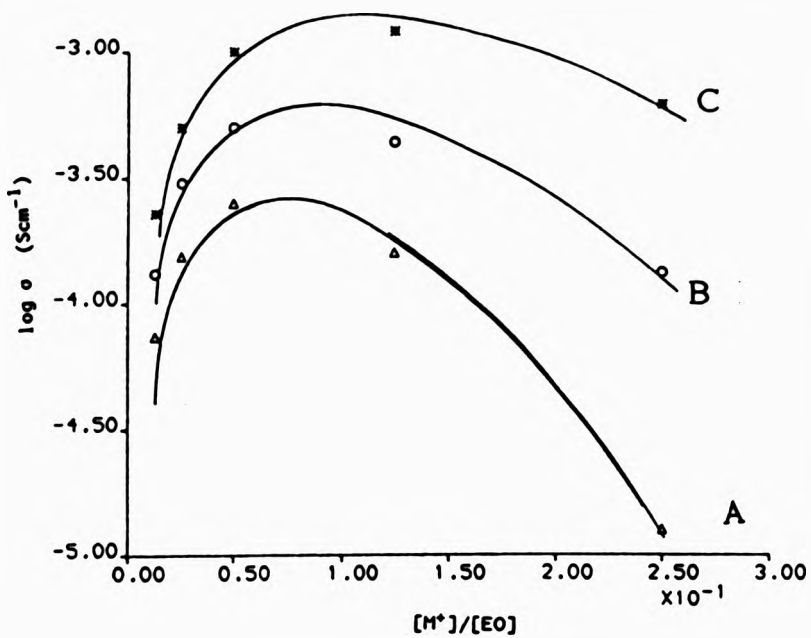


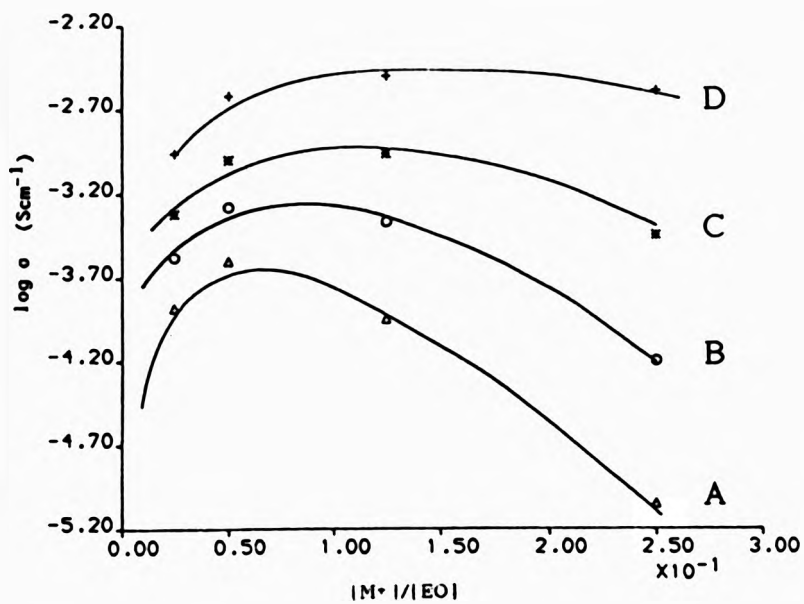
Fig. 6.4.11 Comparison of  $\log \sigma$  against reciprocal temperature for 5% crosslinked  $\text{PVO}_3$  and  $\text{PVO}_3$  lithium perchlorate complexes at a fixed salt concentration  $[\text{M}^+]/[\text{EO}] = 0.250$

5% crosslinked  $\text{PVO}_3/\text{LiClO}_4$  (•)

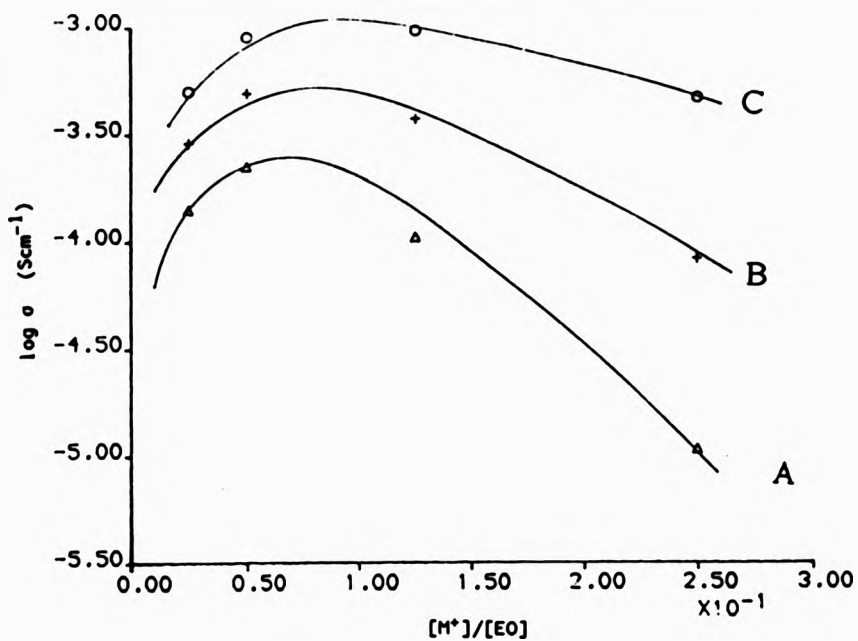
5% crosslinked  $\text{PVO}_3/\text{LiClO}_4$  (◻)



**Figure 6.5.1**  
 Isothermal variation of log conductivity with salt concentration ( $\text{LiClO}_4$ ) for uncrosslinked  $\text{PVO}_3$  measured at temperatures of curve: A, 320 K; B, 340 K; and C, 360 K.



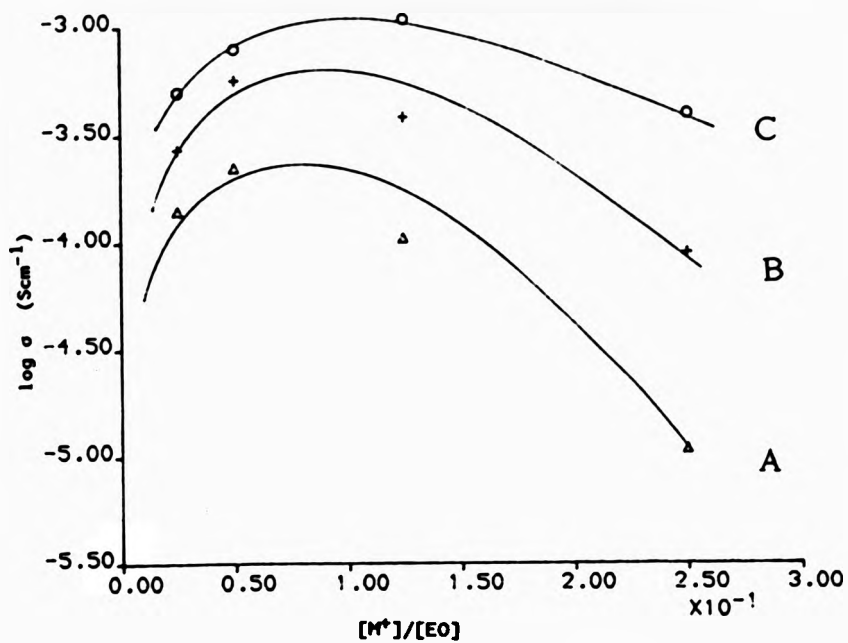
**Figure 6.5.2**  
**Isothermal variation of log conductivity with salt concentration ( $\text{LiClO}_4$ ) for 5% crosslinked  $\text{PVO}_3$  measured at temperatures of curve:**  
**A, 320 K; B, 340 K; C, 360 K and D, 392.15 K.**



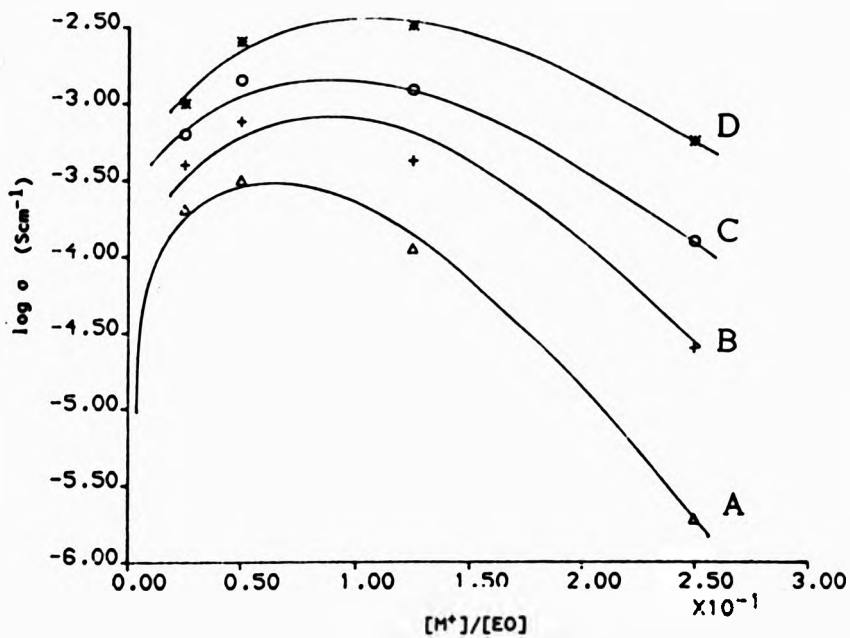
**Figure 6.5.3**

**Isothermal variation of log conductivity with salt concentration ( $\text{LiSO}_2\text{CF}_3$ ) for 5% crosslinked  $\text{PVO}_3$  measured at temperatures of curve:**

**A, 320 K; B, 340 K; C, 360 K.**



**Figure 6.5.4**  
 Isothermal variation of log conductivity with salt concentration ( $\text{LiBF}_4$ ) for 5% crosslinked  $\text{PVO}_3$  measured at temperatures of curve:  
 A, 320 K; B, 340 K; C, 360 K.



**Figure 6.5.5**

**Isothermal variation of log conductivity with salt concentration ( $\text{NaClO}_4$ ) for 5% crosslinked  $\text{PVO}_3$  measured at temperatures of curve:**

**A, 320 K; B, 340 K; C, 360 K and D, 192.15 K.**

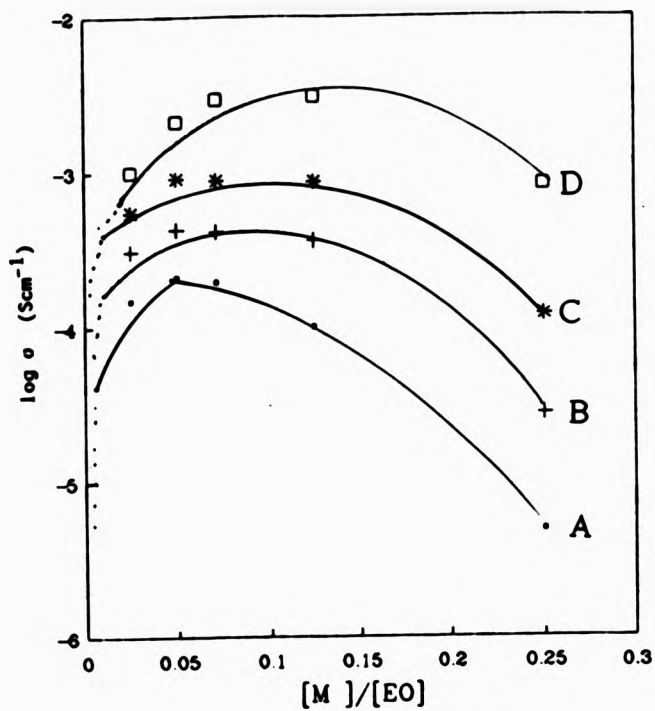


Figure 6.5.6

Isothermal variation of log conductivity with salt concentration ( $\text{LiClO}_4$ ) for 5% crosslinked  $\text{PVO}_{8/7}$  measured at temperatures of curve:

A, 320 K; B, 340 K; C, 360 K and D, 192.15 K.

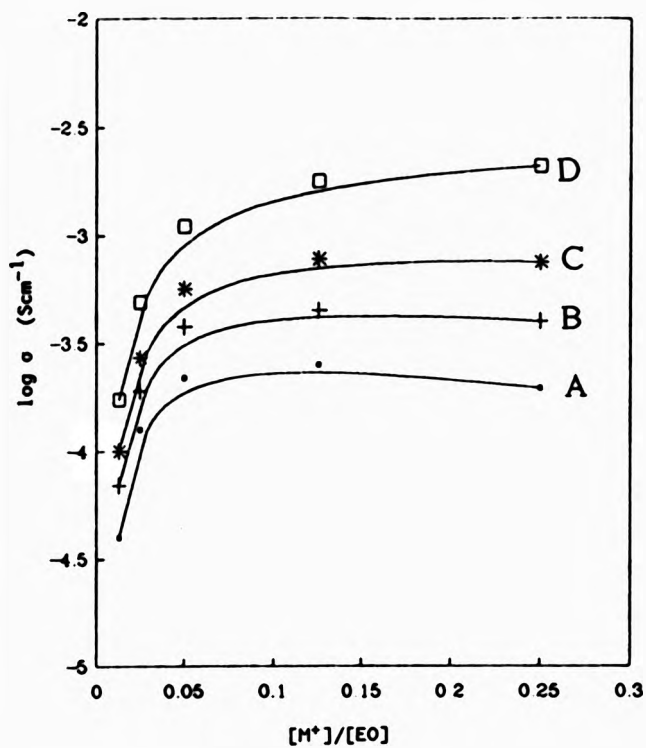


Figure 6.6.7 Plot of  $\log \sigma$  against salt concentrations for  $\text{LiClO}_4$  complexes of uncrosslinked  $\text{PVO}_3$  under various constant reduced temperature conditions.

A:  $T_g + 90 \text{ K}$ ,      B:  $T_g + 100 \text{ K}$   
 C:  $T_g + 110 \text{ K}$ ,    D:  $T_g + 130 \text{ K}$



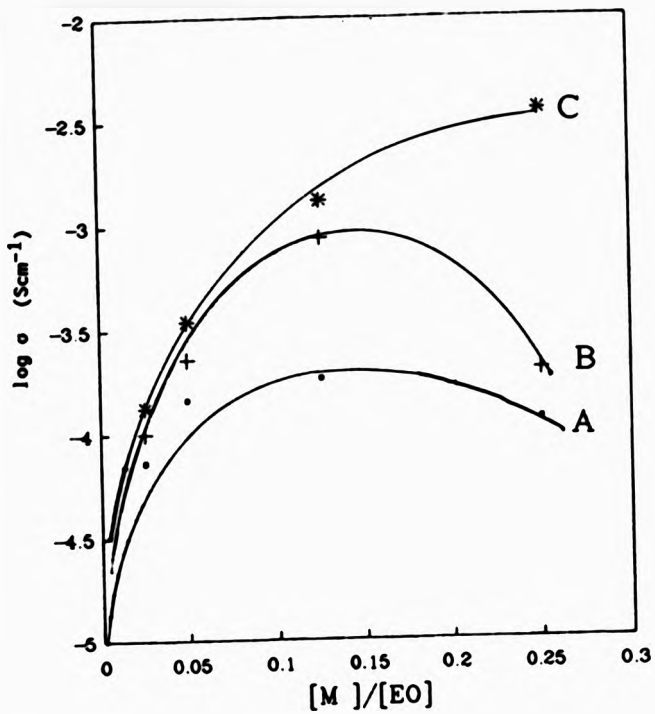


Figure 6.6.8 Plot of  $\log \sigma$  against salt concentrations for  $\text{LiClO}_4$  complexes of 5% crosslinked  $\text{PVO}_2$  under various constant reduced temperature conditions.

A:  $T_g + 80 \text{ K}$ ,      B:  $T_g + 90 \text{ K}$   
 C:  $T_g + 100 \text{ K}$ ,

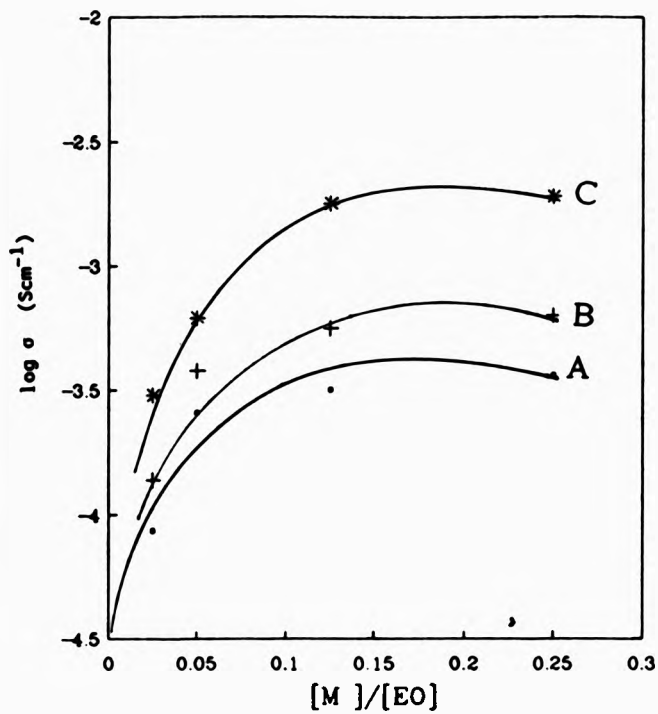


Figure 6.6.9 Plot of  $\log \sigma$  against salt concentrations for  $\text{LiSO}_3\text{CF}_3$  complexes of 5% crosslinked  $\text{PVO}_3$  under various constant reduced temperature conditions.

A:  $T_g + 90 \text{ K}$ , B:  $T_g + 100 \text{ K}$ , C:  $T_g + 120 \text{ K}$

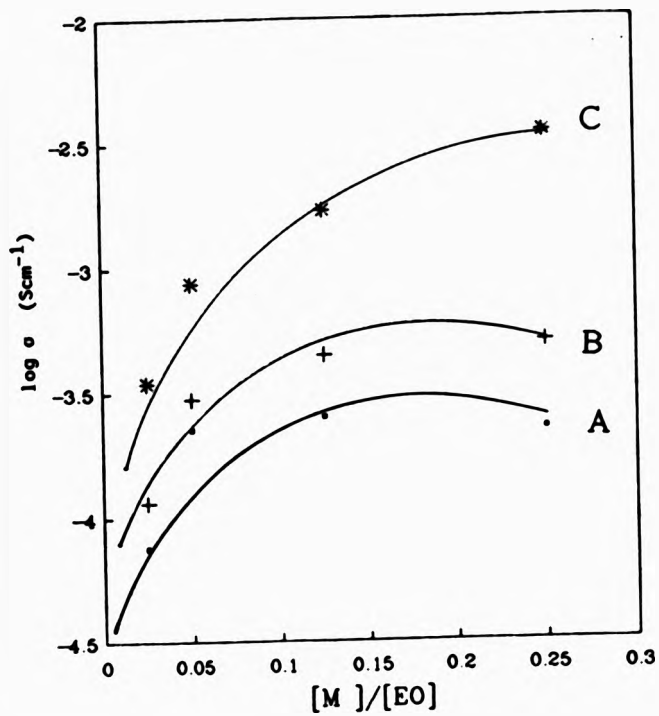


Figure 6.6.10 Plot of  $\log \sigma$  against salt concentrations for  $\text{LiBF}_4$  complexes of 5% crosslinked  $\text{PVO}_2$  under various constant reduced temperature conditions.

A:  $T_g + 90 \text{ K}$ , B:  $T_g + 100 \text{ K}$ , C:  $T_g + 130 \text{ K}$

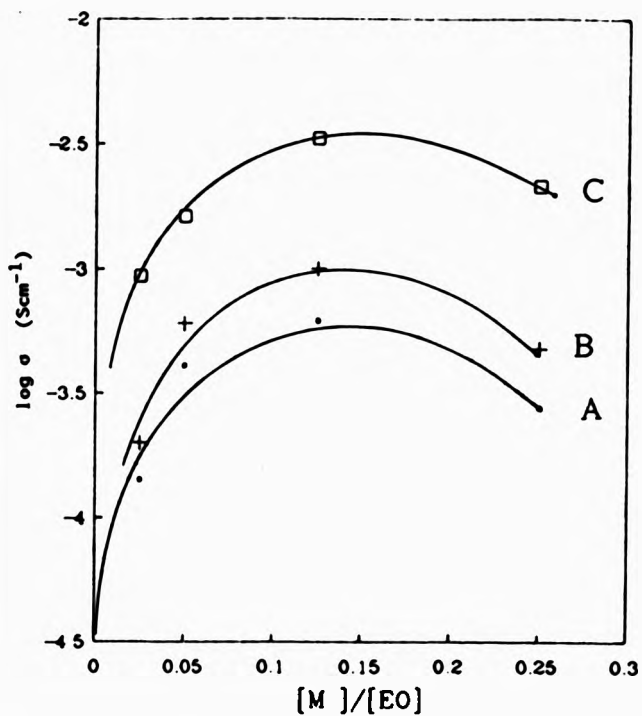


Figure 6.6.11 Plot of  $\log \sigma$  against salt concentrations for  $\text{NaClO}_4$  complexes of 5% crosslinked  $\text{PVO}_3$  under various constant reduced temperature conditions.

A:  $T_g + 90 \text{ K}$ , B:  $T_g + 100 \text{ K}$ , C:  $T_g + 130 \text{ K}$

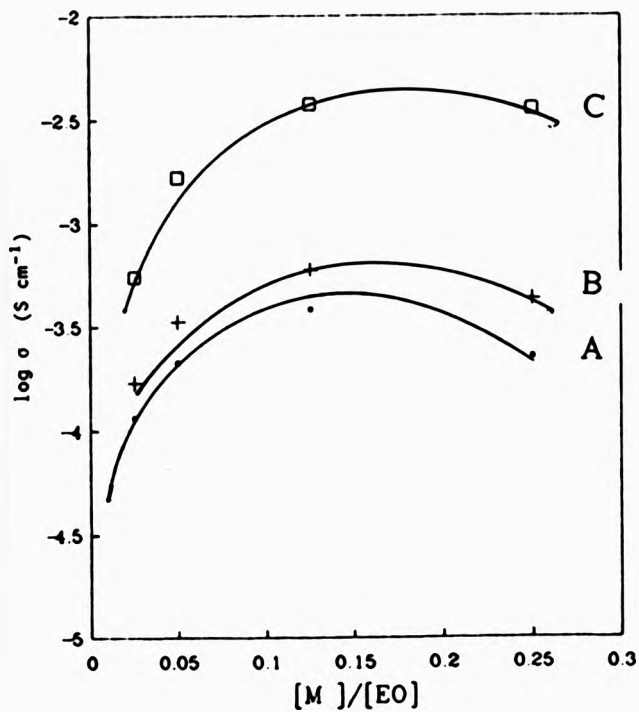


Figure 6.6.12 Plot of  $\log \sigma$  against salt concentration for  $\text{LiClO}_4$  complexes of 5% crosslinked  $\text{PVO}_{6/7}$  under various constant reduced temperature conditions.  
 A:  $T_g + 90 \text{ K}$ , B:  $T_g + 100 \text{ K}$ , C:  $T_g + 130 \text{ K}$

CHAPTER SEVEN  
THEORETICAL TREATMENT OF  
CONDUCTIVITY-TEMPERATURE  
DATA

### 7.1 VTF analysis and theoretical models

When analysing the conductivity data, the normal practice is to use the Vogel-Tammann-Fulcher (VTF) equation<sup>148-150</sup>

$$\sigma(T) = A T^{-x} \exp \left[ \frac{B}{(T - T_0)} \right] \quad (8)$$

to analyse the non-Arrhenius behaviour. Here B and  $T_0$  are constants whose value will depend on the model applied, and A is a factor that subsumes the pre-exponential term normally believed to be proportional to the number of charge carriers in the system. Equation 8 can be interpreted further by using two approaches: the free volume and the configurational entropy models.

With the phenomenological approach of the free volume hypothesis, the equation 8 is readily transformed into the WLF equation which is widely used to describe the relaxational behaviour of polymeric materials in the vicinity of the glass transition temperature. In this model polymer is assumed to contain empty space or "free volume," which will increase with temperature and allow greater freedom of movement for polymer chains in the bulk state. The parameter  $T_0$  is then considered to be the temperature at which the free volume eventually

vanishes. At temperatures above  $T_0$ , when a substantial free volume is present, the ionic species in the polymer matrix will be able to move through the bulk polymer. This movement will be accompanied by polymer chain segmental motion and will be made easier with an increase in temperature. Cheradame and co-workers<sup>64, 67, 66</sup> have shown a clear relation between ionic motion and chain mobility and have used the WLF equation very effectively to describe the behaviour of ion containing networks. In this model  $B$  is then related to the free volume of the system and can be regarded, not as an energy term, but as a function of the expansivity of the polymer-salt mixture.

The major weakness of this theory is that it ignores the obvious kinetic effects associated with long chain molecules. Adam, Gibbs & DiMarzio<sup>71, 72</sup> have proposed an alternative, the configurational entropy model, which attempts to overcome this deficiency. Now the mass transport mechanism is assumed to be a group co-operative rearrangement of the chain rather than a redistribution of free volume,  $T_0$  is the temperature at which configurational entropy is zero, and  $T_0$  is related to  $T_g$  by  $(T_0 = T_g - 50K)$ , whereas  $B$  is a function of the activation energy opposing the rearrangement of the polymer segmental unit.

The approach appears to have merit, and analyses of several polymer-electrolyte systems<sup>151, 9, 123</sup> give



reasonable values of activation energy and values close to 50K for ( $T_g - T$ ). The description is, of course, somewhat inadequate at a molecular level, and Druger, Nitzan, and Ratner<sup>152</sup> proposed a "percolation model" based on the theory proposed by Hammersley<sup>153</sup> to model motion through a random medium.

Ratner proposes that an ion is capable of jumping from one site to a neighbouring site in the polymer matrix if a site is available, and the rate of this process is 1 or 0 depending on whether a site is vacant or not. The theory manages to incorporate the essential aspects of the polymer chain flexibility and the rate at which the chain segments move by recognizing that the dynamics of chain motion will represent an ever changing host environment for the ion, thereby allowing a previously inaccessible site to become available and thus a successful jump to take place.

The theory requires improvement if we are to deal with complicating features such as ion-ion interactions and the influence of ionic species other than single ions.

## 7.2 VTF analyses of the conductivity data

Generally the conductivity data can be treated in three ways with  $\log(\sigma T^{1/2})$  plotted against different reciprocal temperature functions. In method (i) it can be plotted against reciprocal  $(T - T_g)$  where  $T_g$  is the glass transition of the polymer-salt complex. For method two (ii) the plot involves reciprocal  $(T - T_g)$  where  $T_g$  is now assumed as that of the undoped polymer. Finally, in method (iii) a non linear least square analysis of the data has been reported, thereby allowing the unknown parameters A, B and T. to assume values suited to the best fit.

The data when plotted according to methods (i) and (ii) are linear and the slopes of the straight lines correspond to the constant, B, in equation 7 with units of temperature in Kelvin. B has been assumed to be representative of an activation energy ( $E_a'$ ) in many studies<sup>110, 154, 155</sup> and  $E_a'$  values in the range of 3-10  $\text{KJmol}^{-1}$  have been reported previously in the study of polymeric electrolytes.

This conversion frequently reported in the literature, may not be particularly meaningful, however, and it is more instructive to consider how B may be interpreted. This can depend on the model adopted for the system and it has been demonstrated<sup>157</sup> that the VTF equation can be derived from the configurational entropy

approach developed by Gibbs et al<sup>71,72</sup> in which B is expressed as

$$B = \frac{T_0 S_c^* \Delta\mu}{k \Delta C_p T} \quad (10)$$

where  $S_c^*$  is the minimum configurational entropy required for cooperative rearrangement of a polymer chain segment involved in ion transport in the matrix, and  $\Delta\mu$  is the height of the potential energy barrier per monomer unit hindering this type of segmental rearrangement. The heat capacity change is that measured during the change from the glass to the liquid at a temperature T, and k is the Boltzmann constant. Adam and Gibbs<sup>23</sup> have also suggested that it is reasonable to assume that  $S_c^* = k \ln 2$ , hence  $\Delta\mu$  can be estimated from the knowledge of  $\Delta C_p$  and T, has been estimated using VTF equation and  $\Delta C_p$  can be measured directly.

### 7.3 VTF analyses of the crosslinked PVO, conductivity data

Values of A, B and T<sub>0</sub> were estimated from each data set by using a non-linear least square minimisation procedure. If the average value of  $\Delta C_p = 29.45$

$\text{JK}^{-1}\text{mol}^{-1}$ , calculated for the uncrosslinked polymer-salt complex<sup>158</sup> is assumed for the crosslinked samples then  $\Delta\mu$  values can also be obtained using equation 10. The results are listed in Table 7.3.1 for four levels of crosslinking. The model seems to apply reasonably well for samples up to 5% crosslinking for which values of  $(T_g - T_c)$  range between 39 and 61 K, with an average of 50.6 K in good agreement with the prediction. At 11% crosslinking, however, values are much higher and the  $\log \sigma - 1/T$  plots tend towards linearity. This suggests that this approach is no longer applicable to these highly crosslinked networks.

The activation energies for segmental motion range between 40 and 70  $\text{kJ mol}^{-1}$  which are the same order of magnitude as calculated for the uncrosslinked sample<sup>158</sup>. Again, the exception tends to the 11% crosslinked material but if these data are treated using Arrhenius equation then at the lower salt concentrations the calculated activation energies obtained of 42 and 48  $\text{KJ mol}^{-1}$  are comparable.

Thus the effect of low levels of crosslinking on the ion conduction and chain motion is negligible and these polymer-salt mixtures behave like the uncrosslinked sample.

Per cent crosslinking	$\frac{[Li^+]}{[EO]}$	$\ln A$	B (K)	$T_g$ (K)	$(T_g - T_0)$ (K)	$\Delta u$ kJ mol <sup>-1</sup>
0.2	0.025	-6.30	953	176	51.0	50.71
	0.050	-5.79	869	197	42.0	44.71
	0.125	-3.74	1088	211	47.5	56.74
	0.250	-3.55	1019	231	50.0	52.96
1.2	0.0125	-7.42	973	171.7	48.3	52.97
	0.0500	-5.42	893	199.4	39.1	45.39
	0.1250	-4.07	1051	207.0	53.4	56.10
	0.2500	-2.31	1281	225.7	61.3	69.13
5.0	0.0250	-6.49	974	171.0	55.0	54.76
	0.0500	-4.22	1210	178.0	60.0	68.87
	0.1250	-5.07	807	222.0	41.0	40.77
	0.2500	-2.01	1318	228.0	59.0	70.36
11.0	0.0125	-2.41	2998	78.0	158.0	42.25 <sup>a</sup>
	0.0250	-1.59	2613	115.0	114.0	42.50 <sup>a</sup>
	0.0500	-4.10	1248	196.0	68.0	71.44
	0.1250	-2.14	2772	161.0	113.0	200.50

<sup>a</sup> Calculated from the Arrhenius relationship

Table 7.3.1 VTF analysis of conductivity-temperature data for samples with crosslinking.

#### 7.4 VTF analyses of the chain extended poly(vinyl ether)s conductivity data

Using method 1 and 2, linearization of the conductivity temperature data was possible for all the salt complexes prepared from the uncrosslinked PVO<sub>5</sub>, 5% crosslinked PVO<sub>5</sub> and PVO<sub>6,7</sub> based comb-shaped polymers except where Arrhenius behaviour was observed. In Table 7.4.1 the values of constant B, determined from the slope of the linearized data and also Ea' values calculated directly from the B values, are displayed for representative salt complexes prepared from each of the polymeric hosts.

It has been pointed out that discrepancies can arise in the values obtained from the VTF analysis as a result of the choice of reference temperature<sup>122</sup> used in equation 8. In this study it was noted that Ea' values increased as the reference temperature employed in equation 8 was lowered from T<sub>g</sub> to T<sub>g</sub>.. The magnitude of the differences in the results, noted on changing the polymeric host, the incorporated salt or the concentration of salt in the complex, were dependent on whether T<sub>g</sub> or T<sub>g</sub>. was used as the reference temperature and the changes in B and Ea' were of a smaller magnitude when the data were obtained using method 1 rather than method 2. In general B and Ea' increased as the salt concentration in the salt increased. B ranged from 157

Polymer	Salt	$(M^2)/[EO]$	$\frac{B/K}{a}$	$\frac{E_a}{R}$ / $\text{kJmol}^{-1}$
PVO <sub>3</sub> (uncrosslinked)	LiClO <sub>4</sub>	0.25	—	—
	LiClO <sub>4</sub>	0.05	—	—
	LiClO <sub>4</sub>	0.125	563.2	900
	LiClO <sub>4</sub>	0.25	590.5	1530
PVO <sub>3</sub> (5% crosslinked)	LiClO <sub>4</sub>	0.025	—	—
	LiClO <sub>4</sub>	0.05	—	—
	LiClO <sub>4</sub>	0.125	323.1	907
	LiClO <sub>4</sub>	0.25	157.9	1653
	NaClO <sub>4</sub>	0.025	—	—
	NaClO <sub>4</sub>	0.05	455.1	663
	NaClO <sub>4</sub>	0.125	487.6	903
	NaClO <sub>4</sub>	0.25	791.94	1069
PVO <sub>3</sub> /7 (5% crosslinked)	LiClO <sub>4</sub>	0.025	—	—
	LiClO <sub>4</sub>	0.05	—	—
	LiClO <sub>4</sub>	0.07	512.7	720
	LiClO <sub>4</sub>	0.125	473.9	946
	LiClO <sub>4</sub>	0.25	—	—
			—	—
			9.9	14.1
			9.2	18.3

— Arrhenius behaviour

FIGURE 7.4.1 Values of B and E<sub>a</sub> determined from the VTF equation using method 1 (°) and method 2 (aa).

to 791 K and  $E_a'$  was calculated as 3-15  $\text{kJmol}^{-1}$  using method 1. Using method 2, values in the range 663-1889 K and 12.83-36.57  $\text{kJmol}^{-1}$  were determined for B and  $E_a'$  respectively.

$E_a'$  values were obtained using both methods, and produced activation energy values marginally greater than those reported by other workers. However, the results obtained from this part of study are not of particular interest since the reference temperature employed in equation 8 had been approximated using an experimentally determined  $T_g$  value, rather than a reference temperature which had been identified from the conductivity temperature data directly. The use of such a predetermined reference temperature forces an additional unwarranted constant upon the values of the VTF parameters obtained via this technique.

A more acceptable method of analysis which does not prejudice the outcome would be to perform a direct nonlinear least squares analysis on the original data. Therefore, to determine the best fit of the conductivity-temperature data to VTF equation, a least squares analysis was carried out where no assumptions are made. The resulting values of  $\ln A$ , B and T<sub>0</sub> are displayed in Tables 7.4.2 to 7.4.6 for a range of salt complexes prepared from the uncrosslinked PVO<sub>3</sub>, 5% crosslinked and 5% crosslinked PVO<sub>6</sub>, based polymers.

Using the non-linear least squares analysis the



values of B ranged from 283 to 3014 K, depending on the host polymer, the incorporated salt and the concentration of the salt. The value of B generally increased as the concentration of salt in the polymer increased.

The  $T_g$  values determined using this method increased as the concentration of salt in the polymer increased. However, in all complexes  $T_g$  was found to be lower than  $T_g$  values which had been measured experimentally. In all the samples (with the exception of some of those samples which showed Arrhenius behaviour)  $T_g$  has values ranging from 48-80 K below the experimental  $T_g$  determined for each complex. But in some samples with a low concentration of added salt and showing an Arrhenius relationship, the  $(T_g - T_g)$  was found to be well below or above the 48-80 K range observed for the other polymer-salt complexes.

The fact that  $T_g$  values were generally 40-50 degrees below  $T_g$  in these polymer-salt complexes is of great significance since this would suggest that the non-linear least squares analysis of the conductivity-temperature data has identified the "ideal glass transition temperature" of Gibbs and DiMarzio as being more or less the same as the reference temperature,  $T_g$ , in the VTF equation. This ideal glass transition temperature,  $T_g$ , where the configurational entropy of a system vanishes, is defined as being a

temperature below  $T_g$ .

If the average value of  $\Delta C_p = 29.45 \text{ JK}^{-1}$ , calculated for uncrosslinked PVO, is assumed for the chain extended poly(vinyl ether)/salt complexes and using the T, and B values displayed in Tables 7.4.2 to 7.4.6 of these complexes then  $\Delta\mu$  can also be obtained.  $\Delta\mu$ , the activation energy barrier which must be overcome by a minimum chain segment range from 38-74  $\text{kJmol}^{-1}$  and are almost the same order of magnitude as calculated for the uncrosslinked and lightly crosslinked PVO, salt complexes discussed above.

Again, the exceptions tend to be some of the lightly doped materials where conductivity/temperature data showed Arrhenius behaviour. The calculated activation energies for these samples range between 13-35  $\text{kJmol}^{-1}$ , significantly lower than  $\Delta\mu$  values calculated for the same polymer electrolytes with higher concentration of added salt but of almost similar magnitude to that ones calculated using method 1 or 2 described above.

This discrepancy (Arrhenius or VTF behaviour as reported above) has been noted in a number of systems, particularly when analyses are carried out over different temperature ranges, as has been pointed out by Greenbaum et al<sup>73</sup> in connection with the conductivity of MEEP complexed with  $\text{NaCF}_3\text{SO}_3$ <sup>113</sup>. Careful inspection of data has been shown that conductivity values are more "Arrhenius like" at temperatures considerably above the

glass transition temperature than is predicted by VTF-type equations. However, if the temperature range is extended to low enough temperatures, MEEP exhibits VTF behaviour similar to other amorphous polymer electrolytes.

It should also be emphasized that the method of arriving at values of  $A$ ,  $B$  and  $T_0$  for these systems makes no prior assumptions concerning a model, but the actual values obtained from the minimisation procedures used may not always be the best and will depend on the accuracy of the data set used. Thus the  $A$ ,  $B$  and  $T_0$  values quoted must be regarded as averages and any observed trend or lack of trend can not be regarded as necessarily being meaningful. The interpretation here is based on the apparent similarity of the calculated ( $T_g - T_0$ ) values to the Gibbs-DiMarzio prediction which is taken to be significant. If the model is assumed to be applicable and ( $T_g - T_0$ ) fixed at a constant 50 K, the recalculation of  $A$  and  $B$  does not lead to significant changes. So the  $\Delta\mu$  values remain the same order of magnitude as those in Table 7.4.2 to 7.4.6 and no other trend in the data can be seen. In other words no advantage is gained by prejudging the applicability of this model and the approach used seem to be valid.

$\frac{[Li^*]}{[EO]}$	B lnA	$T_g$ (K)	$T_o$ (K)	$(T_g - T_o)$ (K)	$\Delta\mu$ KJ mol <sup>-1</sup>
0.0125	-9.16	283.3	232.5	-14.15	24 <sup>*</sup>
0.025	-7.23	483	212.3	14.7	28.51 <sup>*</sup>
0.05	-6.14	509.9	222.3	10.2	35.29 <sup>*</sup>
0.125	-2.19	1298	185.4	54.6	72.7
0.25	-1.15	1433	211.4	48.6	76.4

\* Calculated from Arrhenius relationship

TABLE 7.4.1 VTF analysis of conductivity-temperature data for uncrosslinked PVO<sub>3</sub> doped with LiClO<sub>4</sub>

$\frac{[Li^+]}{[EO]}$	$\ln A$	B (K)	$T_g$ (K)	$(T_g - T_g)$ (K)	$\Delta\mu$ kJ mol <sup>-1</sup>
0.025	-8.72	156.3	267	-49.75	28 <sup>*</sup>
0.05	-1.84	2156	94.1	137	34 <sup>*</sup>
0.07	-3.966	1142.9	169.9	64.6	51.65
0.125	-2.412	1389.3	176.8	74.7	83.96
0.25	-2.713	3014.1	154.8	123.2	80.68 <sup>*</sup>

\* Calculated from Arrhenius relationship

TABLE 7.4.2 VTF analysis of conductivity-temperature data for  
5% crosslinked PVO<sub>5</sub> doped with LiClO<sub>4</sub>

$\frac{[Li^+]}{[EO]}$	$\ln A$	B (K)	$T_0$ (K)	$(T_g - T_0)$ (K)	$\Delta\mu$ KJ mol <sup>-1</sup>	
0.025	-4.786	1238	143.9	75.1	80	13.3 <sup>*</sup>
0.05	-4.14	1158	155.7	71.3	72	14.3 <sup>*</sup>
0.125	-4.273	757	221.84	43.2	38	—
0.25	-1.52	1173	231.7	68.3	64	—

\* Calculated from Arrhenius relationship

TABLE 7.4.3 VTF analysis of conductivity-temperature data for  
5% crosslinked PVO<sub>3</sub> doped with LiClO<sub>4</sub>.

$\frac{[Li^*]}{[EO]}$	B	$T_0$	$(T_g - T_0)$	$\Delta\mu$	
[EO]	lnA	(K)	(K)	(K)	
0.025	-4.997	1226	138.3	77.2	40 *
0.05	-4.541	1099	157	71	68
0.125	-3.103	1129	194.1	50.1	60
0.25	1.234	2072	187.3	75.2	123

\* Calculated from Arrhenius relationship

TABLE 7.4.4 VTF analysis of conductivity-temperature data for  
5% crosslinked PVO<sub>3</sub> doped with LiBF<sub>4</sub>

$\frac{[Li^+]}{[EO]}$	B	$T_g$	$(T_g - T_g)$	$\Delta\mu$	
[EO]	lnA	(K)	(K)	(K)	$kJ\ mol^{-1}$
0.025	-4.62	1314	137.5	83	31.8 <sup>*</sup>
0.05	-5.79	824	170.1	62.9	48
0.125	-2.47	1328	180.6	66.1	77.1
0.25	0.55	1898	195.7	74.8	111

\* Calculated from Arrhenius relationship

TABLE 7.4.5 VTF analysis of conductivity-temperature data for  
5% crosslinked PVO<sub>3</sub> doped with LiCF<sub>3</sub>SO<sub>3</sub>



$\frac{[Li^+]}{[EO]}$	B	$T_0$	$(T_g - T_0)$	$\Delta\mu$
	lnA	(K)	(K)	(K)
0.025	-7.26	455	208.8	8.8
0.05	-4.2	973	175.8	54.2
0.125	-3.82	759	224.1	32.4
0.25	-2.12	1200	235.4	48.1

\* Calculated from Arrhenius relationship

TABLE 7.4.6 VTF analysis of conductivity-temperature data for  
5% crosslinked PVO<sub>3</sub> doped with NaClO<sub>4</sub>.

$\frac{[Li^+]}{[EO]}$	$\ln A$	$B$ (K)	$T_0$ (K)	$(T_g - T_0)$ (K)	$\Delta\mu$ kJ mol <sup>-1</sup>
0.025	-8.72	156.3	267	-49.75	28 <sup>*</sup>
0.05	-1.84	2156	94.1	137	34 <sup>*</sup>
0.07	-3.966	1142.9	169.9	64.6	51.65
0.125	-2.412	1389.3	176.8	74.7	83.96
0.25	-2.713	3014.1	154.8	123.2	80.68 <sup>*</sup>

\* Calculated from Arrhenius relationship

TABLE 7.4.7 VTF analysis of conductivity-temperature data for  
5% crosslinked PVO<sub>6,7</sub> doped with LiClO<sub>4</sub>

CHAPTER EIGHT

IONIC CONDUCTION IN MIXTURES  
OF SALTS AND POLYPHOSPHAZENE  
WITH PENDANT CROWN ETHERS

### 2.1 Crown ether chemistry

In chapter 2 the aims and objectives for the preparation of a series of novel comb-shaped, copolymer electrolytes was discussed, in which crown ethers were attached to a polyphosphazene backbone using methylene "spacer units" to modify the polymer T<sub>g</sub>.

Crown ether is the general name of a class of macrocyclic polyethers composed of oxyethylene units and homologues. Often, the amine, thiol and ester analogues of the polyethers are included in the classification, although no systematic delineation of the field exists. IUPAC nomenclature for these compounds is often cumbersome and makes key word identification impossible for computer searching.

The regular nature of the macrocyclic structures has led to the much more useful and practical system using the x-crown-y designation. In this system, x represents the total number of atoms in the macrocyclic ring and y the number of heteroatoms.

Crown ethers form stable 1:1 complexes with alkali and alkaline earth cations<sup>166-169</sup> and other metal cations. Some of them have been shown to display selective complexation and cation transport similar to those of the naturally occurring ligands<sup>166-169</sup>. The complexes of cyclic ligands exhibit increased stability over those with an open chain of similar composition.

Cabbiness and Magerum<sup>170</sup> termed this extra stability the "macrocyclic effect". In work on cyclic tetraamine ligands, they note that the macrocyclic effect is about ten times larger than the chelate effect observed for  $\text{Cu}^{2+}$  with multidentate amine complexes. Cyclic polyethers form much more stable complexes than do their corresponding open-chain analogues, as demonstrated by Frensdorff<sup>166</sup> who noted a remarkable increase in the stability of metal complexes of cyclic polyethers over those of linear counterparts by comparing the complexes of  $\text{Na}^+$  and  $\text{K}^+$  with pentaglyme and 18-crown-6 in methanol.

Since the discovery of dibenzo-18-crown-6 and 18-crown-6 by Pearson<sup>171</sup> and other cyclic polyethers<sup>172</sup> together with the knowledge that these potentially exolipophilic compounds selectively complex alkali and alkaline earth metal cations in their endopolarophilic cavity<sup>173</sup>, efforts have continued to modify the widely useful properties<sup>174-176</sup> of such crown ethers by variation of all possible structural parameters in order to make accessible new ligand systems and to study the relationship between structure and cation selectivity as well as their complex chemistry<sup>177</sup>.

Variable parameters included the number of ether oxygen atoms, ring size, length of the  $(\text{CH}_2)_n$  bridge, substitution by other heteroatoms (N, S), introduction of aromatic (benzene, biphenyl, naphthalene) and

heteroatomic systems (pyridine, furan, thiophene) in the ring<sup>178</sup>. Figure 8.1.1 shows such crown ethers.

The possibilities of structural variation are still not exhausted. An important development in the neutral ligand topology is linked with the ability of large bicyclic diamines (catapinands, see Figure 8.1.2) to take up protons and anions inside their three dimensional cavity<sup>179</sup>. This has led to the design of cryptands - three-sidedly enclosed endopolarophilic / exolipophilic cavities in which metal cations can be firmly trapped<sup>180</sup>. The complexes are called cryptates. Numerous structural variations are also possible here, as shown in Figure 8.1.2.

The selectivity of these synthetic ligands toward metal cations is primarily due to the geometry of intramolecular cavity containing the cation. The order of selectivity is strongly dependent on the relative size of the cation and the ligand cavity<sup>177,186,173</sup>, e.g. the selectivity order of various crown ethers in methanol<sup>177(b)</sup> was found to change from  $\text{Na}^+ > \text{K}^+$  for perhydrodibenzo[14]-crown-4, to  $\text{K}^+ > \text{Na}^+$  for [18]-crown-6 and dibenzo[18]-crown-6 to  $\text{K}^+ = \text{Cs}^+ \gg \text{Na}^+$  for dibenzo[21]-crown-7 to  $\text{Cs}^+ > \text{K}^+$  for dibenzo[24]-crown-8.

The stable complex formation and high selectivity for metal cations (especially alkali and alkali earth cations) displayed by crown ethers have aroused

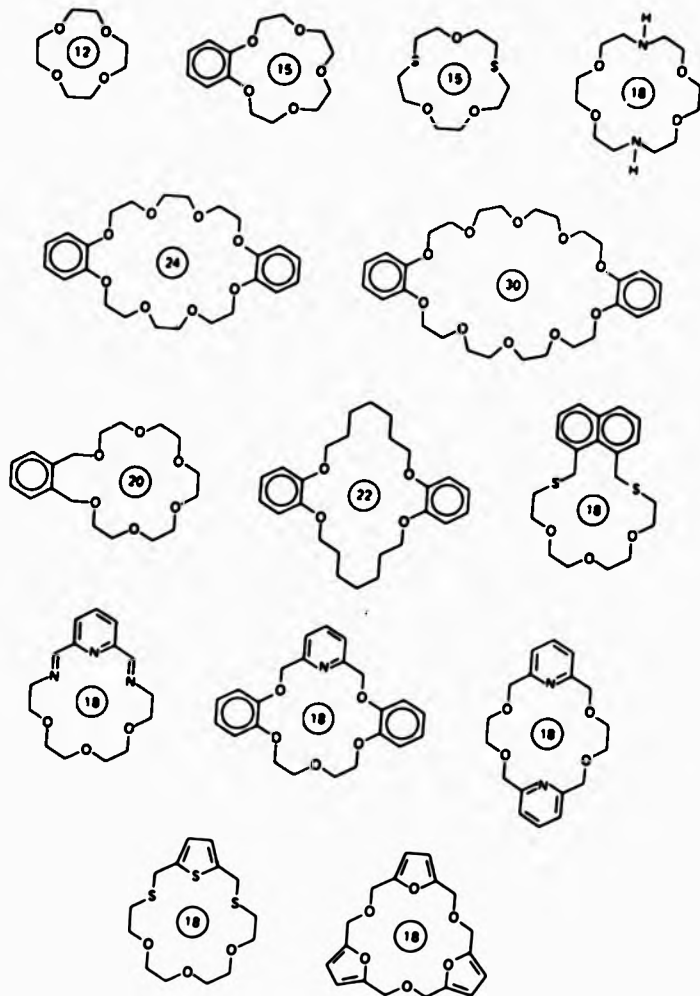


Figure 8.1.1 Some monocyclic crown ether type neutral ligands.

considerable interest in the field of cation transport across membranes, phase transfer catalysis and many other chemical and biological processes. Detailed kinetic results for some of these synthetic ligands<sup>181-183</sup> have been reported and have increased the understanding of cation transport by these ligands. Investigations of cation transport properties of synthetic ligands have been reported<sup>168,169</sup>.

Metal complexation in solution is generally a very quick reaction<sup>184</sup>. Nuclear magnetic resonance<sup>185</sup> and relaxation curves<sup>186</sup> have shown however that complex formation does not occur instantaneously, and it is not a simple one step reaction between ligand and cation. Often complexation includes a series of intermediate steps like substitution of one or several solvent molecules from the inner co-ordination shell of the metal ion and/or internal conformational rearrangements of the ligand, in particular, when the ligand is a multidentate one (crown ether, cryptand)<sup>177(b)</sup>.

The "complexation reaction" can occur essentially by two border mechanisms<sup>187</sup> :

- (1) The solvent molecule leaves the cation decreasing its coordination number, prior to entry of the ligand: *S<sub>N</sub>1*-type mechanism.
- (2) The ligand forces its way through the solvent



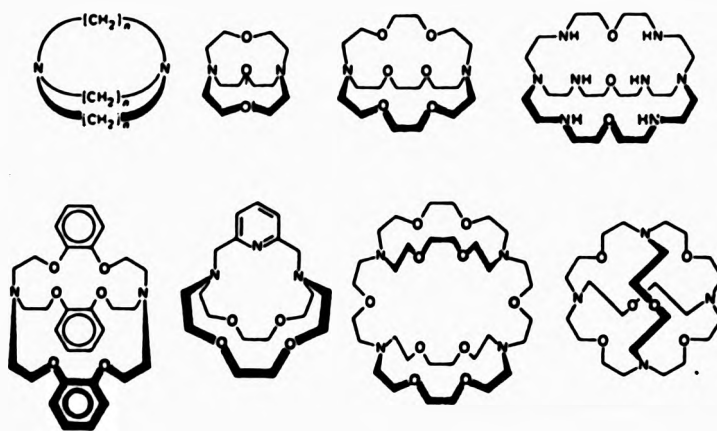


Figure 8.1.2 Some selected cryptand molecules.

envelope of the cation, increasing the coordination number of the latter and then displace a solvent molecule:  $S_N2$ -mechanism.

In the first case, the rate of substitution depends only on the solvated metal ion, in the latter case it is also ligand dependent.

In aqueous solution, solvent/ligand exchange reactions with main-group metal ions proceed via the  $S_N1$  mechanism<sup>188</sup>, whilst  $S_N2$  mechanisms are generally associated with metal ions having deformed coordination envelopes<sup>189</sup>. In reality, a hybrid mechanism resembling more a "push-pull" type process must be taken for granted<sup>177(b)</sup>.

Solvent effects on both the kinetics of complex formation and the stability of the complex have been widely studied<sup>190-192</sup>. The results show that the change of solvent dramatically alters the stability of metal complexation; e.g. on changing from water to methanol the complex stabilities are increased by a factor of about  $10^2$ - $10^3$ .

## 8.2 Ionic conduction in mixtures of salts and polyphosphazene with pendant 16-crown-5 ethers

Both lithium perchlorate and sodium perchlorate were found to dissolve readily in the polymer, code-named PFC1 (see chapter 3), to produce homogeneous mixtures. The concentrations are expressed as the ratio of the amount of cation ( $M^+$ ) per (ethylene oxide) unit in the ring (five in each ring). Above  $[M^+]/[EO]$  ratios of 0.12 the mixtures tended to become brittle and difficult to handle, and so the measurements were confined to samples with lower salt concentrations.

As expected, the  $T_g$  of the polymer-salt complexes shift to higher transition temperatures upon addition of salt, due to crosslinking and coordination of the cation by the polyether chains which are stiffened by this interaction. This effect can be seen from the data in Table 8.2.1. The extent of solvation of  $LiClO_4$  and  $NaClO_4$  by the polymer to form ions rather than ion pairs is reflected in the relative change in  $T_g$  as shown in Figure 8.2.1.

Large increases in  $T_g$  have been equated in the previous chapters and elsewhere<sup>97,101</sup> with effective dissolution and partial ionisation of the salt by the polymer. The relative increase in  $T_g$  of the polymers with different salt types but similar salt concentrations indicate that at rather low salt

concentrations the response of the two systems are comparable. But at medium to high salt content, the electrolyte containing the sodium salt show a greater increase in  $T_g$  of the polymer as shown in Figure 8.2.1 .

This may suggests that  $\text{NaClO}_4$ , is more effectively ionised by the crown ether (16-crown-5) and thereby causing a greater stiffening of the polymer backbone. The sodium ion is normally thought to be more tightly complexed by the 16-crown-5 ether than the lithium ion which is smaller and does not fit the crown ether cavity as well as  $\text{Na}^+$ .

This is reflected in the measured conductivities of the polymer/ $\text{NaClO}_4$ , and polymer/ $\text{LiClO}_4$ , electrolytes as a function of temperature and salt concentration, as shown in Figures 8.2.2 and 8.2.3, which show that the system with largest increase in  $T_g$ , has the highest conductivity levels. The smaller radius of the  $\text{Li}^+$  ion leads to less effective coordination by the crown ether and this appears to influence the conductivity level achieved. Nevertheless weakly associated crown ether complexes were seen to form and perhaps the poorer conductivity levels observed for  $\text{Li}^+$ /polymer mixtures could be due to this poor dissociation of the salt and extensive ion pairing in the matrix. In order to achieve better conductivity levels for the Li systems, one can opt to use smaller crown ether rings sizes where  $\text{Li}^+$  can be more effectively complexed, thereby enabling greater

dissociation of the salt to occur in the polymer. This idea is discussed more fully later in this chapter.

The dependence of conductivity on temperature is non-Arrhenius as seen from the curvature of the  $\log \sigma$  against  $1/T$  plots in Figures 8.2.2 and 8.2.3.

Salt	[M <sup>+</sup> ]/[EO]	T <sub>g</sub> /K	ΔT <sub>g</sub> /K
LiClO <sub>4</sub>	0.0125	260	27
	0.0166	262	29
	0.0208	266	33
	0.0417	275	42
	0.0833	278	45
NaClO <sub>4</sub>	0.0125	258	25
	0.0166	273	40
	0.0208	283	50
	0.0286	285	52
	0.0417	305	72
	0.0833	339	106
	0.1250	363	130

Table 8.2.1 The effect of added salt on the T<sub>g</sub> of the

PFC1

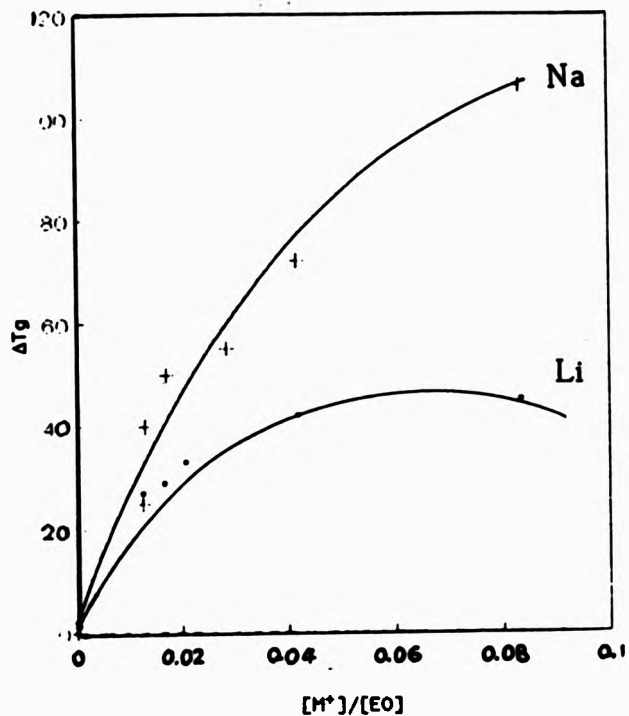


Figure 8.2.1 The relative change in  $T_g$  ( $\Delta T_g$ ) upon salt addition ( $LiClO_4$  and  $NaClO_4$ ) for the PPCl electrolyte.

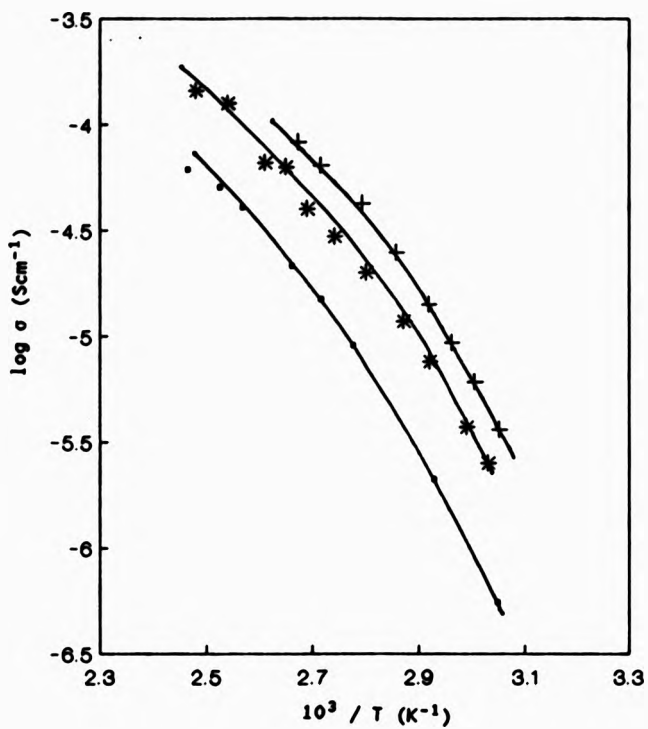


Figure 8.2.3 Arrhenius plot of log conductivity against reciprocal temperature for the PPCl/NaClO<sub>4</sub> complexes.

[Li<sup>+</sup>]/[EO] ratios: 0.0125 (-)

0.0208 (\*)

0.0417 (x)



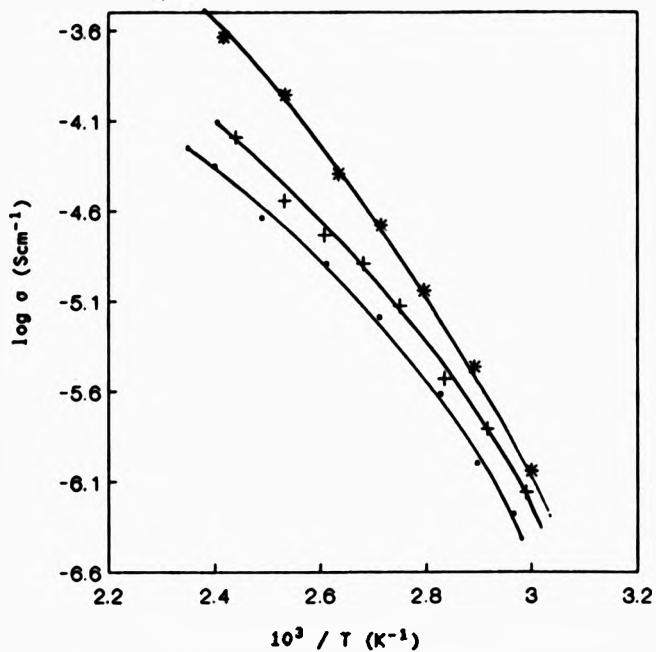


Figure 8.2.2 Arrhenius plot of log conductivity against reciprocal temperature for the PPCl/LiClO<sub>4</sub> complexes.

[Li<sup>+</sup>]/[EO] ratios: 0.0125 (•)

0.0208 (x)

0.0417 (\*)

### 2.1 The effect of spacer length on the conductivity of the PFC1/Sodium perchlorate mixtures

The conductivity levels obtained for the PFC1/salt complexes, discussed above, are reasonably good but generally lower than those obtained in comparable comb-shaped structures with short Poly(ethylene oxide) chains. The salt-free structure investigated above had the crown ether attached directly to the main chain via an oxygen bridge and this had a glass transition temperature of 233 K which is higher than the comb-shaped polymers with linear oxyethylene side chains.

Conductivity levels have been found to improve in amorphous systems when the T<sub>g</sub> value is lowered due to the increased flexibility of the polymer matrix. It is possible to decrease the T<sub>g</sub> of the crown-ether substituted polyphosphazenes by inserting flexible units between the bulky crown-ether rings and the main polymer chain. This serves to "plastize" the system internally which should decrease the T<sub>g</sub> and lead to a consequential increase in conductivity when salt is added to the polymer.

On this basis two polymers were prepared where 16-crown-5 ether was chemically attached by spacer units of differing lengths, 3 and 6, to the polyphosphazene. The polymers containing 3 and 6 methylene spacer units

were code-named PPC2 and PPC3 respectively (see chapter 3).

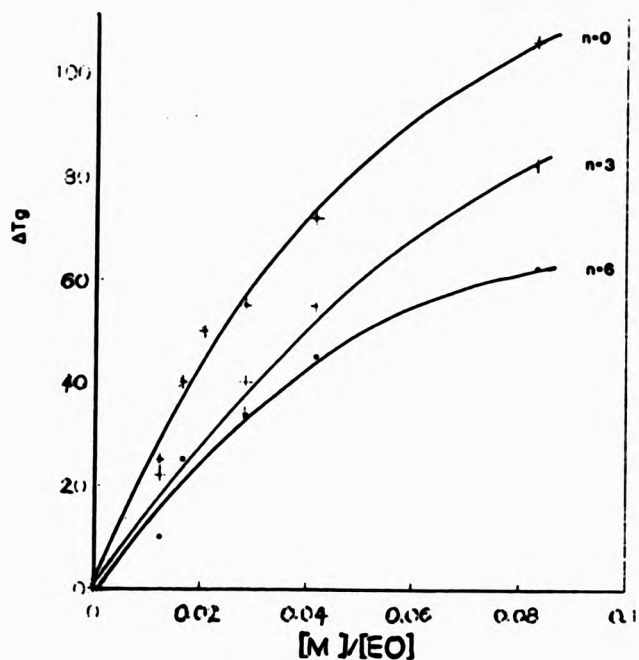
Glass transition temperatures for the undoped polymers were found to decrease as the number of methylene units in the chain, between the ring and the backbone, increased. This is shown in Table 8.3.1, where it can be seen that there is a decrease of 9 K when  $n$  increases from 0 to 6. While this is not a particularly large effect the relative increase in  $T_g$  when  $\text{NaClO}_4$  is added to the polymers is much smaller for the sample with  $n = 6$  than for the other two samples (see Table 8.3.1 and Figure 8.3.1). Thus the differences  $\Delta T_g$  between the undoped and doped sample at, say, a  $[\text{Na}^+]/[\text{EO}]$  ratio of 0.0417 decrease from 72 to 55 to 45 K for  $n = 0, 3$  and 6, respectively. Consequently there is a smaller net increase in  $T_g$  for the polymer-salt mixtures over the entire composition range when  $n = 6$ , which is reflected in the conductivities of the complexes as shown in Figures 8.3.1, 8.3.2. This effect can be seen more clearly in Figure 8.3.3 where the temperature dependence of the  $\log \sigma$  data are plotted for a fixed  $[\text{Na}^+]/[\text{EO}]$  ratio of 0.0417. The conductivities of the complexes are found to be almost an order of magnitude larger when  $n$  is increased from 0 to 6, and for the latter polymer PPC3, these conductivity levels are comparable to some of the comb-shaped structures<sup>17</sup>.

These results are in accordance with the suggestion

that ionic mobility is assisted by flexibility in the polymer matrix and that this will increase as the temperature is increased.

[Na <sup>+</sup> ] [EO]	n = 0		n = 3		n = 6	
	Tg (K)	ΔTg	Tg (K)	ΔTg	Tg (K)	ΔTg
0.000	233.0	0	226.0	0	224.5	0
0.0125	256.0	25.0	248.0	22.0	234.5	10.0
0.0167	273.0	40.0	260.0	34.0	249.5	25.0
0.0286	285.0	52.0	266.0	40.0	258.0	33.5
0.0417	305.0	72.0	281.0	55.0	269.5	45.0
0.0833	339	106	308.5	82.5	287.5	62.5

Table 8.3.1 Effect of spacer length on the glass transition temperature for poly(phosphazene-crown-ether)-NaClO<sub>4</sub> complexes.



**Figure 8.3.1** The comparison of change in Tg ( $\Delta T_g$ ) as a function of salt concentration ( $\text{NaClO}_4$ ) for the PPC1, PPC2 and PPC3 ( $n = 0, 3$  and  $6$  respectively) polymer electrolytes.

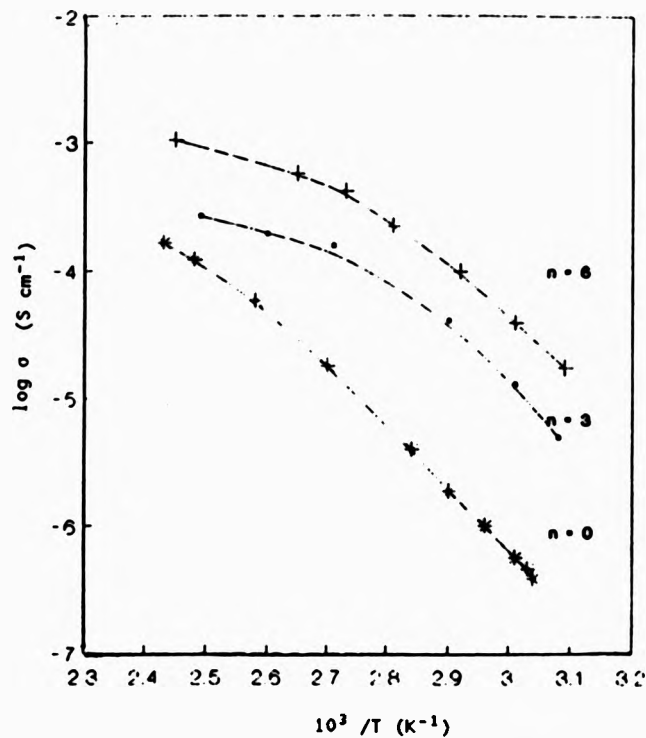


Figure 8.3.1 Arrhenius plot of log conductivity against reciprocal temperature for PPC1, 2 and 3 / NaClO<sub>2</sub> salt mixtures (n = 0, 3 and 6 respectively) at fixed salt concentration of [Na<sup>+</sup>]/[EO] = 0.0417.

**8.4 Ionic conduction in mixtures of salts and polyphosphazenes with pendant 2-hydroxy-15-crown-5 and 2-hydroxy 12-crown-4 ethers**

For comparison with the above electrolytes a 15-crown-5 derivative of polyphosphazene with one methylene spacing unit was prepared and code-named, as PFC5. The glass transition temperature for the undoped polymer was found to be 228 K, about 5 K lower than the PFC1 and about 2 K higher than PFC2. Sodium perchlorate was found to dissolve readily in the polymer to produce a homogeneous mixture with a subsequent increase in T<sub>g</sub> as shown in Table 8.4.1.

For added NaClO<sub>4</sub>, at  $[Na^+]/[EO] = 0.0417$  the conductivity was found to be significantly higher than the PFC1 and PFC2 electrolytes and only marginally lower than PFC3 complex where 16-crown-5 was chemically attached by six methylene spacer units to the backbone of polyphosphazene. This effect can be seen in Figure 8.4.1. Here, the implication is that if the number of methylene spacer units is raised to six for the system containing 15-crown-5, a further improvement in ionic conductivity can be achieved. The conductivity levels for this type of systems then would be comparable with some of the comb-shaped structures with short ethylene oxide chains.

Although the stability constants for the unattached



[Na <sup>+</sup> ]/[EO]	T <sub>g</sub> /k	ΔT <sub>g</sub>
0.00	228	0
0.0125	240	12
0.0166	255	27
0.0147	275	47
0.0833	300	72

TABLE 8.4.1 The effect of added salt (NaClO<sub>4</sub>) on the glass transition temperature of PPC1

15-c-5

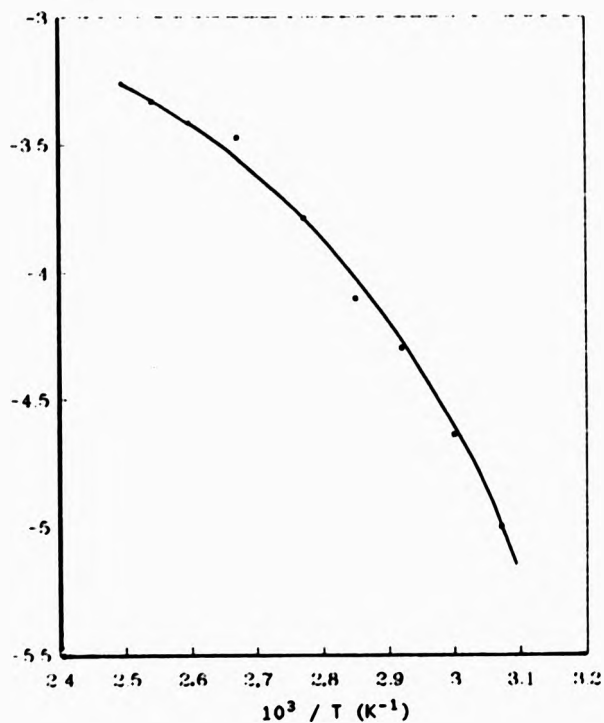


Figure 8.4.1 Arrhenius plot of log conductivity against reciprocal temperature for PPC5 /NaClO<sub>4</sub> salt mixture at a fixed salt concentration of  $[\text{Na}^+]/[\text{EO}] = 0.0417$ .

16-crown-5 and 15-crown-5 sodium salt complexes are only slightly different as shown in Table 8.4.2, it seems that due to some other additional factors, the two polymer electrolytes give varying levels of conductivity. It is difficult to offer a meaningful explanation for this behaviour in the absence of hard physical data on these type of materials. Although the stability constants and ion selectivity of these ligands provide a good guide regarding their choice as polymer electrolytes, but once attached to polymers various effects can alter the properties of these ligands. For example, Polyvinyl macrocyclic polyethers (see Figure 8.4.3) were found to be more efficient in complexing cations than their monomeric analogues, especially in those cases where the diameter of the polyether ring is smaller than that of cation<sup>193</sup>.

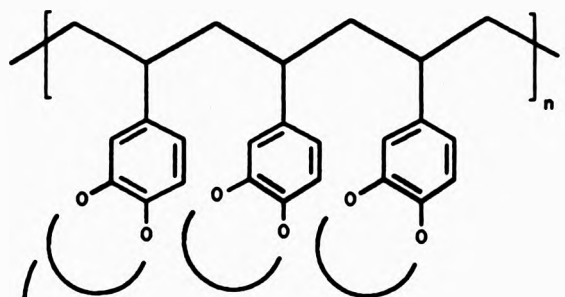
For example,  $\log K$ , of  $K^+$ -poly(4'-vinyl)benzo-[15]-crown-5 complex is found to be  $>5$ , where as that for the corresponding monomer benzo[15]crown-5 potassium salt complex is 3.7. This has been explained by cooperative effects, where two neighbouring crown ether rings combine with a single cation.

According to the published literature, based on the cavity size of crown ethers and ionic radius of the metal ions, 16-crown-5 or 15-crown-5 are not suitable candidates for efficient complexation of lithium ions. It has been reported that, for example, with 18-crown-6

Crown ether	log K <sup>(a)</sup>	
	Sodium cation	Potassium cation
Hydroxy 16-crown-5	3.03	2.53
15-crown-5	3.30	3.34

(a) crown ether + M<sup>+</sup>  $\xrightleftharpoons{K_1}$  (crown ether M<sup>+</sup>) in methanol

TABLE 8.4.2 Stability constants



crown ether moieties with various number of ethylene oxide units

Figure 8.4.3 Polystyrene macrocyclic polyethers<sup>183</sup>.

two types of adducts can be observed: a 1:1 complex with  $\text{LiClO}_4$ , and a 1:2 complex with  $\text{LiSCN}$ , both including a two additional moles of water<sup>194</sup>. 18-crown-6 ring skeleton is too large for the small  $\text{Li}^+$ . It is effectively narrowed by encapsulating a water molecule in its cavity. The water has a double role, acting as a coordinating agent toward  $\text{Li}^+$  and donating its protons to the ether agents.

In a large series of ligands, all containing four ether oxygen binding sites, the association of  $\text{Li}^+$  is characterised by pentacoordination with square-pyramidal geometry as shown in Figure 8.4.4 For example, in the 1:1 complex between 16-crown-4 and  $\text{LiSCN}$  the metal ion is coordinated to four ether oxygens and to the nitrogen of the anion. Similarly, in the 1:1 complexes of  $\text{LiNO}_3$  with benzo-14-crown-4 the  $\text{Li}^+$  ligates to the four oxygens with the bidentate  $\text{NO}_3^-$  counter ion, being displaced from the plane of the former towards the adjacent nitrate<sup>195</sup>.

The association of  $\text{Li}^+$  and 12-crown-4 is also characterised by a square-pyramidal pentacoordination. a suitable example includes 1:1 complexes of this ligand with  $\text{LiSCN}$ <sup>196</sup>. In these structure the coordination sphere around  $\text{Li}^+$  consist of four basal oxygens and an apical N-site of the thiocyanate. In other examples of this host the lithium ions exhibit a coordination number of 8. This includes 2:1 complexes between 12-crown-4 and

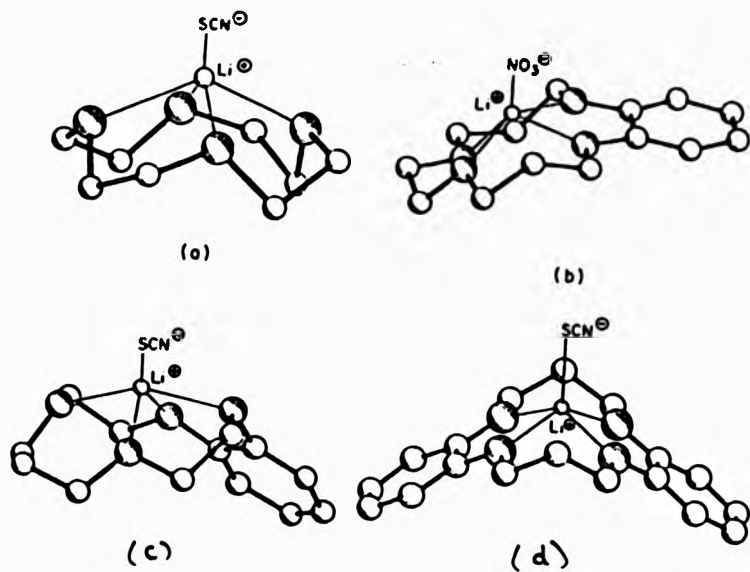
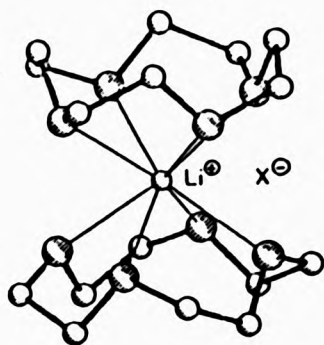
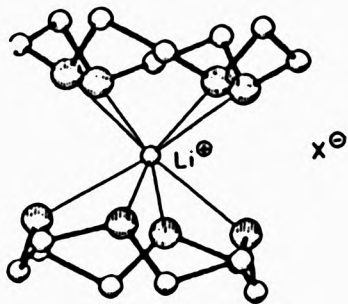


Figure 8.4.4 Complexes of  $\text{Li}^+$  salts with (a) 12-crown-4 (b) benzo-14-crown-4, (c) benzo-13-crown-4 and (d) dibenzo-14-crown-4.



(a)



(b)

Figure 8.4.5 2:1 complexes of 12-crown-4 with (a) diphenyl phosphide and (b) dimethylcopper(I) lithium salts, showing 8 coordination of the cation ( $X^-$  represents the corresponding counter ions).



the lithium cation with diphenylarsenide, diphenylphosphide<sup>197</sup>, dimethylcopper and diphenylcopper as counter ions<sup>198</sup>. Here the Li<sup>+</sup> is surrounded by two separate crown ether entities to form a puckered sandwich arrangement [Li(12-crown-4)<sub>2</sub>]<sup>+</sup>, being coordinated only by the crown ether oxygens (Figure 8.4.5).

These structure types demonstrate the use of a crown ether in effecting metal cation and organometalloid anion separation. In a closed packed disordered system based on the comb-shaped polymers, migration of cations would be difficult, with extensive ion-pairing which effectively reduces the number of charge carriers. The use of 12-crown-4, however, may offer two advantages:

- i) the crown rings provide an inbuilt free volume in the polymer matrix
- ii) the Li<sup>+</sup> ions are shielded from the ClO<sub>4</sub><sup>-</sup> anions

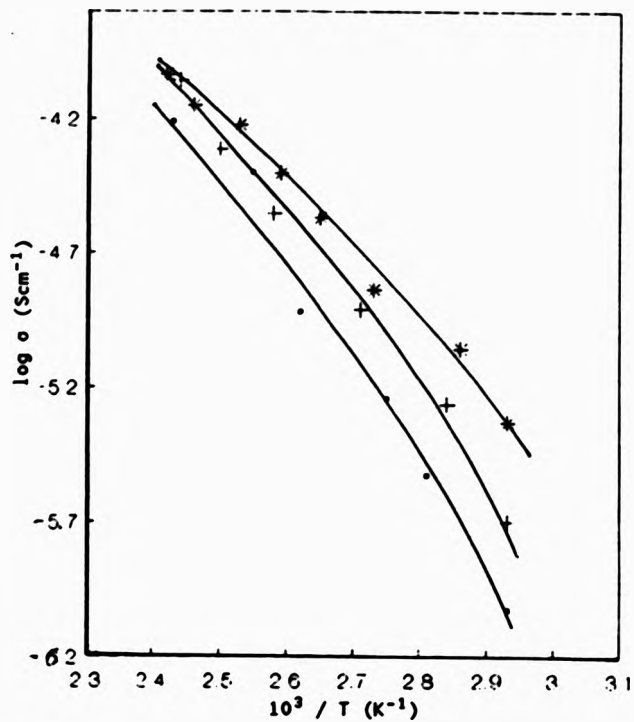
This idea was tested by chemically attaching 12-crown-4 to a polyphosphazene backbone. This material which was code-named PPC6 (see chapter 3) was then doped with LiClO<sub>4</sub>. The glass transition temperature of the undoped polymer was found to be 225.5 K and progressively increased upon salt addition as shown in Table 8.4.3.

The relative change in T<sub>g</sub>, upon salt addition, for

[Li <sup>+</sup> ]/[EO]	T <sub>g</sub> (K)	ΔT <sub>g</sub>
0	225.5	0
0.0125	252.5	27
0.0208	268.0	42.5
0.0417	280.5	55
0.0833	293.0	67.5

TABLE 8.4.3 The effect of added salt (LiClO<sub>4</sub>) on the T<sub>g</sub> of PPC6 polymer electrolyte.

these complexes at low salt concentrations is very similar to the 16-crown-5 /Li- salt complexes, but at medium to high ratios of salt the change in T<sub>g</sub> seem to be much greater. This probably implies that in this system the ionisation of the salt occurs more efficiently which results in a decrease in the mobility of the polymer. This is reflected in the measured conductivities of this electrolyte as shown in Figure 8.4.6 at various salt concentrations.



*Fig.* 8.4.6 Arrhenius plot of log conductivity against reciprocal temperature for the PPC6/LiClO<sub>4</sub> salt mixtures.

[Li <sup>+</sup> ]/[BO] ratios:	0.0125	(o)
	0.0208	(x)
	0.0417	(*)

### 8.5 VTF analysis of the conductivity-temperature data

For all the polyphosphazene-crown salt complexes studied above, dependence of conductivity on temperature is non-Arrhenius as seen from the curvature of the logs against  $1/T$  plots. These can be linearized by using the Vogel-Tammann-Fulcher (VTF) equation (equation 8).

According to this equation  $A$  and  $B$  are constants and  $T_0$  has been variously regarded as the  $T_g$  of the original polymer, that of the polymer-salt complex, or the temperature below which the configurational entropy is zero. By making no assumptions, the values of  $A$ ,  $B$  and  $T_0$  were obtained by a minimisation procedure for some of the systems described above.

The VTF parameters for polymer PFC1/salt systems and PFC2, PFC3 with  $[Na^+]/[EO] = 0.0147$  are shown in Tables 8.5.1 and 8.5.2 respectively. According to the Adam-Gibbs analysis of the VTF equation, which is based on the configurational entropy approach, predicts that  $T_g - T_0 = 50$ . One can see that this approximate value is approached only at higher salt concentrations for the PFC1/salt complexes (when  $n$ , the number of methylene spacer units is 0). This type of behaviour has been seen in other systems and commented in the previous chapters. This analysis may suggest that the model applied here is not the best model to use for these systems.

Salt	[M <sup>+</sup> ]/[EO]	ln A	B/K	T <sub>0</sub> /K	T <sub>g</sub> /K	(T <sub>g</sub> - T <sub>0</sub> )
LiClO <sub>4</sub>	0.0125	-8.44	746.0	254.3	260	5.7
	0.0208	-7.76	851.7	243.5	266	22.5
	0.0417	-3.06	1700	210.1	275	65.0
NaClO <sub>4</sub>	0.0125	-8.04	699.7	252.7	258	5.3
	0.0167	-8.30	573.0	261.2	273	11.8
	0.0286	-6.81	854.1	234.6	285	50.4
	0.0417	-8.16	458.1	264.9	305	40.1

TABLE 8.5.1 Glass transition temperature T<sub>g</sub> and VTF parameters for the polymer

PPCl/salt complexes.

n	ln A	B (K)	T <sub>g</sub>	T <sub>g</sub> (K)	(T <sub>g</sub> - T <sub>g</sub> )
0	-8.16	458.1	284.9	305.0	40.1
3	-9.63	162.0	295.0	281.0	14.0
6	-7.97	248.0	282.0	269.5	-12.5

TABLE 3.41 VTF parameters for poly(phosphazene-crown-ether)-  
NaClO<sub>4</sub> complexes with [Na<sup>+</sup>]/[EO] = 0.0417 .

### Conclusions:

The results presented in this chapter show that the polymer/ $\text{NaClO}_4$  (PFC1) system gives higher conductivity levels, for comparable salt concentrations, than mixtures containing  $\text{LiClO}_4$ . This suggests that  $\text{NaClO}_4$  is more effectively ionised by the crown ether and thereby makes available a greater number of charge carriers to the system. The sodium ion is normally thought to be more tightly bound by the 16-crown-5 ether than the lithium ion which is smaller and does not fit the crown ether cavity as well as sodium ion. Thus it appears that the more effective the cation binding by the crown ether the better the conductivity. The implication is then that the anion may be largely responsible for the conduction in these systems, rather than the cation, and that significant amounts of the former exists as free ions which are shielded from back coordination with the complexed cation, thereby remaining free to move within the polymer matrix. The measurements of ionic transport numbers is hoped to clarify this point.

It was also shown above that conductivity levels can be improved by lengthening the spacer and decreasing the initial  $T_g$  of the polymer where the system with six methylene spacer units exhibited higher conductivity levels similar to some of the linear side chain



structures. The system based on 15-crown-5 was shown to be promising and by introducing spacer units it is hoped that, yet, higher levels of conductivity can be achieved. Finally, it was expected that a decrease in crown ether ring size would improve the complexing of the  $\text{Li}^+$  ion, but the structure with one methylene spacer and a 12-crown4 ring did not result in great improvement in conductivity levels.

CHAPTER NINE

CONCLUTIONS AND FUTURE WORK

### 2.1 Effect of crosslinking on polymer properties:

1. It has been shown in this work that comb-shaped polymers can be synthesised which have properties similar to those characteristic of polyethylene oxide, and amorphous complexes can be prepared on addition of inorganic salt to these materials.
2. The Majority of comb-shaped polymer electrolytes have poor mechanical properties: at room temperature they most resemble viscous melts and tend to flow at elevated temperatures. This problem is a serious drawback for potential commercial applications where long term stability is required. However, in this study it was shown that, by using a facile crosslinking procedure the material can be converted into a stable, non tacky, rubber-like material, which improves the handling characteristics significantly without loss of performance.
3. Another useful aspect of the crosslinking procedure used in this work is that crosslinked films with various thicknesses can be fabricated by carrying out the crosslinking reaction in a layer of monomers and an initiator spread on a glass plate. This produces the material in a more convenient sheet form.
4. Due to crosslinking, the  $T_g$  of the networks increases because of the restrictions imposed by the crosslinks on

the freedom of the motion of the polymer backbone. After an initial small increase, the  $T_g$  remains constant up to 5% crosslinking, after which there is a sharper rise up to 11% which slows down at higher cross link densities.

5. A loss of flexibility is noted in each of the polymeric hosts on dissolution of salt. The effect is increased as the number of cations solvated by the polymer is increased until at the solubility limit of the salt in the polymer no further loss of flexibility occurs.

6. The loss of flexibility noted in the polymer on addition of particular concentration of salt was found to be similar for the lightly crosslinked (up to 5% crosslinked) and uncrosslinked materials.

7. The temperature dependence of ionic conductivity in the crosslinked polymer/salt mixtures remains unaffected by network formation up to an apparent crosslink density of 5%.

8. Thus the effect of low levels of crosslinking on the ion conduction and chain motion is negligible and these polymer/salt complexes behave like the uncrosslinked material.

9. Finally all of the network structures reported in this work swell to varying degrees in organic solvents and this feature was used to prepare the polymer/salt complexes by immersing the network in a methanol solution of the required salt. The extent of swelling

was dependent on crosslink density and the type of solvent. Chloroform caused greater swelling. Longer EO side chains in PVO<sub>3</sub> and PVO<sub>6,7</sub> samples caused greater swelling in polar solvents such as methanol.

### 3.2 The effect of chain extension on polymer properties

1. When the number of EO units in the side chain is increased from 3 to 5 (mono-dispersed), or 6/7 (average number of EO units), a significant improvement in ionic conductivity is achieved. This is in line with the other findings that, the conductivity determined for systems containing the same salt and concentration of salt increased as the length of the side chain in the polymeric host was extended from one to (on average) seven EO units. The enhanced conductivity in these materials is generally thought to be due to greater flexibility of the polymer chains. But in this work, no further flexibility is achieved when the number of EO units is raised to 5 or 6/7. The T<sub>g</sub> of the chain extended polymers are in fact slightly higher than the system with only 3 EO units in the side chain.

2. Unlike PVO<sub>3</sub>/salt complexes, the temperature dependence of log conductivity for these systems show a linear temperature dependence. This is particularly noticeable at low to medium salt concentrations.

3. The comparison of the two uncrosslinked PVO<sub>3</sub> and PVO<sub>3</sub>/LiClO<sub>4</sub> complexes show that the relative rise in T<sub>g</sub> for the PVO<sub>3</sub> complex was significantly greater than the one observed in PVO<sub>3</sub> complexes, especially at high concentrations of the added salt.

4. This suggests that the dissociation of the salt and therefore the number of charge carriers, ionic mobility, ion-ion, ion-polymer interactions and other related effects are not similar in these two materials.

5. The electrical conductivity shown by these electrolytes is noticeably superior to the salt complexes prepared from siloxane or polyphosphazene based comb-shaped polymers.

### 2.3 Polyphosphazene-crown ether electrolytes:

1. For the unspaced structure (PFC1) the increase in T<sub>g</sub> is greater when NaClO<sub>4</sub> is used compared with the system containing LiClO<sub>4</sub>.

2. This is reflected in the conductivity levels which are significantly better in the NaClO<sub>4</sub> polymer system.

3. The implication is that 16-crown-5 is a more effective binding agent for sodium ions than the Li<sup>+</sup> and so there is a larger number of charge carriers and fewer ion pairs produced in the system containing NaClO<sub>4</sub>.

4. Conductivity levels can also be improved by spacers which decrease the initial  $T_g$  of the polymer.
5. The system with six methylene units achieves conductivity levels similar to some of the linear side chain structures.
6. According to the VTF analysis of the conductivity data, which is based on the configurational entropy model, the prediction that  $T_g - T_c = 50$  K is approached only at high concentrations for PPCl/salt complexes. Therefore, the model applied here may not be the best model to use for this type of systems.

#### 2.4 Closing Remarks and Future Work:

Although the study of the electrical properties of comb-shaped polymer-salt complexes was initiated only fairly recently, it has already been established that these materials demonstrate many interesting features which could be developed further to allow the preparation of materials exhibiting high levels of ionic conductivity at low temperatures.

The ultimate goal in this area of research is the development of a material which are both highly conductive, and which also possess suitable electrochemical, mechanical and thermal stability over

long periods of time. Notwithstanding the above points, it is vital, from a purely academic point of view to study the various factors which give rise to significant ionic conductivity in these polymeric materials.

PEO/salt complexes have been under continuous investigation for nearly 20 years, and, at present certain aspects of these materials are still not fully understood. It is hoped that by studying the different aspects of these materials a clearer picture regarding the mechanism of ion transportation, the nature of charge carrier(s) and the processes involved in charge carrier(s) generation would emerge. It will then be possible to predict various parameters that result in the desired properties anticipated from these materials.

The relationship established between conductivity and  $T_g$  suggests that research would be worthwhile on solvating polymers with very low  $T_g$ . Throughout this work, it was shown that polyvinyl ethers and polyphosphazenes have chains that offer very high flexibility, allowing cooperative polymer conformation fluctuations as needed for cation solvation and mobility. In this respect, these polymers probably present the ultimate as far as chain flexibility is concerned.

Therefore, to achieve conductivity levels higher than the ones reported in this work, the rise in  $T_g$  of the polymer, upon salt addition, should be kept to a



minimum. Literature data suggest that if the polymer can solvate the ions efficiently then there is a supply of free ions to act as charge carriers but this also raises the  $T_g$ , because the complexed ions crosslink and stiffen the polymer chains. When the ionisation of the salt in the polymer is low, the  $T_g$  of the mixture is also low but there are only a few ions to act as charge carriers and so the conductivity is correspondingly low.

Although this was found to be the case in polyphosphazene-crown ether salt mixtures, the comparison between PVO, an PVO<sub>3</sub>/LiClO<sub>4</sub> mixtures shows the opposite. The rise in  $T_g$  upon salt addition in PVO<sub>3</sub> is lower than the PVO, system (note that the two polymers were found to have almost similar chain flexibility), yet the former material exhibits much higher conductivity levels. If higher conductivity in the chain extended electrolyte is due to a more efficient dissociation of the salt, this should cause, by the virtue of the argument given above, a greater stiffening of the polymer chains. Here, this effect is not observed and demonstrates that the nature of ionic conductivity in polymer electrolytes is a very complex one indeed and requires further elucidation.

An added attraction of vinyl ethers used in this work is the ease with which they can copolymerise with a variety of other monomers and this property can be utilised to modify the polymer structure, thus affecting

its properties (for example: inclusion of self-ionisable side chains may result in pure cation conductors, by having the anion fixed to the polymer).

Regarding the crown ether based polymer electrolytes, while conductivity levels achieved in these materials match the other PEO/salt mixtures, none were significantly better. However, the importance of ring size and firm cation binding was demonstrated but requires further exploration and may lead to a further improvement in performance.

Also, it has to be established whether we are dealing with cation or anion conduction and measurement of transport numbers is essential to an understanding of the mechanism of conduction.

The use of a phosphazene backbone provided us with a very flexible backbone for chemical attachment of the rings, but having two bulky groups on the same monomeric unit of the polymer may cause unnecessary hindrance which might reduce efficient ion complexation.

Therefore it is more desirable to have one crown ether per repeat unit. This can be done in many ways, and a vinyl type of polymer backbone similar to the polyvinyl ethers is suggested. Two brief reaction schemes for the preparation of the crown based monomers is outlined in Figure 9.1.

It should also be noted that if a more efficient dissociation of the salt is desired then an electron

donor side arm on the crown ring would stabilise the complex further according to Figure 9.2. Finally, another family of ligands of interest which might be considered is cryptands which form more stable complexes with alkali metal ions than crown ethers. In this type of structure the metal ion is well encapsulated within the dimensional cavity of the 3 cryptand cup and is effectively shielded from its counter ion.

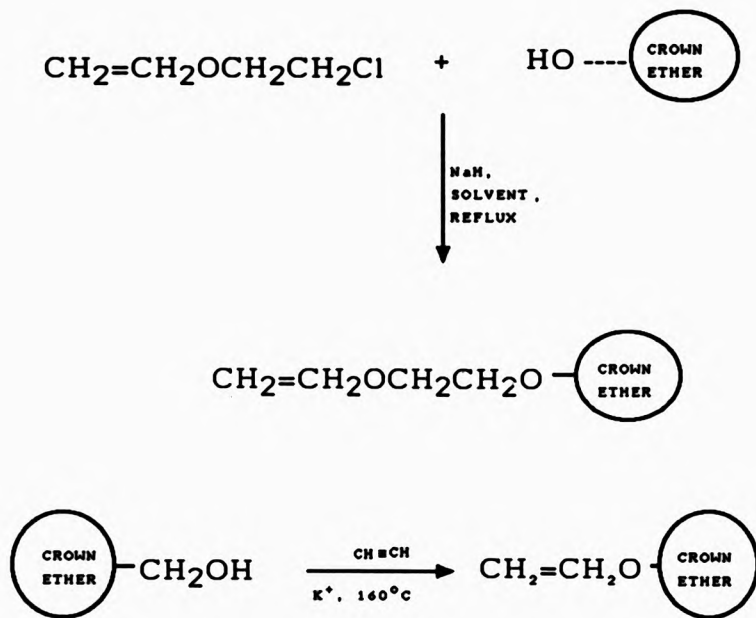
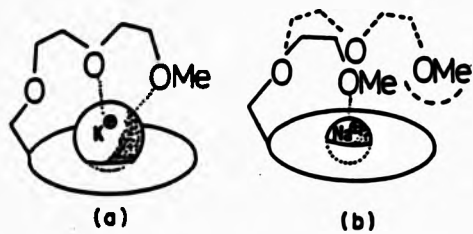


FIGURE 9.1 Routes to polymerisable vinyl ethers containing crown ethers



**Fig 9.2** Schematic drawings of lariat-cation interactions (crown ether represented by a simple ring)

## REFERENCES

1. H. Shirakawa, E.J. MacDiarmid, A.G. Chiang, *J. Chem. Soc. Chem. Com.*, (1977), 578.
2. M.B. Armand, J.M. Chabango, M. Duclot, in "Fast Ion Transport in Solids", Ed. P. Vashista, J.N. Mundy, J.K. Shenoy, p.131, New York: North Holland (1979).
3. A. Eisenberg, M. King in "Ion Containing Polymers", Ed. R.S. Stein, New York: Academic.
4. D.E. Fenton, J.M. Parker, P.V. Wright, *Polymer*, (1973), 14, 589.
5. M.B. Armand, J.M. Chabango, D. Duclot, Second international conference on solid electrolytes, St. Andrews, 1987.
6. C. Berthier, W. Goreki, M. Minier, M.B. Armand, J.M. Chabango and P. Rigaud, *Solid State Ionics*, (1983), 11, 91.
7. M.B. Armand, Six international conference on solid State Ionics, Garmisch-partenkirchen, 1987, paper A4.
8. J.J. Fontanella, M.C. Wintersgill, J. Smith, A. Semancik, and C.G. Andeen, *J. Appl. Phys.*, (1986), 60, 2665.
9. J.J. Fontanella, M.C. Wintersgill, J.P. Calame, A. Smith, and C.G. Adneen, *Solid State Ionics*, (1986), 18/19, 253.

10. D.J. Bannister, G.R. Davies, I.M. Ward and J.E. McIntyre, *Polymer*, (1984), 25, 1291.
11. J.R. Owen, in "Electrochemical Science and Technology of Polymers-1", ed. R.G. Linford, Elsevier, London, 1987.
12. M.J. Smith, *Portugaliae Electrochemica Acta*, (1986), 4, 225.
13. M.B. Armand, *Ann. Rev. Sci.*, (1986), 16, 245.
14. D.F. Shriver in "Polymers in Electronics", CRC press, Cleveland Ohio, to be published.
15. C.A. Vincent, *Prog. Solid State Chem.*, (1987), 17, 145.
16. P.V. Wright, *J. Macromol. Sci.*, to be published.
17. *Polymer Electrolytes Reviews 1*, ed. J.R. MacCallum and C.A. Vincent, Elsevier, London, 1987.
18. a) M. Miamoto, M. Sawamoto, T. Higashimura  
*Macromolecules*, (1984), 17(3), 265.  
b) M. Miamoto, M. Sawamoto, T. Higashimura  
*Macromolecules*, (1985), 18(2), 123.  
c) S.Aoshima, K. Ebara, T. Higashimura  
*Polymer Bull.*, (1985), 14, 425.  
d) T. Nakamura, S. Aoshima, T. Higashimura  
*Polymer Bull.*, (1985), 14, 515.  
e) M. Sawamoto, S. Aoshima, T. Higashimura  
*Makromol. Chem., Makromol. Symp.*, (1988),  
13/14, 513.  
f) T. Higashimura, S. Aoshima, M. Sawamoto,

*Makromol. Chem., Makromol. Symp.*, (1988),  
13/14, 457.

19. S.R. Sandler, W. Karo, "Polymer synthesis Vol. II" Chapter 7, Academic Press (1977).
20. M.B. Armand M. Duclot, Eur. pat. 0013199, prior.
21. B.L. Papke, Doctoral thesis, North western University, (1982), Available from university microfilms International.
22. J.M. Chabango, Doctoral thesis, university of Grenoble, 1980.
23. D.F. Shriver, B.L. Papke, M.A. Ratner, R. Dupon, T. Wong, and M. Brodwin, *Solid State Ionics*, (1981), 5, 83.
24. R.G. Pearson, *J. Am. Chem. Soc.*, (1963), 85, 3533.
25. R.G. Pearson, *J. Chem. Ed.*, (1968), 45, 643.
26. P.G. Bruce, F. Krok and C.A. Vincent, (1983), *Solid State Ionics*.
27. Y. Marcus, *Ion Solvation*, Wiley, Chichester, 1985.
28. M.B. Armand and F. Elkadiri, Proc. of the Symp. on Lithium batteries (San Diago, 1986), *The electrochemical Soc.*, New Jersey, p. 502.
29. M. Gauthier, *Int. Symp. on Polymer Electrolytes*, St. Andrews, Scotland, June 1987.
30. L.L. Yang, A.R. Maghie, and C.G. Farrington, *J. Electro Chem. Soc.*, (1986), 133, 1380.
31. R. Huq and C.G. Farrington, *Extended abstract of the*



- N     *Electrochemical Society, Fall Meeting, San Diego, California, (1986), Abstract 765.*
32. A. Patrick, M. Glasse, R. Linford, *Solid State Ionics*, (1986), 18, 1063.
33. D.J. Bannister, G.R. Davies, I.M. Ward, and J.E. MacIntyre, *Polymer*, (1984), 25, 1291.
34. J.S. Tong, P.M. Blonsky, D.F. Shriver, H.R. Allcock, P.E. Austin, T.S. Neenan and T. Sisko, *Proc. of the Symp. on Lithium Batteries (San Diego 1986)*, Vol. 87-1.
35. T. Takagishi, S. Okuda, N. Kuroki, H. Kozuka, *J. Polym. Chem.*, (1985), 23, 2109.
36. J. Moacanin, E.F. Cuddihy, *J. Polym. Sci. Part C*, (1966), 14, 313.
37. M. Watanabe, K. Nagaoka, K. Kanba, and M. Ashinohara, *Polymer J.*, (1982), 14, 877.
38. R.D. Lundberg, F.E. Bailey and R.W. Callard, *J. Polym. Sci. A-1*, 1966, 4, 1563.
39. M. Watanabe, J. Ikeda and J. Shinohara, *Polymer J.*, (1983), 15, 175.
40. G.G. Cameron, M.D. Ingram and G.A. Sorrie, *J. Electroanal. Chem.*, (1986), 198, 205.
41. P.M. Blonsky, D.F. Shriver, P. Austin and H.R. Allcock, *Solid State Ionics*, (1986), 18/19, 258.
42. J.J. Fontanella, M.C. Wintergill, J.P. Calame and G.G. Adneen, *J. Polym. Sci. Polym. Phys.*, (1985), 23, 113.

43. E.E. Wetton, D.B. James and W. Whiting,  
*J. Polym. Sci. Polym. Lett.*, (1976), **14**, 577.
44. D.B. James, R.E. Wetton and D.S. Brown,  
*Polymer*, (1979), **20**, 187.
45. D.B. James, R.E. Wetton and D.S. Brown,  
*Am. Chem. Soc. Div. Polym. Chem.*, (1978), **19**, 347.
46. M.J. Hannon, K.F. Wissbrun,  
*J. Polym. Sci. Polym. Phys.*, (1975). **13**, 113.
47. K.F. Wissbrun, M.J. Hannon,  
*J. Polym. Sci. Polym. Phys.*, (1975). **13**, 223.
48. D.W. Xia, D. Soltz, J. Smid, *Solid State Ionics*,  
(1984), **14**, 221.
49. K. Nagaoka, H. Naruz and I. Shinohara,  
*J. Polym. Sci.*, (1984), **22**, 659.
50. J.M.G. Cowie, "Polymers: Chemistry and Physics of  
*Modern Materials*", Intertext, Aylesbury 1973.
51. J.F. Le Nest, A. Gandini and H. Cheradame,  
*Brit. Polym. J.*, (1988), **20**, 185.
52. G.W. Castellan, "Physical Chemistry", Addison  
Wesley, California, (1964), p.577.
53. S. Gladstone, "Textbook of Physical Chemistry",  
MacMillan and Co., London, 1962, p.884.
54. Z. Ohtaki, *J. Appl. Phys.*, (1985), **57**, 123.
55. M. Watanabe, N. Ogata, "Polymer Electrolyte Reviews  
1", Ed. J.R. MacCallum, C.A. Vincent., Elsevier  
Applied Science Publishers, Essex, 1987, p.39.
56. K.S. Cole, R.H. Cole, *J. Chem. Phys.* (1941), **2**,

341.

57. J.R. MacDonald, *J. Chem. Phys.*, (1973), 58, 4282.
58. J.R. MacDonald, "Superionic Conductors", Ed. G.D. Mahan, W.L. Roth, Plenum Press, New York, 1980.
59. S. Smedley, "The Interpretation of Ionic conductivity in Liquids", Plenum Press, New York, 1980.
60. H. Cheradame, J.F. Le Nest, Abstracts, *Int. Symp. on polymer Electrolytes*, St. Andrews, Scotland, June 1987.
61. J.F. Le Nest, H. Cheradame, F. Dalard, D.J. Deroo, *Appl. Electrochem.* (1986), 16, 75.
62. H. Cheradame, in *IUPAC Macromolecules*, Pergamon press, New York, 1982, p.251.
63. A. Killis, J.F. Le Nest, H. Cheradame, *Makromol. Chem. Rapid Commun.*, (1980), 1, 595.
64. A. Killis, J.F. Le Nest, H. Cheradame, G. Gandini, *J. Polym. Sci. Polym. Phys. Ed.*, (1981), 19, 1073.
65. M. Levesque, J.F. Le Nest, H. Cheradame, *Makromol. Chem. Rapid Commun.*, (1983), 4, 497.
66. A. Killis, J.F. Le Nest, A. Gandini, H. Cheradame, J.P. Cohen-Addad, *Solid State Ionics*, (1984), 14,
67. A. Killis, J.F. Le Nest, A. Gandini, H. Cheradame, *Makromol. Chem.*, (1982), 183, 1037.
68. A. Killis, J.F. Le Nest, A. Gandini, H. Cheradame, A. Gandini, *Makromol. Chem.*, (1982), 183, 2835.
69. A. Killis, J.F. Le Nest, A. Gandini, H. Cheradame,

- J.P. Cohen-Addad, *Polym. Bull.*, (1982), **4**, 351.
70. B.L. Papke, M.A. Ratner, D.F. Shriver,  
*J. Electrochem. Soc.*, (1982), **129**, 1694.
71. J.H. Gibbs, E.A. Di Marzio, *J. Chem. Phys.*, (1958),  
**28**, 373.
72. G. Adam, J.H. Gibbs, *J. Chem. Phys.*, (1965), **43**,  
139.
73. S.G. Greenbaum, K.J. Adamic, Y.S. Pak, M.C.  
Wintersgill, J.J. Fontanella, *Six international  
conference on solid state ionics,  
Garmisch-Partenkirchen*, (1987), paper P3-3.
74. N. Kobayashi, M. Uchiyama, K. Shigehara, E.  
Tsuchida, *Phy. Chem.*, (1985), **82**, 987.
75. J.R.M. Giles, *Solid State Ionics*, (1987), **24**, 155.
76. J.R. MacCallum, A.S. Tomlin, C.A. Vincent,  
*Eur. Polym. J.*, (1986), **22**, 787.
77. C.D. Robitaille, T. Jacobson, *J. Electrochem. Soc.*,  
(1986), **133**, 315.
78. M.B. Armand, D. Muller, M. Duval, P.E. Harvey,  
U.S. Pat. No. 4578326.
79. J.R.M. Giles, J. Knight, C. Booth, R.H. Mobbs, J.R.  
Owen, PCT No. WO 86/01643.
80. I.M. Ward, J.E. MacIntyre, D.J. Bannister, P.J.  
Hall, PCT No. 85/02713.
81. J.M. Chabango, *Doctoral Thesis, University of  
Grenoble*, (1980).
82. D.W. Xia, J. Smid, *J. Polym. Sci.*, (1984), **22**, 617.

83. M. Leveque, Doctoral Thesis, University of Grenoble, (1986).
84. D. Andre, J.F. Le Nest, H. Cheradame, U.S. pat. 4357401, 1982.
85. M. Watanabe, J. Ikeda, J. Shinohara, *Polymer J.*, (1983), 15, 65.
86. M. Watanabe, K. Sanui, N. Ogata, *Macromolecules*, (1986), 19, 815.
87. M. Watanabe, K. Sanui, N. Ogata, T. Kobayashi, *Macromolecules*, (1984), 17, 2908.
88. J.R. MacCallum, M.J. Smith, C.A. Vincent, *Solid State Ionics*, (1984), 11, 307.
89. P.M. Blonsky, D.F. Shriver, P.E. Austin, H.R. Allcock, *J. Am. Chem. Soc.*, (1984), 106, 6854.
90. H.R. Allcock, P.E. Austin, T.X. Neenan, J.T. Sisko, P.M. Blonsky, D.F. Shriver, *Macromolecules*, (1986), 19, 1508.
91. P.G. Hall, G.R. Davies, J.E. MacIntyre, I.M. Ward, D.J. Bannister, K.M.P. Le Brocq, *Polymer Comm.*, (1986), 27, 98.
92. D. Fish, I.M. Khan, J. Smid, *Makromol. Chem. Rapid. Comm.*, (1986), 7, 115.
93. W.W. Xia, D. Soltz, J. Smid, *Solid State Ionics*, (1984), 14, 221.
94. D.W. Xia, J. Smid, *J. Polym. Sci. Letters*, (1984), 22, 617.
95. N. Kobayashi, M. Uchiyama, E. Tsuchida,

- Solid State Ionics*, (1985), **17**, 307.
96. J.M.G. Cowie, A.C.S. Martin,  
*Polymer Comm.*, (1985), **26**, 298.
97. J.M.G. Cowie, R. Ferguson,  
*J. Polym. Sci., Polym. Phys. Ed.*, (1985), **23**, 2181.
98. G.G. Cameron, J.L. Harvey, M.D. Ingram, G.A.  
Sorrie, *Brit. Polym. J.*, (1988), **20**, 199.
99. F.M. Gray, J.R. MacCallum, C. Vincent,  
*Solid State Ionics*, (1985), **18/19**, 282.
- 100 J.M.G. Cowie, R. Ferguson, A.C.S. Martin,  
*Polymer. Comm.*, (1987), **28**, 130.
101. J.M.G. Cowie, A.C.S. Martin, A.M. Firth,  
*Brit. Polym. J.*, (1988), **20**, 247.
102. J.M.G. Cowie, A.C.S. Martin,  
*Polymer*, (1987), **28**, 627.
103. J.R.M. Giles, F.M. Gray, J.R. MacCallum, C.A.  
Vincent, *Polymer*, (1987), **28**, 1977.
- 104 F.M. Gray, J.R. MacCallum, C.A. Vincent, J.R.M.  
Giles, *Macromolecules* , in press.
105. M. Mali, J. Ross, D. Brinkman, C. Berthier, M.B.  
Armand, *Proceedings XXIII Congress AMPERE*, Zurich,  
(1986), p.240.
106. J.F. Le Nest, *Doctoral Thesis*,  
University of Grenoble, (1985).
107. D. Muller, J.F. Le Nest, H. Cheradame, J.M.  
Chabagno, M. Laveque, *Eur. Patent*, 021 3985, 1987.
108. N. Kobayashi, T. Hamada, H. Ohno, E. Tuschida,

- Polym. J.*, (1986), 18, 661.
109. C.K. Chang, G.T. Davis, C.A. Harding, T.A. Takahoshi, *Macromolecules*, (1985), 18, 825.
110. C.S. Harris, D.F. Shriver, M. Ratner, *Macromolecules*, (1986), 19, 606.
111. S. Clancy, D.F. Shriver, L.A. Ochrymoycz, *Macromolecules*, (1986), 19, 606.
112. M. Watanabe, M. Rikukawa, K. Sanui, K. Ogata, H. Kato, T. Kobayashi, *Macromolecules*, (1984), 17, 2902.
113. J.S. Tonge, D.F. Shriver, *J. Electrochem. Soc.*, (1987), 134, 270.
114. H. Hooper, J.M. North, *Solid State Ionics*, (1983), 2, 1161.
115. M. Guathier, D. Fauteus, G. Vassort, M. Duval, P. Ricoax, D. Muller, P. Reguad, M.B. Armand, D. Deroo, *Second international meeting on Li batteries*, Paris, (1984).
116. G. Vassort, M. Gauthier, P.E. Harvey, F. Bruchu, M.B. Armand, *Proceedings of the Symp. on Primary and Secondary Ambient Temperature Li Batteries*, The Electrochemical Society, Philadelphia, PV88-6, (1988), p.780.
117. J.R. Upton, J.R. Owen, R. Rudkin, B.C.H. Steele, J. Benjamin, P. Tufton, *Solid State Ionics*, (1988),
118. J.R. Owen, J. Drennan, G.E. Lagos, P.C. Spudens, B.C.H. Steele, *Solid State Ionics*, (1981), 5, 343.

119. F. Pantaroni, S. Passerini, B. Scrosati,  
*J. Electrochem. Soc.*, (1987), 134, 753.
120. G.J. Kleywegt, W.L. Driessen,  
*Chem. Br.*, (1988), 24, 447.
121. F. Defendini, M.B. Armand, W. Gorecki, C. Berthier,  
*Electrochem. Soc. Extended Abstr.*, (1986), 86(2),  
893.
122. K.J. Adamic, S.G. Greenbaum, M.C. Wintersgill, J.J.  
Fontanella, *J. Appl. Phys.*, (1986), 60, 1342.
123. M.C. Wintersgill, J.J. Fontanella, M.K. Smith, S.G.  
Greenbaum, K.J. Adamic, C.G. Andeen, *Polymer*,  
(1987), 28, 633.
124. P.G. Hall, G.R. Davies, J.R. MacIntyre, I.M. Ward,  
D.J. Bannister, K.M.F. LeBroq, *Polym. Commun.*,  
(1986), 27, 98.
125. J. Smid, D. Fish, I.M. Khan  
*Makromol. Chem., Rapid Commun.*, (1986), 7, 115.
126. A.R.P. Le Mehaute, G. Crepy, G. Marceline, T.  
Hamaid, A. Guyot, *Polymer Bull.*, (1985), 14, 233.
127. C. Carre, T. Hamaid, A. Guyot, C. Mai,  
*First Int. Symp. On Polymer electrolytes*, St.  
Andrews, Scotland, 1987.
128. S.D. Druger, M.A. Ratner, A. Nitzan,  
*Solid State Ionics*, (1986), 18/19, 106.
129. E.S. Watson, M.J. O'Neil, J. Justin,  
N. Brenner, *Anal. Chem.*, (1964), 36, 1233.
130. M.J. O'Neil, *Anal. Chem.*, (1964), 36, 1238.



131. H.R. Allcock, *J. Polym. Sci., Part A*, (1967),  
1, 355.
132. L.J. Mathias, J.B. Canterbury, M. South,  
*J. Polym. Sci., Polym. Lett.*, (1982), 20, 473.
133. T. Suzuki, T. Tomono,  
*J. Polym. Sci., Polym. Chem. Ed.*, (1984), 22, 2829.
134. I. Ikeda, T. Katayama, K. Tauchiya, M. Okahara,  
*Bull. Chem. Soc. Jpn.*, (1983), 56, 2473.
135. D.K. Dishong, C.J. Dimond, M.I. Cinoman, J.W. Gokel  
, *J. Am. Chem. Soc.*, (1983), 105, 586.
136. T. Miyazaki, S. Yanagida, I. Itoh, M. Okahara,  
*Bull. Chem. Soc. Jpn.*, (1982), 55, 2005.
137. H.R. Allcock, R.L. Kugel, K.J. Valen,  
*J. Am. Chem. Soc.*, (1965), 87, 4215.
138. H.R. Allcock, R.L. Kugel, K.J. Valan,  
*Inorg. Chem.*, (1966), 5, 1709.
139. D.F. Shriver, B.L. Papke, M.A. Ratner, R. Dupon, T.  
Wong, *Solid State Ionics*, (1981), 5, 83.
140. As review, J. Smid, *Angew. Chem. Internat. Ed.*  
*Engl.*, (1972), 11, 112.
141. See for example, J.G. Heffernan, W.M MacKenzie,  
and D.C. Sherrington, *J. Chem. Soc., Perkin II*,  
(1981), 514.
142. B. Tummler, G. Maass, F. Vogtle, H. Sieger, U.  
Heimnnn and E. Weber, *J. Am. Chem. Soc.*, (1979),  
101, 2588.
143. R. Fornasier, F. Montanari, G. Podda, P. Tando,

- Tetrahedron lett., (1974), 1381.
144. F. Vogtle and E. Weber, *Angew. Chem. Internat. Ed. Eng.*, (1974), 13, 814.
145. Toshinobu Higashimura, Sadahito Aoshima, *Polymer Bulletin*, (1987), 17, 389.
146. C. A. Angell, R.D. Bressel, *J. Phys. Chem.*, (1972), 76, 3244.
147. C.A. Angell, *Solid State Ionics*, (1983), 9 & 10.
148. H. Vogel, *Phys. Z.*, (1921), 22, 645.
149. V.G. Tammann, W.Z. Hesse, *Anorg. Allg. Chem.*, (1926), 156, 245.
150. G.S. Fulcher, *J. Am. Chem. Soc.*, (1925), 38, 339.
151. C.A. Angell, *Solid State Ionics*, (1986), 18 & 19, 72.
152. S.D. Druger, M.A. Ratner, A. Nitzan, *Solid state Ionics*, (1983), 9 & 10, 1115.
153. J.M. Hammersley, *Proc. Cambridge Philos. Soc.*, (1957), 53, 642.
154. J.R. MacCallum, M.J. Smith, C.A. Vincent, *Solid State Ionics*, (1984), 11, 307.
155. J.R.M. Giles, M.P. Greehall, *Polym. Comm.*, (1986), 27, 360.
156. A. Bouridah, F. Dalard, D. Deroo, H. Cheradame, J.F. LeNest, *Solid state Ionics*, (1985), 15, 233.
157. B.L. Papke, M.A. Ratner, D.F. Shriver, *J. Electrochem. Soc.*, (1982), 129, 1694.
158. J.M.G. Cowie, A.C.S. Martin, A.M. Firth,

- Brit., Polym. J.*, (1988), 20, 247.
159. J. Wislicenus, *Justus Liebigs Ann. Chem.*, (1878), 192, 106.
160. W. Chalmers, *Can. J. Res.*, (1932), 113.
161. W. Chalmers, *J. Am. Chem. Soc.*, (1934), 56, 912.
162. D.D. Eley, J. Saunders, *J. Chem. Soc.*, (1952), 4167.
163. D.D. Eley, A.W. Richards, *Trans. Faraday Soc.*, (1949), 45, 425.
164. W. Reppe, O. Schlichting:  
U.S. Patent 2,104,000, (1937).  
U.S. Patent 2,104,002, (1937).  
U.S. Patent 2,098,108, (1937).
165. C.E. Schildknecht, "Vinyl and Related Polymers", pp. 593-634., Wiley, New York, (1952) and N.M. Bicals, *Encycl. Polym. Sci. Techno.*, (1971), 14, 511.
166. H.K. Frensdorff, *J. Am. Chem. Soc.*, (1971), 93, 600.
167. M. Kirch, J.M. Lehn, *Angew. Chem. Internat. Ed. Eng.*, (1975), 14, 555.
168. J.M. Lehn, *Pure and Appl. Chem.*, (1977), 49, 857.
167. J.M. Lehn, *Pure and Appl. Chem.*, (1978), 50, 871.
168. J.M. Lehn, *Pure and Appl. Chem.*, (1979), 51, 979.
169. J.D. Lamb, T.J. Christensen, J.L. Oscaranson, B.L. Neilsen, B.W. Asay, R.M. Izatt., *J. Am. Chem. Soc.*, (1980), 102, 6820.

170. D.K. Cabbiness, D.W. Margerum, *J. Am. Chem. Soc.*, (1969), 91, 6540.
171. (a) C.J. Pedersen, *J. Am. Chem. Soc.*, (1967), 89, 2495, 7017.  
(a) C.J. Pedersen, *Org. Synth.*, (1972), 52, 66.  
(c) For the history of the discovery of the crown ethers see *Aldrichia Acta*, (1971), 4.
172. D.J. Pedersen, *J. Am. Chem. Soc.*, (1970), 92, 391.
173. (a) D.J. Pedersen, *Fed. Proc.*, (1986), 27, 1305.  
(b) J.J. Christensen, J.O. Hill, R.M. Izatt, *Science*, (1971), 174, 459.  
(c) C.J. Pedersen, H.K. Frensdorff, *Angew. Chem.*, (1972), 84, 16.
174. Concerning problems of synthesis and reaction mechanism (reviews):  
(a) G.W. Gokel, H.D. Durst, *Synthesis*, (1976), 168.  
(b) G.W. Gokel, H.D. Durst, *Aldrichia Acta*, (1976), 2, 3.  
(c) A.C. Knipe, *J. Chem. Education.*, (1976), 53, 618.  
(d) W.P. Weber, G.W. Gokel, in "Phase Transfer Catalysis in Organic Synthesis : Reactivity and Structure Concept in Organic Chemistry", Vol. 4, Springer Verlag, New York, 1977.  
(e) F. Vogtle, E. Weber, *Kontakte (Merck)*, (1977),

16(2) and 36(3).

175. Concerning Analytical Problems:

- (a) E. Blasius, K.P. Janzen, W. Adrian, G. Klautke  
, R. Lorschneider, J. Stockmer,  
*Anal. Chem.*, (1977), 284, 337.
- (b) Review: E. Weber, F. Vogtle, *J. Chem. Educ.*,  
(1978), 55, 350.

176 Biological, Physiological and toxicological Uses:

- (a) YU. a. Ovechinnikov, V.I. Ivanov, A.M. Shkrob,  
in *"Membrane Active Complexons*, B.B.A Library  
Vol. 12., Elsevier Scientific Publishing  
Company, 1974.
- (b) B.C. Pressman, *Annual Reviews of Biochemistry*,  
Vol. 5 (Eds. E.E. Snell, P.D. Boyer, A. Meister  
, C.C. Richardson), Palo Alto, California,  
1976.
- (c) Review: F. Vogtle, E. Weber, U. Elben,  
*Kontakte (Merck)*, 32(3), (1978).

177. Reviews:

- (a) *Structure and Bonding*, Vol.16., Springer  
Verlag, (1973).
- (b) W. Burgermeister, R. Winkler-Oswatitsch, in  
*"Inorganic Biochemistry II"*, Topics in Current  
Chemistry, Vol. 69, Springer Verlag, 1977.
- (c) R.M. Izatt, J.J. Christensen (Eds.),  
*"Synthetic Multidentate Macrocyclic Compounds"*  
, Academic Press, 1978.

- (d) R.M. Izatt, J.J. Christensen, *Progress in Macrocyclic Chemistry*, Wiley, New York, 1979.
178. Reviews:
- (a) D.St.C. Black, A.J. Hartshorn, *Coor. Chem. Rev.*, (1972), 2, 219.
  - (b) J.J. Christensen, D.J. Eatough, R.M. Izatt, *Chem. Rev.*, (1974), 74, 351.
  - (c) J.S. Bradshaws, J.Y.K Hui, *J. Hetrocycl. Chem.*, (1974), 11, 649.
  - (d) G.R. Newkome, A. Nayak, J. Otemaa, D.A. Van, *J. Org. Chem.*, (1978), 43, 3362.
179. (a) H.E. Simmons, C.H. Park, *J. Am. Chem. Soc.*, (1968), 90, 2428.
- (b) C.H. Park, H.E. Simmons, *J. Am. Chem. Soc.*, (1968), 90, 2431.
180. (a) B. Dietrich, J.M. Lehn, P. Savage, *Tetrahedron Letters*, (1969), 2885.
- (b) B. Dietrich, J.M. Lehn, P. Savage, *Tetrahedron*, (1969), 22, 1629.
181. G.E. Liesegang, M.M. Farrow, F.A. Vazquez, N. Purdie, E.R. Eyring, *J. Am. Chem. Soc.*, 99, (1977), 99, 3240.
182. B.G. Cox, H. Schneider, R.G. Wilkins, *J. Am. Chem. Soc.*, (1978), 100, 4746.
183. V.M. Loyola, R. Pizer, R.G. Wilkins, *J. Am. Chem. Soc.*, (1977), 99, 7185.
184. E.A. Moelwyn, in *"Kinetics of Reactions in*

*Solution*<sup>m</sup>, Clarendon Press, Oxford, 1942.

185. For example F. de Jong, D.N. Reinhoudt, R. Huis, *Tetrahedron Letters*, (1977), 3985.
186. for example K. Henco, B. Tunnler, G. Maass, *Angev. Chem. Intern. Ed. Engl.*, (1977), 16, 538.
187. M. Eigen, *Ber. Bunsenges. Phys. Chem.*, (1963), 67, 753.
188. Review: K.O. Hodgson, *Intra. Sci. Chem. Rept.*, (1974), 2, 27.
189. M. Eigen, G. Geier, W. Kurse, *Essays in Coord. Chem. Exper., Suppl. IX.*, (1964), 164.
190. B.G. Cox, J. Garcia-rosas, H. Schneider, *J. Am. Chem. Soc.*, (1981), 103, 1384.
191. B.G. Cox, J. Garcia-rosas, H. Schneider, *J. Am. Chem. Soc.*, (1981), 103, 1054.
192. I.M. Kolthoff, M.K. Chantooni, *Anal. Chem.*, (1980), 52, 1032.
193. S. Kopolow, T.E. Hogen Esch, J. Smid, *Macromolecules*, (1971), 4, 359.
194. J.D. Dunitz, P. Seiler, *Acta Cryst.*, (1974), B30, 27.
195. N.S. Poonia, B.P. Yado, B.W. Bhagwat, V. Naik, H. Manohar, *Inorg. Nucl. Chem. Letters*, (1977), 13, 119.
196. B. Dietrich, J.M. Lehn, J.P. Sauvage, *J. Chem. Soc. Chem. Comm.*, (1970), 1055.
197. (a) Cassol, A. Seminaro, G.D. Paoli, *Inorg. Nucl.*

*Letters*, (1973), 2, 1163.

(b) R.B. King, P.R. Heckley, *J. Am. Chem. Soc.*,  
(1974), 96, 3118.

(c) A. Seminaro, G. Siracusa, A. Cassol, *Inorg.*  
*Chim. Acta.*, (1976), 20, 105.

(d) M. Ciaampoloni, N. Nardi, *Inorg. Chim. Acta*,  
(1979), 32, L9.

198. Review: D.K. Koppikar, P.V. Sivapullaiah, L.  
Ramarkkrishnan, *Struct. Bonding*, (1978), 34, 135.